UNCLASSIFIED

AD 402 776

Reproduced
by the
DEFENSE DOCUMENTATION CENTER
FOR
SCIENTIFIC AND TECHNICAL INFORMATION
CAMERON STATION, ALEXANDRIA, VIRGINIA

UNCLASSIFIED

NOTICE: When government or other drawings, specifications or other data are used for any purpose other than in connection with a definitely related government procurement operation, the U. S. Government thereby incurs no responsibility, nor any obligation whatsoever; and the fact that the Government may have formulated, furnished, or in any way supplied the said drawings, specifications, or other data is not to be regarded by implication or otherwise as in any manner licensing the holder or any other person or corporation, or conveying any rights or permission to manufacture, use or sell any patented invention that may in any way be related thereto.

402776

AS AD

ANTENNA LABORATORY

Technical Report No. 68

A STUDY OF WAVE PROPAGATION OF HELICES

by

Paul William Klock

Contract No. AF33(657)-10474
Hitch Element Number 62405484
760 D-Project 6278, Task 6278-01

MARCH 1963

Sponsored by
AERONAUTICAL SYSTEMS DIVISION
WRIGHT-PATTERSON AIR FORCE BASE, OHIO
Project Engineer — James Rippin — ASRNCF-3

ASTIA
APR 30 1963

ELECTRICAL ENGINEERING RESEARCH LABORATORY
ENGINEERING EXPERIMENT STATION
UNIVERSITY OF ILLINOIS
URBANA, ILLINOIS

Antenna Laboratory

Technical Report No. 68

A STUDY OF WAVE PROPAGATION ON HELICES

by

Paul William Klock, Ph.D.

Contract No. AF33(657)-10474
Hitch Element Number 62405484
760 D-Project 6278, Task 6278-01

March 1963

Sponsored by

AERONAUTICAL SYSTEMS DIVISION

WRIGHT-PATTERSON AIR FORCE BASE, OHIO

Project Engineer - James Rippin - ASRNCF-3

Electrical Engineering Research Laboratory
Engineering Experiment Station
University of Illinois
Urbana, Illinois

ABSTRACT

The determinantal equation for a narrow tape helix is derived of two methods, and complex-valued solutions for the phase constant are obtained.

The complete k - β diagram (Brillouin diagram) is given as a function of tape width and pitch angle. In order that the solutions be continuous functions of k and β, it is necessary to change branches of the square root which appears in the determinantal equation. A discussion of solutions which are physically admissible as complex wave solutions is given, and the phase constants corresponding to the complex wave solutions are used to represent the current on a helix. Two source problems are investigated, one an infinite helix, the other a finite helix. Comparison with experiments is made with good agreement.

ACKNOWLEDGEMENT

The author wishes to thank his teachers.

TABLE OF CONTENTS

TABLE OF CONTENTS (continued)

LIST OF ILLUSTRATIONS

LIST OF ILLUSTRATIONS (continued)

LIST OF ILLUSTRATIONS (continued)

LIST OF ILLUSTRATIONS (continued)

LIST OF ILLUSTRATIONS (continued)

LIST OF ILLUSTRATIONS (continued)

1. INTRODUCTION

Analysis for the helix was first reported in 1897 by Pocklington[1] who assumed a very thin perfectly conducting wire and formulated an integral equation whose approximate solutions predicted an axial phase velocity equal to the velocity of light c for very low frequencies and c sin ψ, where ψ is the pitch angle of the helix, for larger frequencies. These results agree with the results reported in the present work for the limiting cases of very narrow tape and low frequencies.

In 1910 Nicholson[2] formulated the helix problem exactly but was forced to make unreasonable approximations to obtain a solution.

Ollendorf[3] in 1926 reported the solution of the sheath helix for the mode in which no angular variation of the fields exist. Solutions for the higher order modes of the sheath helix were given by Phillips and Malin[4].

A more complete analysis which was motivated by the use of the helix in traveling wave tubes and as antennas was given by Kornhauser[5] in 1949.

An excellent history and an extensive bibliography through 1955 is given by Sensiper[6] who also explains the relationship of his thesis[7] to the total literature. In these publications he formulated and solved the determinantal equation for the tape helix for the phase constant β. He limited himself to the real-valued solutions of this equation.

Following Sensiper, Pierce and Tien[8] obtained an approximate solution of the determinantal equation of the tape helix using Pierce's[9] coupled mode theory.

Abstracts of 66 papers and reports on the helical beam antenna through May 1959 are given by Wong and Thomas[10].

None of the works referred to above indicated the possibility of the existence of complex-valued solutions of the helix determinantal equation. In fact, Sensiper and also Pierce voiced doubts as to the existence of complex-valued

phase constants. Sensiper's proof on the non-existence of complex solutions was based on the condition of total finite energy.

The existence of the complex roots and their importance to the helical antenna problem was first pointed out by Mittra[11]. In that paper he also explained as a consequence of the presence of a particular symmetry in the helix structure which makes its effective period to be infinitesimally small, why the determinantal equation of the helix, unlike the equation for other periodic structures, does not have periodic solutions. As a further consequence of the above geometry it was shown that there exist no harmonic terms in the representation of the current along the tape and that a single term of the type $e^{-j\beta_w s}$ (s = distance along the tape, β_w = phase constant) is sufficient to represent this current.

A major contribution of the present work is the detailed study of the determination and application of the complex solutions of the helix determinantal equation. Except for a brief mention by Mittra, a discussion of these solutions has not been reported elsewhere. The complex valued solutions of the helix equation have been found very useful in explaining the current distribution on the helix, both uniform and log-periodic, and for predicting the radiation pattern of a helical antenna. A further discussion on the interpretation and usefulness of the complex solutions of the determinantal equation in an open periodic structure appears later.

An alternative approach to the solution for the current distribution on the helical structure has been reported by Patton[12]. He obtained the Fourier transform of the current distribution on the semi-infinite bifilar helix by a Wiener-Hopf technique. The Fourier transform of the current was related to the radiation pattern, and the calculated patterns were compared with experimental results also obtained by Patton. The effect of wire size was studied.

Three related papers have recently been written by MacLean[13,14,15]. In the first he compares the different approaches to the helical antenna. The results

of the report state that a "simple engineering approach" (i.e., one without Bessel Functions) "is adequate for most purposes." The second paper is a theoretical study assuming that waves travel both axially and helically along the antenna. It is shown that the existence of the helical waves is responsible for what are the cut off frequencies of the antenna. Study is also made of the effect of the ground plane. The last is an analysis based on the sheath-helix mode. He obtains, among other things, the determinantal equation for the sheath helix with a concentric perfectly conducting core. The results are given for relative phase velocity when the fields have one axial variation, i.e., $e^{-jn\phi}$, $n = 1$.

Kraus[16] in 1948 and later Kornhauser[17] calculated the radiation pattern of a helical antenna operation on the axial or beam mode by assuming a sinusoidal current with an empirically determined phase constant which corresponded to a slow wave on the antenna. They obtained satisfactory results by using the empirically determined phase constant which may now be obtained by using the phase constant determined from the solution to the determinantal equation.

The current distribution on a helical antenna was measured by Marsh,[18] and he was able to fit his measured results well by assuming there existed two waves on the antenna, one corresponding to a complex-valued phase constant with the real part representing a wave traveling at the velocity of light and the other corresponding to a real valued phase constant representing a slow wave. His empirically determined phase constants agree well with the complex-valued phase constants which are solutions to the determinantal equation.

Now return to a brief discussion of complex solutions. The solutions corresponding to complex-valued phase constants are not proper modes since the fields corresponding to these modes do not satisfy the radiation condition everywhere at infinity. However, Marcuvitz[19] suggested that these solutions might be used to approximately represent the near fields, and used as an alter-

nate to the continuous eigen-value spectrum and as an approximate representation of the far fields of a structure in a certain range of observation points. The solutions corresponding to the improper modes were given the name leaky modes by Marcuvitz who showed that the zero of the determinantal equation which corresponds to the leaky mode is on the improper Riemann sheet in the phase constant plane. The far fields may also be calculated by Kirchhoff type integration by treating the near field representation in terms of the leaky wave fields as equivalent sources.

Radiation properties of a class of periodic structures may be conveniently analyzed in terms of their Brillouin (k- β) diagram provided this diagram exhibits both real and complex solutions in slow as well as fast wave regions. Early workers on periodic structures were primarily interested in the surface wave, (real valued solution to the determinantal equation), on open periodic structures, and it was customary to name the fast wave regions forbidden regions. Recently it has been well demonstrated that not only do there exist complex-valued solutions for the phase constant of some structure in the forbidden region where $\beta_r < k$ but also in the slow wave regions where $\beta_r > k$. Since leaky waves have become synonymous with fast waves, it is suggested here that the name complex waves be associated with the waves corresponding to complex-valued phase constants in fast or slow wave regions or that the term leaky wave be generalized to include both slow and fast waves. The physical interpretation of complex waves was given by Marcuvitz[19]. Olner[20] gives an excellent discussion on the range of permitted observation points and the position of the complex wave zero of the determinantal equation. In a class of structures excited by a given source, where the dominant part of the field has its total representation in terms of the continuous spectrum of spatial frequencies, complex waves have been found useful in representing the fields. This alternate repre-

sentation is approximate.

Goldstone and Oliner[21,22] obtained good results using complex waves in the analysis of a class of leaky-wave structures. The relationship between complex waves and the radiation pattern of leaky wave antennas is discussed by Hessel.[23] Oliner also gives other examples of the use of complex waves in electromagnetic phenomena.

To date, very few structures have been analyzed for their complete Brillouin, (k-ß), diagram, other than on an approximate and perturbational basis. This generalization is excepting some idealized structures such as the constant reactance or modulated reactance surfaces, the anisotropic sheet structures and a few others. Although the analysis of the above structures is quite useful, their application to practical devices is good only in an approximate sense.

The tape helix, which is very much a practical structure, yielded to solution for its complete k-ß diagram which, with its applications to helical antennas, is the subject of this report. The determinantal equation for a narrow tape helix may be formulated in at least two different ways. One involves the Floquet expansion of the fields and the assumed current, with unknown phase constant, on matching boundary conditions at the cylindrical surface which contains the tape. The second method is based on an integral equation formulated for the current distribution on the tape. The second method is similar to the method used by Kogan[24] on the round wire version of the helix. The same determinantal equation is obtained by both methods. The determinantal equation and its solutions for the phase constant are extensively studied for real-valued as well as complex-valued phase constants.

The solutions in the k-ß plane are continuous. In order that the solutions be continuous it is necessary to change branches of the square

root in the argument of the IK product in determinantal equation. Different branches give rise to different solutions which are physically interpreted. The root-tracking procedure on different Riemann sheets which is outlined here may find applications in the study of other structures where the locus in the k-β plane appears to be discontinuous.

The complex-valued solutions to the determinantal equation are used in the analysis of two different source problems. The first source problem obtains the solution for the relative amplitude of the waves corresponding to real and complex roots for an infinite helix excited at the center. The second considers the same problem for a finite helix excited at the center. A variational principle is used to formulate the latter source problem. Theoretically computed values of the real and complex solutions are used to explain the experimentally measured current distributions by Marsh[18]. As previously mentioned, complex wave analysis given in this report may be used to interpret Marsh's results which were empirical.

It is felt that the current distribution on the tapered version of the helix, viz., the equiangular spiral on a cone, may also be explained by extending the present work to tapered structures.

2. THE DETERMINANTAL EQUATION

2.1 Introduction

In this chapter the determinantal equation for the infinite tape helix will be derived by two methods. The functions of a complex variable which appear will be multivalued, and determination of the appropriate branches will be discussed. The geometry of the tape helix used is shown in Figure 2.1.

The tape lies in a cylindrical surface whose radius is "a" and whose axis is the z axis. Perfect conductivity and infinitesimal radial thinness are assumed; however, the width of the tape is taken as δ as measured in the z direction. Points on the surface of the cylinder are given by the coordinates ϕ and ζ. The azimuthal angle, ϕ, locates a point on the center line of the tape as given by the parametric equations

$$x = a \cos \phi$$

$$y = a \sin \phi$$

$$z = \frac{p}{2\pi} \phi = \bar{p} \phi$$

where p is the pitch of the helix. The coordinate ζ is the distance in the z direction from the point determined on the center line of the tape by specifying ϕ.

The equation of the tape may then be written as

$$-\infty < \phi < \infty$$

$$-\frac{\delta}{2} \leq \zeta \leq \frac{\delta}{2}$$

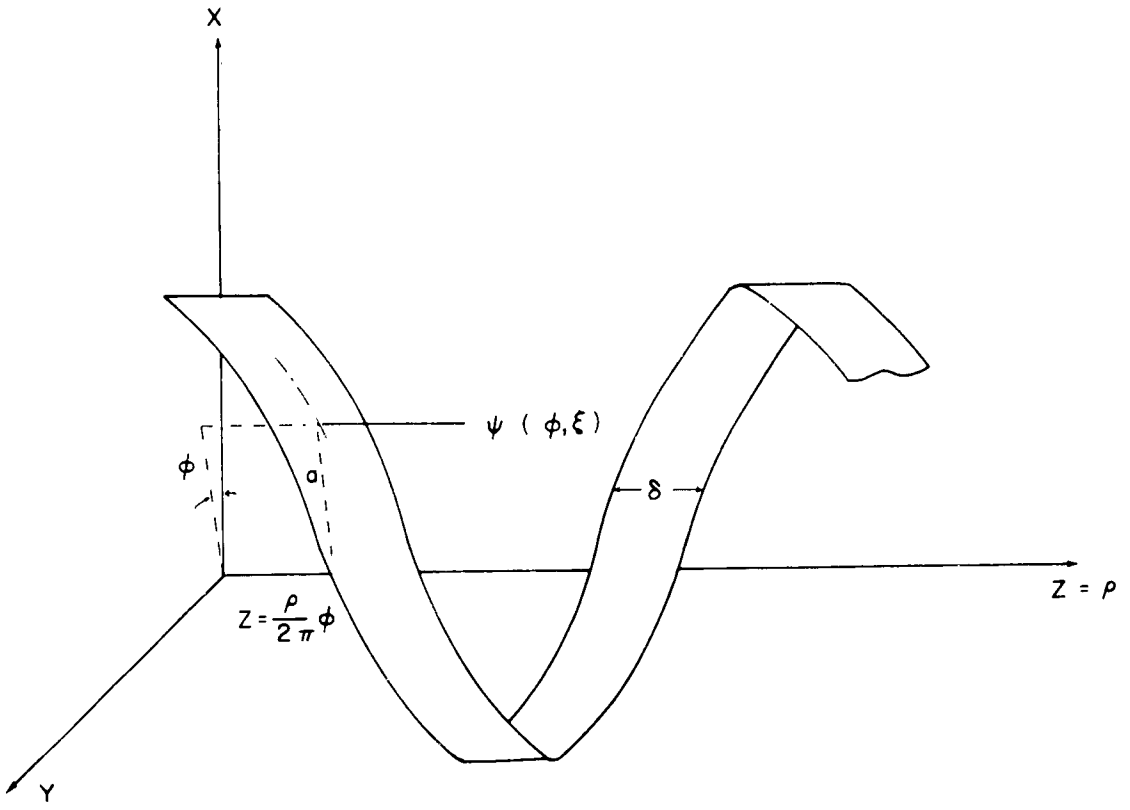

Figure 2.1. The geometry of the tape helix.

2.2 Derivation by Application of Boundary Conditions

The determinantal equation for the tape helix is derived in this section by expanding the fields and current in space harmonics[25] and then matching boundary conditions at r = a.

The helix shows a great amount of symmetry. If one displaces the infinite helix a distance p in the z direction, the helix transforms into itself. The translational period is p. If the helix is rotated through an angle, $\phi = 2\pi$, the helix transforms into itself. The rotational period is 2π. These symmetries are not the only symmetries. In addition, any arbitrary translation z_o followed by a rotation ϕ_o where $\phi_o = \frac{z_o}{\bar{p}}$ transforms the helix into itself. Therefore the period in $\zeta = z - \bar{p}\phi^1$, where $\phi^1 = \frac{z}{p}$, is zero. Now if $\zeta = z - \bar{p}\,\phi^1$ and ϕ is fixed then ζ is periodic with period p. If z is fixed ζ is also periodic with period p. This property, the generalized period being zero, is a unique property of the helix. Of course, uniform structures have zero translational period. This unique symmetry property of the helix has important consequences which will be discussed later.

The field equations used are expressed in circularly cylindrical coordinates. Starting from the source free Maxwell's equation one obtains the wave equation for E_z and H_z as

$$\frac{1}{r}\frac{\partial}{\partial r}\left(r\frac{\partial\psi}{\partial r}\right) + \frac{1}{r^2}\frac{\partial^2\psi}{\partial\phi^2} + \frac{\partial^2\psi}{\partial z^2} - \frac{1}{c^2}\frac{\partial^2\psi}{\partial t^2} = 0 \qquad (2.1)$$

where $\psi = E_z$ or H_z and is a function of r, ϕ, z and t.

Assuming the time variation as sinusoidal and that Equation (2.1) may

be separated as

$$\Psi (r, \phi, z, t) = R(r) \bar{\Phi}(\phi) Z(z) e^{i\omega t}$$

one obtains

$$\frac{1}{r} \frac{d}{dr} \left(r \frac{dR}{dr} \right) - \left[\frac{n^2}{r^2} + \left(\frac{\beta m}{\bar{p}} \right)^2 - k^2 \right] R = 0 \qquad (2.2)$$

where

$$\frac{d^2 \bar{\Phi}}{d\phi^2} + n^2 \bar{\Phi} = 0 \qquad (2.3)$$

and

$$\frac{d^2 Z}{dz^2} + \left(\frac{\beta m}{\bar{p}} \right)^2 Z = 0 \qquad (2.4)$$

$$k^2 = \omega^2 \mu \epsilon$$

A solution to Equation (2.3) is

$$\bar{\Phi} = A^1 e^{-in\phi} \qquad (2.5a)$$

and, since the fields are periodic in ϕ with period 2π, n must be an integer.

A solution of Equation (2.4) is

$$Z = A^{11} e^{-i \frac{\beta m}{\bar{p}} z} \qquad (2.5b)$$

The solution for Equation(2.2) is

$$R = A_n I_n \left(\tau_m \frac{r}{p}\right) + B_n K_n \left(\tau_m \frac{r}{p}\right) \tag{2.5c}$$

where

$$\tau_m = \sqrt{\beta_m^2 - (k\bar{p})^2}$$

If the fields are to be finite at r = 0 or r = ∞, then the fields are of the form

$$\psi(r,\phi,z) = \sum_{m,n=-\infty}^{\infty} A_{mn} \frac{I_n\left(\tau_m \frac{r}{p}\right)}{K_n\left(\tau_m \frac{r}{p}\right)} e^{-in\phi} e^{-i\frac{\beta_m}{p} z} \tag{2.6}$$

Floquet's Theorem[25] states that the fields at z = z + p are related to the fields at z by a complex constant. If $\beta_m = \beta + m$ then Equation(2.6) may be written

$$\psi(r,\phi,z) = e^{-i\beta\frac{z}{p}} \sum_{m,n=-\infty}^{\infty} A_{mn} \frac{I_n\left(\tau_m \frac{r}{p}\right)}{K_n\left(\tau_m \frac{r}{p}\right)} e^{-in\phi} e^{-im\frac{z}{p}} \tag{2.6a}$$

Now Equation (2.6a) satisfies Floquet's Theorem since

$$\psi(r,\phi,z + p) = e^{-i\beta 2\pi} \psi(r,\phi,z)$$

When z is changed to $z + z_o$ and ϕ changed simultaneously to $\phi + \phi_o$ where

$z_o = \bar{p}\,\phi_o$, the fields must be the same except for a complex constant. The property that the fields differ only by a complex constant after the above combination of translation and rotation is the result of "The Generalized Floquet Theorem[26] ". In "The Generalized Floquet Theorem" use is made of the periodicity not only in the translation alone or in the rotation alone but in the combination of translation, rotation, and other kinds of reflection symmetries.

The Generalized Floquet Theorem is satisfied for the helix whose fields are described by Equation (2.6a) if and only if n = -m. Equation (2.6a) becomes

$$\psi(r,\phi,z) = e^{-i\frac{\beta}{\bar{p}}z} \sum_{n=-\infty}^{\infty} A_n \frac{I_n\left(\tau_n \frac{r}{\bar{p}}\right)}{K_n\left(\tau_n \frac{r}{\bar{p}}\right)} e^{-in\left(\frac{z}{\bar{p}} - \phi\right)} \tag{2.7}$$

Let the logitudinal fields be

$$E_z^{i,0} = e^{-i\frac{\beta}{\bar{p}}z} \sum_{n=-\infty}^{\infty} \frac{A_n^{1} I_n\left(\tau_n \frac{r}{\bar{p}}\right)}{A_n^{o} K_n\left(\tau_n \frac{r}{\bar{p}}\right)} e^{-i\frac{n}{\bar{p}}\zeta} \tag{2.8}$$

$$H_z^{i,0} = e^{-i\frac{\beta}{\bar{p}}z} \sum_{n=-\infty}^{\infty} \frac{B_n^{1} I_n\left(\tau_n \frac{r}{\bar{p}}\right)}{B_n^{o} K_n\left(\tau_n \frac{r}{\bar{p}}\right)} e^{-i\frac{n}{\bar{p}}\zeta} \tag{2.9}$$

where i and 0 refer to $r < a$ and $r > a$ respectively.

By applying Maxwell's equation the other fields are

$$E_p^{i,0} = e^{-i\frac{\beta}{p}z} \sum_{n=-\infty}^{\infty} \begin{bmatrix} -n\frac{\beta_n}{p} & A_n^{\,i} I_n\left(\tau_n \frac{r}{p}\right) & -\frac{i\omega\mu}{\tau} & B_n^{\,1} I_n^{\,1}\left(\tau_n \frac{r}{p}\right) \\ \hline \left(\frac{\tau_n}{p}\right)^2 r & A_n^{\,o} K_n\left(\tau_n \frac{r}{p}\right) & \frac{n}{p} & B_n^{\,o} K_n^{\,1}\left(\tau_n \frac{r}{p}\right) \end{bmatrix} e^{-i\frac{n}{p}\zeta} \qquad (2.10)$$

$$E_r^{i,0} = e^{-i\frac{\beta}{p}z} \sum_{n=-\infty}^{\infty} \begin{bmatrix} i\frac{\beta_n}{p} & A_n^{\,i} I_n^{\,1}\left(\tau_n \frac{r}{p}\right) & \frac{n\omega\mu}{\tau_n^{\,2}} & B_n^{\,1} I_n\left(\tau_n \frac{r}{p}\right) \\ \hline \frac{\tau_n}{p} & A_n^{\,o} K_n^{\,1}\left(\tau_n \frac{r}{p}\right) & \frac{}{p} r & B_n^{\,o} K_n\left(\tau_n \frac{r}{p}\right) \end{bmatrix} e^{-i\frac{n}{p}\zeta} \qquad (2.11)$$

$$H_\phi^{i,0} = e^{-i\frac{\beta}{p}z} \sum_{n=-\infty}^{\infty} \begin{bmatrix} \frac{i\omega\epsilon}{\tau} & A_n^{\,i} I_n^{\,1}\left(\tau_n \frac{r}{p}\right) & -\frac{n\frac{\beta_n}{p}}{\left(\frac{\tau_n}{p}\right)^2} & B_n^{\,i} I_n\left(\tau_n \frac{r}{p}\right) \\ \hline \frac{\tau_n}{p} & A_n^{\,o} K_n^{\,1}\left(\tau_n \frac{r}{p}\right) & r & B_n^{\,o} K_n\left(\tau_n \frac{r}{p}\right) \end{bmatrix} e^{-i\frac{n}{p}\zeta} \qquad (2.12)$$

$$H_r^{i,0} = e^{-i\frac{\beta}{p}z} \sum_{n=-\infty}^{\infty} \begin{bmatrix} \frac{n\omega}{\left(\frac{\tau_n}{p}\right)^2} & A_n^{\,i} I_n\left(\tau_n \frac{r}{p}\right) & i\frac{\beta_n}{p} & B_n^{\,i} I_n^{\,1}\left(\tau_n \frac{r}{p}\right) \\ \hline r & A_n^{\,o} K_n\left(\tau_n \frac{r}{p}\right) & \frac{}{\tau} & B_n^{\,o} K_n^{\,1}\left(\tau_n \frac{r}{p}\right) \\ & & \frac{n}{p} & \end{bmatrix} e^{-i\frac{n}{p}\zeta} \qquad (2\ 13)$$

The boundary conditions for the tape helix at r = a are:

1) Tangential electric field is continuous everywhere on the cylinder r = a.

2) Tangential magnetic intensity is discontinuous by the surface current.

The surface current will be assumed to have the following form

$$J_{11} = \begin{cases} J_{0} e^{-\beta\phi} & \frac{p}{}\phi < z < \frac{p}{}\phi + \delta \\ 0 & \end{cases}$$

$$J_1 = 0 \qquad \text{elsewhere in } 0 \leq z \leq p \tag{2.14}$$

Such an assumption is justified because the fields at $\phi + \phi_1$ are related to the fields at ϕ exactly in the manner in which the fields at $\phi^1 + \phi_1$ are related to the fields at ϕ^1, where ϕ, ϕ^1 and ϕ_1 are arbitrary. The reason for the previous statement is that if the helix is infinite then one cannot distinguish between the fields at ϕ and ϕ^1 except by the complex constant as shown in Equation (2.7). Later, in Chapter 5, it will be shown that the solution for an infinite helix fed at the origin will be of the form $e^{-i\beta_1\phi}$. This current is confined to the tape and is flowing only in the parallel direction. In addition the current has a phase shift only when ϕ of the center line is changed. Thus the current satisfies Floquet's Theorem. If one is to be successful in matching boundary conditions the current must be expanded in the form of Equation (2.7), viz.

$$J_{11} = e^{-j\frac{\beta}{p}z} \sum_{n=-\infty}^{\infty}{}' j_{11n} e^{-j\frac{n}{p}\zeta} \tag{2.15}$$

This form for the current is identical to the form for the fields,

Equation (2.7), and permits the matching of the boundary conditions.

If one examines Equation (2.15), Equation (2.14) would be rewritten as

$$J_{11} = \begin{cases} J_o e^{-\imath \beta \frac{z}{\bar{p}}} e^{-i \frac{\beta}{\bar{p}} \zeta} & 0 < \zeta < \delta \\ 0 & \text{elsewhere} \end{cases} \qquad (2.16)$$

The current of Equation (2.16) is easily expressed in a Fourier series of the form of Equation (2.15). The coefficients are found to be

$$j11n = \frac{1}{p} \int_0^{\delta} J_o e^{-\imath \frac{\beta}{\bar{p}} \zeta} e^{\imath \frac{n}{\bar{p}} \zeta} d\zeta$$

$$J11n = \frac{J_o \delta}{p} e^{-\imath \beta_n \frac{\delta}{2\bar{p}}} \frac{\sin \frac{\beta_n \delta}{2\bar{p}}}{\frac{\beta_n \delta}{2\bar{p}}} \qquad (2.17a)$$

$$j\phi n = j11n \cos \Psi \qquad (2.17b)$$

$$jzn = j11n \sin \Psi \qquad (2.17c)$$

Now since all the fields and currents are expanded in similar series of linear independent functions, the boundary conditions must apply to each term of the series or space harmonic. The boundary conditions are

$$E_{zn}^{\,i} = E_{zn}^{\,o} \tag{2.18a}$$

$$E_{\phi n}^{\,i} = E_{\phi n}^{\,o} \tag{2.18b}$$

$$J_{\phi n} = H_{zn}^{\,i} - H_{zn}^{\,o} \tag{2.18c}$$

and

$$J_{zn} = H_{\phi n}^{\,o} - H_{\phi n}^{\,1} \tag{2.18d}$$

If Equations (2.8) through (2.13) are substituted into Equation (2.18) the following equations are obtained.

$$A_n^{\,1} I_n\left(\tau_n \frac{a}{p}\right) - A_n^{\,o} K_n\left(\tau_n \frac{a}{p}\right) = 0 \tag{2.19a}$$

$$A_n^{\,i} I_n\left(\tau_n \frac{a}{p}\right) + \frac{i\omega\mu \dfrac{\tau_n}{p}}{n\beta_n \dfrac{\beta_n}{p}} B_n^{\,1} I_n^{\,1}\left(\tau_n \frac{a}{p}\right) - A_n^{\,o} K_n\left(\tau_n \frac{a}{p}\right)$$

$$- \frac{-\omega\mu \dfrac{\tau_n}{p}}{n\beta_n \dfrac{\beta_n}{p}} B_n^{\,o} K_n^{\,1}\left(\tau_n \frac{a}{p}\right) = 0 \tag{2.19b}$$

$$B_n^{\,i} I_n\left(\tau_n \frac{a}{p}\right) - B_n^{\,o} K_n\left(\tau_n \frac{a}{p}\right) = j l i n \cos\psi \tag{2.19c}$$

$$A_n^{o} K_n^{1}\left(\tau_n \frac{a}{p}\right) - \frac{n\beta n/p}{\frac{\tau_n}{p} a i\omega\epsilon} B_n^{o} K_n\left(\tau_n \frac{a}{p}\right) - A_n^{i} I_n^{i}\left(\tau_n \frac{a}{p}\right)$$

$$+ \frac{n\frac{\beta_n}{p}}{\frac{\tau_n}{p} a i\omega\epsilon} B_n^{i} I_n\left(\tau_n \frac{a}{p}\right) = j l l n \sin\psi \qquad (2.19d)$$

The above four equations can be solved for $A_n^{i,o}$ and $B_n^{i,o}$. These solutions yield

$$A_n^{i} = \frac{K_n\left(\tau_n \frac{a}{p}\right)\frac{\tau_n a}{p}}{i\omega\epsilon} j l l n \left[\frac{n\frac{\beta_n}{p}}{\tau_n \frac{a}{p}} \cos\psi - \frac{\tau_n}{p} \sin\psi\right] \qquad (2.20a)$$

$$B_n^{1} = - K_n^{1}\left(\tau_n \frac{a}{p}\right) \frac{\tau_n a}{p} j l l n \cos\psi \qquad (2.20b)$$

$$A_n^{o} = A_n^{i} \frac{I_n\left(\tau_n \frac{a}{p}\right)}{K_n\left(\tau_n \frac{a}{p}\right)} \qquad (2.20c)$$

$$B_n^{o} = B_n^{i} \frac{I_n^{1}\left(\tau_n \frac{a}{p}\right)}{K_n^{1}\left(\tau_n \frac{a}{p}\right)} \qquad (2.20d)$$

where use of the Wronskian, $I_n^{1}(x)\, K_n(x) - I_n(x)\, K_n^{1}(x) = \frac{1}{x}$, was made.

The component of electric field parallel to the helix may now be written as

$$E_{ll} = \sum_{n=-\infty}^{\infty} E_{lln} \tag{2.21}$$

where

$$E_{lln} = E_{zn} \sin \psi + E_{\phi n} \cos \psi \tag{2.22}$$

If Equations (2.8), (2.10) and (2.20) are substituted into Equation (2.22), E_{lln} is obtained viz.

$$E_{lln} = \frac{i\, e^{-i \frac{\beta}{p} z}\, e^{-i \frac{n}{p} \zeta} \sin^2 \psi}{\omega \epsilon a} \quad jlln \left\{ I_n K_n \left[\left(\frac{\tau_n \alpha}{p} \right)^2 + \left(\frac{n \beta_n a}{p \frac{\tau_n \alpha}{p}} \right)^2 \right] \operatorname{ctn}^2 \psi \right.$$

$$\left. -2n \frac{\beta_n \alpha}{p} \operatorname{ctn} \psi \right] + k^2 a^2 I_n^1 K_n^1 \operatorname{ctn}^2 \psi \Bigg\} \tag{2.23}$$

If Equation (2.23) is substituted in Equation (2.21) and E_{ll} set equal to zero along the center line of the tape, i.e., $\zeta = 0$, then the determinantal equation for β is obtained

$$0 = \frac{ie^{-i\frac{\beta}{\bar{p}}z} J \sin^2\psi}{\omega\epsilon ap} \sum_{n=-\infty}^{\infty} \left\{ I_n K_n \left[\left(\frac{\tau_n a}{\bar{p}} \right)^2 + \left(\frac{\frac{n\beta_n a}{\bar{p}}}{\frac{\tau_n a}{\bar{p}}} \right)^2 \operatorname{ctn}^2\psi - 2n\frac{\beta_n a}{\bar{p}} \operatorname{ctn}\psi \right] \right.$$

$$\left. + k^2 a^2 I_n^1 K_n^1 \operatorname{ctn}^2\psi \right\} \frac{\sin\frac{\beta_n \delta}{2\bar{p}}}{\frac{\beta_n \delta}{2\bar{p}}} \qquad (2.24)$$

Equation (2.24) has been found by Sensiper[7]. It was reproduced here using the concept of generalized periodicity. The factor outside the summation cannot be zero. Therefore both sides of Equation (2.24) may be divided by the non-zero factor. If the following relations among the Bessel functions

$$I_n(x)\, K_n(x) = \frac{-x^2}{4n^2} \left[I_{n-1} K_{n-1} + I_{n+1} K_{n+1} - I_{n-1} K_{n+1} - I_{n+1} K_{n-1} \right]$$

$$I_n^1(x)\, K_n^1(x) = -\frac{1}{4} \left[I_{n-1} K_{n-1} + I_{n+1} K_{n+1} + I_{n-1} K_{n+1} + I_{n+1} K_{n-1} \right]$$

are substituted into Equation (2.24), one obtains

$$0 = \sum_{n=-\infty}^{\infty} \left[\left(\frac{\beta^2}{\bar{p}^2} - k^2 \right) a^2 I_n K_n - \frac{k^2 a^2}{2} \operatorname{ctn}^2\psi \left(I_{n-1} K_{n-1} + I_{n+1} K_{n+1} \right) \right] D_n \qquad (2.25)$$

where

$$D_n = \frac{\sin \frac{\beta_n \delta}{2\bar{p}}}{\frac{\beta_n \delta}{2\bar{p}}}$$

The argument of each IK product in Equations (23, 24 and 25) is $\tau_n \frac{a}{\bar{p}}$.

If

$$A_i = \sum_{n=-\infty}^{\infty} I_{n+1}\left(\tau_n \frac{a}{\bar{p}}\right) K_{n+1}\left(\tau_n \frac{a}{\bar{p}}\right) D_n$$

then Equation (2.25) may be written as

$$\frac{\beta^2 - \frac{k^2 \bar{p}^2}{\sin^2 \psi}}{k^2 \bar{p}^2 \operatorname{ctn}^2 \psi} = \frac{A_{+1} + A_{-1} - 2A_o}{2A_o} \qquad (2.26)$$

Equation (2.26) is the determinantal equation for the tape helix derived by assuming a surface current uniform across the tape with phase shift along the length of the tape. The form of Equation (2.26) is suitable for studying the behavior of β as a function of k.

2.3 Derivation by Transform Techniques

In this section the integral equation for the electric field on an infinite helix is derived. The determinantal equation is then obtained by taking the Fourier transform of the electric field along the helix.

A current $I(\phi)$ is assumed along the center line of the helix and then the electric field is calculated by finding first the vector potential

$$\bar{A} = \frac{\mu}{4\pi} \int \bar{I} \frac{e^{-ikR}}{R} \, dL \tag{2.27}$$

and second the electric field

$$\bar{E} = - i\omega\bar{A} + \frac{\text{grad div } \bar{A}}{i\omega\mu\epsilon} \tag{2.28}$$

The calculation gives

$$\bar{E} = \frac{-i\omega\mu}{4\pi} \int \bar{I} \frac{e^{-ikR}}{R} \left[1 - \frac{1}{k^2R} (ik + \frac{1}{R})\right] dL$$

$$+ \frac{i\omega\mu}{4\pi} \int \bar{I} \hat{a}_R \hat{a}_R \frac{e^{-ikR}}{R} \left[1 - \frac{3}{k^2R} (ik + \frac{1}{R})\right] dL \tag{2.29}$$

where $\hat{a}_R$ is unit vector pointing toward the observation point from the source point. The component of electric field parallel to the center line is given by $E_{11} = \bar{E} \hat{a}_{11}$. On the surface of the cylinder

$$E_{11}(\phi,\zeta) = \frac{-i\omega\mu}{4\pi(a^2+\bar{p}^2)^{1/2}} \left\{ \int_{-\infty}^{\infty} I(\phi^1) \left[a^2 \cos(\phi-\phi^1) + \bar{p}^2\right] f_1(R) \, d\phi^1 \right.$$

$$\left. - \int_{-\infty}^{\infty} I(\phi^1) \frac{\left\{a^2 \sin(\phi-\phi^1) + \bar{p}^2 [\phi-\phi^1+\zeta]^2\right\}^2}{R^2} f_2(R) \, d\phi^1 \right\} \tag{2.30}$$

$$R^2 = 2a^2 [1 - \cos(\phi - \phi^1)] + \bar{p}^2 (\phi - \phi^1 + \zeta)^2$$

$$f_1(R) = \frac{e^{-ikR}}{R} \left[1 - \frac{1}{k^2 R} (ik + \frac{1}{R})\right]$$

$$f_2(R) = \frac{e^{-ikR}}{R} \left[1 - \frac{3}{k^2 R} (ik + \frac{1}{R})\right]$$

$$f = \frac{\zeta}{\bar{p}}$$

$$\bar{p} = \frac{p}{2\pi}$$

The expression may be written as

$$E_{11}(\phi, \zeta) = \frac{-i\omega\mu}{4\pi k^2 (a^2 + \bar{p}^2)^{1/2}} \int_{-\infty}^{\infty} I(\phi^1) \left\{ \frac{\partial^2}{\partial \phi^{12}} + k^2 [a^2 \cos(\phi - \phi^1) + \bar{p}^2] \right\} \frac{e^{-ikR}}{R} d\phi^1 \tag{2.31}$$

and, integrating by parts twice, the differentiation may be thrown over to the current as

$$E_{11}(\phi, \zeta) = \frac{-i\omega\mu}{4\pi k^2 (a^2 + \bar{p}^2)^{1/2}} \int_{-\infty}^{\infty} \left\{ \frac{\partial^2 I(\phi^1)}{\partial \phi^{12}} + k^2 I(\phi^1) [a^2 \cos(\phi - \phi^1) + \bar{p}^2] \right\} \frac{e^{-ikR}}{R} d\phi^1 \tag{2.32}$$

where I and $\frac{dI}{d\phi^1}$ at $\pm \infty$ are zero.

Equation(2.31) is written symbolically as

$$E_{11}(\phi, \zeta) = \int_{-\infty}^{\infty} I(\phi^1) \, Z(\phi - \phi^1, \zeta) d\phi^1 \tag{2.33}$$

The Fourier Transform may easily be taken since the integral is of the convolution type. The transform, denoted by $\tilde{}$, with respect to ϕ

$$\tilde{E}(\beta,\zeta) = \tilde{I}(\beta)\ \tilde{Z}(z,\zeta) \tag{2.34}$$

β is the transform variable and ζ is to be treated as a parameter. If the factor $\frac{-i\omega\mu}{4\pi(a^2+R^2)^{1/2}}$ is ignored and $z = \bar{p}\,\phi$ in the non-periodic part, $Z(\phi,\zeta)$ may be written as

$$Z(\phi,z,\zeta) = [a^2\cos\phi + \bar{p}^2]\ \frac{e^{-ikR}}{R} + \left(\frac{\bar{p}}{k}\right)^2 \frac{d^2}{dz^2}\ \frac{e^{-ikR}}{R} \tag{2.35}$$

Note that when a derivative with respect to z is taken, ϕ is a function of z. Now $Z(\phi,z,\zeta)$ is periodic in ϕ with period 2π. If $Z(\phi,z,\zeta)$ is expanded in a Fourier series with z and ζ as parameters the result is

$$Z(\phi,z,\zeta) = \sum_{n=-\infty}^{\infty} z_n(z,\zeta)\ e^{in\phi} \tag{2.36}$$

where

$$Z_n(z,\zeta) = \frac{1}{2\pi}\int_0^{2\pi} Z(\phi,z,\zeta)\ e^{-in\phi}d\phi \tag{2.37}$$

If z is replaced by $\bar{p}\phi$ in Equation (2.36) the result is

$$Z(\phi,\bar{p}\phi,\zeta) = \sum_{n=-\infty}^{\infty} Z_n(\bar{p}\phi,\zeta)\ e^{in\phi}$$

If the Fourier Transform of $Z_n(\bar{p}\phi,\zeta)$ with respect to ϕ is $\tilde{Z}_n(\beta,\zeta)$ the transform of $Z(\phi,\bar{p}\phi,\zeta)$ is

$$\tilde{Z}(\beta,\zeta) = \sum_{n=-\infty}^{\infty} \tilde{Z}_n(\beta+n) \tag{2.38}$$

with

$$\tilde{Z}_n(\beta,\zeta) = \frac{1}{2\pi} \int_{-\infty}^{\infty} Z_n(\bar{p}\phi,\zeta)\, e^{i\beta\phi} d\phi \tag{2.39}$$

If $Z_n(\bar{p}\phi,\zeta)$ is replaced by using Equation (2.37) one obtains, after an interchange in the order of integration,

$$\tilde{Z}_n(\beta,\zeta) = \left(\frac{1}{2\pi}\right)^2 \int_0^{2\pi} e^{-in\phi^1} d\phi^1 \int_{-\infty}^{\infty} Z(\phi^1,\bar{p}\phi,\zeta) e^{i\beta\phi} d\phi \tag{2.40}$$

The integration with respect to ϕ may now be effected by

$$\int_{-\infty}^{\infty} \frac{e^{-ik(g^2+\sigma^2)^{1/2}}}{2(g^2+\sigma^2)^{1/2}}\, e^{2\beta g} dg = K_o[\sigma(\beta^2-k^2)^{1/2}] \tag{2.41}$$

using Campbell and Foster[27] pair 917.

Making the change of variable $\alpha = \phi + \frac{\zeta}{\bar{p}}$ in Equation (2.35) results in

$$Z(\phi^1, \alpha) = [a^2 \cos \phi^1 + \bar{p}^2] \frac{e^{-ikR}}{R} + \frac{1}{k^2} \frac{\partial^2}{\partial \alpha^2} \frac{e^{-ikR}}{R}$$

$$\text{with} \quad R^2 = 2a^2 (1 - \cos \phi^1) + (\bar{p}\alpha)^2$$

The interesting integral in Equation (2.40) is

$$\int_{-\infty}^{\infty} \frac{e^{-ikR}}{R} \, e^{i\beta(\alpha - \frac{\zeta}{\bar{p}})} \, d\alpha \tag{2.42}$$

which is equal to

$$\frac{2}{\bar{p}} \, e^{-i\beta \frac{\zeta}{\bar{p}}} \, K_o \left[\sigma(\beta^2 - \bar{p}^2 k^2)^{1/2}\right]$$

where

$$\sigma^2 = 2 \left(\frac{a}{\bar{p}}\right)^2 (1 - \cos \phi^1)$$

The inner integral in Equation (2.40) is

$$\frac{2}{\bar{p}} \, e^{-i\beta \frac{\zeta}{\bar{p}}} \, K_o \left[\sigma(\beta^2 - \bar{p}^2 k^2)^{1/2}\right] \left[a^2 \cos \phi^1 + p^2 - \frac{\beta^2}{k^2}\right] \tag{2.43}$$

Now from Erdelyi[28] p. 102 No. 35, K_o is expanded as

$$K_o(w) = I_o(z) \, K_o(z) + 2 \sum_{n=1}^{\infty} I_n(z) \, K_n(z) \cos n\phi \tag{2.44}$$

where

$$w = \sqrt{2} \, a \, (1 - \cos \phi)^{1/2}$$

If

$$w = \sqrt{2}\, z\, (1 - \cos\phi)^{1/2} (\beta^2 - \bar{p}^2 k^2)^{1/2}$$

then z is

$$z = \frac{a}{\bar{p}} (\beta^2 - \bar{p}^2 k^2)^{1/2}$$

If Equation (2.44) is substituted into integral (2.40) and integrated, the result for $\tilde{Z}_n(\beta,\zeta)$ is

$$\tilde{Z}_n(\beta,\zeta) = a^2 e^{-i\beta \frac{\zeta}{\bar{p}}} \frac{2}{\bar{p}} [I_{n+1}K_{n+1} + 2BI_nK_n + I_{n-1}K_{n-1}] \qquad (2.45)$$

where

$$B = \frac{1}{a^2} (\bar{p}^2 - \frac{\beta^2}{k^2})$$

and all arguments are

$$\frac{a}{\bar{p}} (\beta^2 - \bar{p}^2 k^2)^{1/2}$$

Therefore from Equations (2.38) and (2.45) $\tilde{Z}(\beta,\zeta)$ is

$$\tilde{Z}(\beta,\zeta) = \frac{2a^2}{\bar{p}} \sum_{n=-\infty}^{\infty} e^{-i(\beta+n)\frac{\zeta}{\bar{p}}} [I_{n+1}K_{n+1}(\tau_n) + 2BI_nK_n(\tau_n) + I_n K_{n-1}(\tau_n)] \qquad (2.46)$$

where

$$\tau_n = \frac{a}{\bar{p}} [(\beta+n)^2 - \bar{p}^2 k^2]^{1/2}$$

Now if the boundary condition on $E_{11}(\phi_1\zeta)$ is that the average of the electric field with respect to ζ be zero for all ϕ, then the condition of $\tilde{Z}(\beta,\zeta)$ is

$$\frac{1}{\delta}\int_{-\delta/2}^{\delta/2} \tilde{Z}\ (\beta,\zeta)\ d\zeta = 0 \tag{2.47}$$

The result of Equation (2.47) yields the determinantal equation, viz.

$$0 = \frac{2a^2}{\bar{p}}\delta \sum_{n=-\infty}^{\infty} [I_{n+1}K_{n+1}\ (\tau_n) + 2B\ I_nK_n(\tau_n) + I_{n-1}K_{n-1}(\tau_n)]\ D_n \tag{2.48}$$

where

$$D_n = \frac{\sin\ (\beta+n)\ \frac{\delta}{2\bar{p}}}{(\beta+n)\ \frac{\delta}{2\bar{p}}}$$

If

$$A_i = \sum_{n=-\infty}^{\infty} I_{n+1}\ (\tau_n)\ K_{n+i}\ (\tau_n)\ D_n$$

Equation (2.48) may be written as

$$\frac{\beta^2 - \frac{k^2\bar{p}^2}{\sin^2\psi}}{k^2\bar{p}^2\ \mathrm{ctn}^2\psi} = \frac{A_{+1} + A_{-1} - 2A_o}{2A_o} \tag{2.49}$$

Equation (2.49), derived by transform techniques, is the same as Equation (2.26)

derived by applying boundary conditions. Patton[12] obtained the determinantal equation for the round wire version of the helix by using the transform techniques. The approximations used for the round wire version were that the current is concentrated in a filament at the center of the wire and that the electric field is zero on a line which is either the smallest or largest distance from the z axis. The transform technique had not previously been applied to the tape helix. The approximations used were that the current is concentrated in a filament at the center of the tape and that the average of the electric field over the tape is zero.

2.4 Interpretation of the Determinantal Equation as a Complex-Valued Equation

In addition to the real valued solutions for the determinantal equation found by Sensiper[7] it will be shown in Chapter 4 that there exist solutions where the phase constant, β, is complex-valued if the determinantal equation is interpreted as a complex-valued equation. The interpretation of the determinantal equation as a complex-valued equation is now considered.

If there exists a solution for β which is complex-valued, then the arguments, τ_m, of the $I_n K_n$ products are complex-valued since

$$\tau_m = [(\beta+m)^2 - \bar{p}^2 k^2]^{1/2} \frac{a}{\bar{p}}$$

The question of which branch of the square root to choose for τ_m will be discussed shortly. Again consider the determinantal equation. If the arguments of the IK products are complex-valued, then the IK products are

complex-valued. It is seen that if β is complex-valued then τ is complex-valued and then, in turn, the $I_n K_n$ products are complex-valued. Each side of the determinantal equation, Equation (2.49) is complex-valued. It remains, of course, to show that there exist solutions for β which are complex-valued. This will be done.

Which branch of the square root for τ_m should be chosen? If τ_n written as

$$\tau_n = (\tau_n^2)^{1/2} = |\tau_n| e^{i\theta_n} = \tau_{nr} + i\,\tau_{ni}$$

where

$$\theta_n = \tan^{-1} \frac{\tau_{ni}}{\tau_{nr}}$$

the question is reduced to choosing the appropriate the branch of the arc tangent for θ_n. One set of solutions of the determinantal equation was found choosing the principle value of the arc tangent for each θ_n. A second set of solutions was found by adding $\pm \pi$ to the principle value of the arc tangent for θ_{-1} and choosing the principle value of the arc tangent for θ_n, $n \neq -1$. The + or - sign is chosen to make $|\arg \tau_{-1}| \leq \pi$. A third set of solutions was found by adding $\pm \pi$ to the principle value of the arc tangent of both θ_{-1} and θ_{-2} and choosing the principle value of the arc tangent for θ_n, $n \neq -1, -2$. The + or - sign is chosen to make $|\arg \tau_{-1}| \leq \pi$, $n = -1, -2$. For a set of solutions each argument is treated as a continuous function of k. To understand this continuous treatment consider

$$\tau_{-1} = \left[(\beta_r - 1)^2 - (k^2 + \beta_1^2) + 2i\,\beta_1 (\beta_r - 1) \right]^{1/2} \frac{a}{p}$$

with

$$2\theta_{-1} = \tan^{-1} \frac{2\,\beta_i(\beta_r-1)}{(\beta_r-1)^2-(\bar{k}^2+\beta_i^2)}$$

where

$$\tau_{-1} = |\tau_{-1}|\, e^{i\theta_{-1}}, \quad \bar{k} = k\,\tilde{p}$$

and

$$\beta = \beta_r + i\,\beta_i$$

Suppose the k-β diagram has a solution $\bar{k} = \beta_r \sin\psi$ with $\beta_i < 0$ and small. Figure 2.2a and 2b shows the k-β diagram. The salient features of the locus of τ_{-1}^2 as a function of $\bar{k}$ are shown in Figure 2.3. For $k > 0$ and small the real part of τ_{-1}^2 is positive since $(\beta_r-1)^2 > \bar{k}^2 + \beta_i^2$. The imaginary part of τ_{-1}^2 is also positive since $\beta_i(\beta_r-1)$ is positive. With both the real and imaginary parts of τ_{-1}^2 positive the τ_{-1}^2 as a function of $\bar{k}$ lies in the first quadrant. The locus remains in the first quadrant until a value of $\bar{k}$ is reached such that

$$(\beta_r-1)^2 = \bar{k}^2 + \beta_i^2$$

This value of $\bar{k}$ is approximately $\bar{k} = 1-\beta_r$ since β_i is small. As $\bar{k}$ is increased the locus enters the second quadrant to remain until

$$\bar{k} = \sin\psi, \text{ i.e. } \beta_r = 1$$

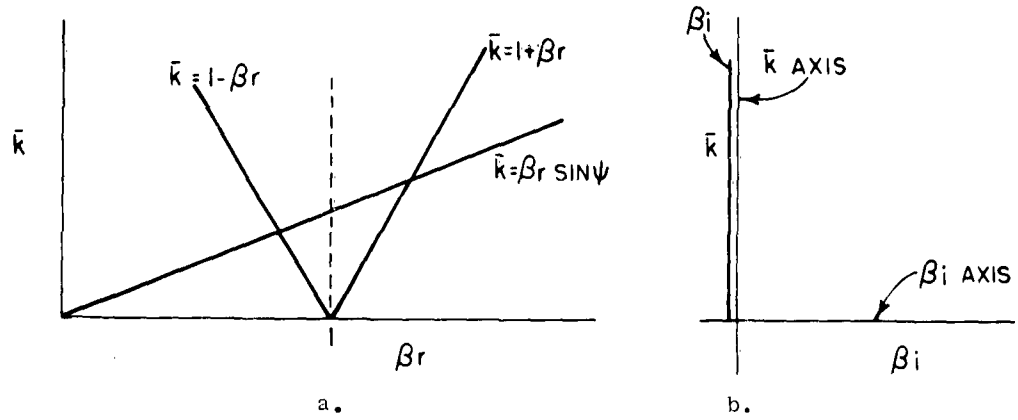

Figure 2.2. A k - ß diagram for consideration of τ_{-1}.

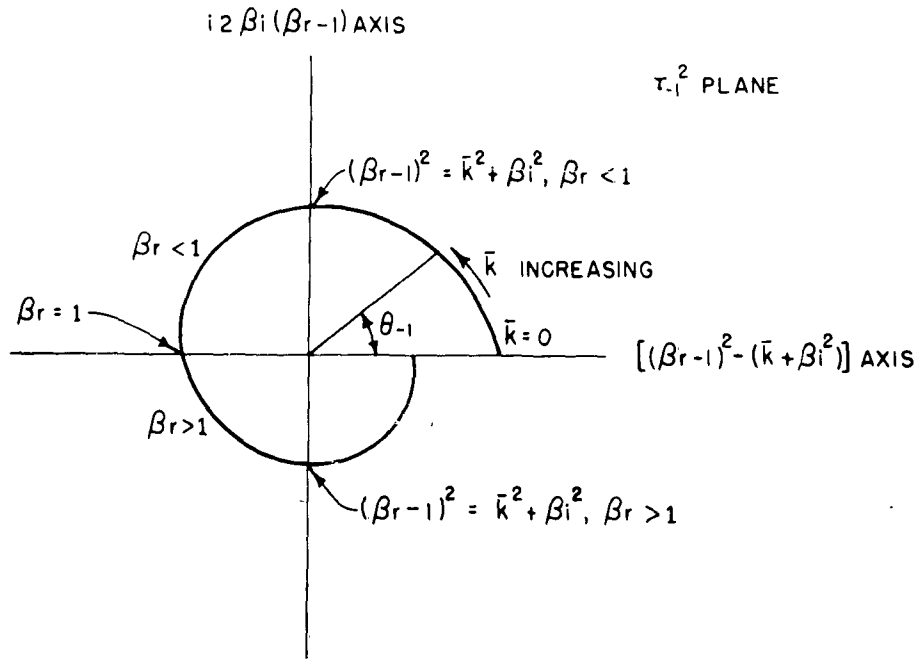

Figure 2.3. The continuous locus in the τ_{-1}^2 plane.

Now as $\bar{k}$ is increased the locus of T_{-1}^2 enters the third quadrant since $\beta_i < 0$ and $\beta_r - 1 > 0$. As $\bar{k}$ is further increased $(\beta_r - 1)^2 = \bar{k}^2 + \beta_i^2$ and the locus leaves the third quadrant.

Now for $\bar{k}$ increasing the locus enters the fourth quadrant since $(\beta_r - 1)^2 > \bar{k}^2 + \beta_i^2$ and $\beta_i < 0$. The other arguments are treated similarly as continuous functions.

2.5 Summary

The same determinantal equation for the tape helix has been derived by two methods making slightly different assumptions. In the derivation by matching boundary conditions a uniform current over the entire width of the tape was assumed. For the derivation by Fourier Transforms a current was concentrated in a filament in the center line of the helix, and E_{11} on the tape was averaged to zero.

If the phase constant β is complex-valued then the determinantal equation is complex-valued. Further, if the phase constant is complex-valued one knows how the arguments of the IK products can be treated as continuous functions. The determinantal equation is now ready for study.

3. STUDY OF TWO SIMPLIFIED EQUATIONS

3.1 Introduction

The determinantal equation, Equation (2.26), is somewhat complex as well as being complex valued if the phase constant, β, is complex valued. It will be instructive to study two simplified equations so that one will gain an insight into the behavior of the determinantal equation. This study will be done in the next two sections.

3.2 The First Simplified Equation

The determinantal equation with $\bar{k} = k\bar{p}$ may be written as

$$\frac{\beta^2 - \dfrac{\bar{k}^2}{\sin^2\psi}}{\bar{k}^2 \operatorname{ctn}^2\psi} = \frac{\sum_{n=-\infty}^{\infty} \left[I_{n+1}K_{n+1}(\tau_n) + I_{n-1}K_{n-1}(\tau_n) - 2\, I_nK_n(\tau_n) \right] D_n}{2 \sum_{n=-\infty}^{\infty} I_nK_n(\tau_n)\, D_n} \tag{3.1}$$

where

$$\tau_n = \frac{a}{\bar{p}} \left[(\beta+n)^2 - \bar{k}^2 \right]^{1/2}$$

and

$$D_n = \frac{\sin (\beta+n) \dfrac{\delta}{2\bar{p}}}{(\beta+n) \dfrac{\delta}{2\bar{p}}}$$

The I_nK_n products all have branch points at the origin. To see this consider

a small argument approximation[28] for the hyperbolic Bessel functions. For $|z| \ll 1$

$$I_n(z) \simeq \left(\frac{z}{2}\right)^n \frac{1}{n!} \quad , \; n \neq 0$$

$$I_o(z) \simeq 1, \; K_o(z) \simeq -\ln \frac{z}{2}$$

$$K_n(z) = (-1)^{n+1}\left(\frac{z}{2}\right)^n \ln \frac{z}{2} + \frac{1}{2}\left(\frac{2}{z}\right)^n (n-1)! + 0\left[\left(\frac{2}{z}\right)^{n-2}\right], \; n \neq 0$$

if

$$n \neq 0$$

$$\lim_{\tau_m \longrightarrow 0} I_n(\tau_m)K_n(\tau_m) = \frac{1}{2n} \quad , \text{ a constant}$$

However, the first term in the small argument approximation for $K_n(z)$ is logarithmic and has branch point at the origin. This branch point remains, although in the limit as $z \longrightarrow 0$ the term containing the logarithmic factor tends to zero. For $n = 0$ the $\lim_{\tau_m \longrightarrow 0} I_o(\tau_m)K_o(\tau_m)$ has logarithmic character. Consequently, if the argument of I_oK_o is small, that term will make a substantial contribution to the determinantal equation.

If one inspects τ_{-1}

$$\tau_{-1} = \frac{a}{p}\left[(\beta_r-1)^2-(\beta_i^2+\bar{k}^2)+i2\beta_i(\beta_r-1)\right]^{1/2}$$

where $\beta = \beta_r + i\beta_i$, it is seen that in the region where β_r is near unity τ_{-1} will change rapidly. These facts that τ_{-1} changes rapidly when β_r is near unity and that if the argument of $I_o K_o$ will make a substantial contribution to the determinantal equation, suggest that a simplified equation that would behave like the determinantal equation near $\beta_r = 1$ would be obtained by replacing the sum in the numerator of Equation (3.1) by

$$I_o K_o(\tau_{-1}) + I_2 K_2(\tau_{-1}) - 2 I_1 K_1(\tau_{-1})$$

Inspection of the denominator of Equation (3.1) shows that the denominator is slowly varying with β. This additional result leads one to the following simplified equation

$$\frac{\beta^2 - \frac{\bar{k}^2}{\sin^2\psi}}{\bar{k}^2 \cos^2\psi} = \frac{I_o K_o(\tau_{-1}) + I_2 K_2(\tau_{-1}) - 2 I_1 K_1(\tau_{-1})}{A} \qquad (3.2)$$

where A is a parameter.

The parameter A is picked to be about equal to $2A_o$ for the values of the helix parameter studied.

As the tape is made more narrow the sum A_o increases.

The solutions for β as a function of k are shown in Figures 3.1a through 3.10b for various values of A. The real and imaginary parts of the phase constant are given on individual figures with the real part as a function of $\bar{k}$ on the figures with suffix "a" and the imaginary part as a function of $\bar{k}$ on the figures with suffix "b".

The line $\bar{k} = \beta_r \sin \Psi$ is shown on all the $\bar{k} - \beta_r$ planes. The line separates the $\bar{k} - \beta_r$ plane into two regions, one the region above the line $\bar{k} = \beta_r \sin \Psi$ where the solutions correspond to fast waves, i.e. waves which have a phase constant corresponding to a phase velocity greater than velocity of light, and two the region below the line where the solutions correspond to slow waves, i.e., waves which have a phase constant corresponding to a phase velocity less than the velocity of light. The lines $\beta_r = 1 \pm \bar{k}$ are also shown on the $\bar{k} - \beta_r$ planes. Inside the "v" shaped region formed by the lines $\beta_r = 1 \pm \bar{k}$ the argument τ_{-1} has non-zero imaginary part. Outside the "v" shaped region formed by the lines $\beta_r = 1 \pm \bar{k}$ the argument τ_{-1} may have zero imaginary part.

The immediate observation upon examining Figures 3.7a and 3.7b is that for fixed $\bar{k}$ there are several values of β. Some of the solutions correspond to choosing $+ \tau_{-1}$ as the argument of the IK products and others to choosing $- \tau_{-1}$. The solutions are named mode 1, mode 2 and mode 3 with the determination of the argument for mode 1 as $+ \tau_{-1}$ and the determination of the argument for mode 2 and mode 3 as $- \tau_{-1}$. Let $\bar{k}_{c1}$ be the smallest value of $\bar{k}$ such that mode 1 has a solution for β with a non-zero imaginary part.

The mode 1 solution for $\bar{k} < \bar{k}_{c1}$ agrees with the solution shown by Sensiper[7] for the real valued determinantal equation. The mode 2 solution also agrees with the solution found by Sensiper.

The character of the solution is different depending on whether the parameter A is greater than A_{c1} or less than A_{c1}. The mode 1 solution for $\bar{k} > \bar{k}_{c1}$ is typical of the solutions when $A > A_{c1}$ where A_{c1} will be defined later. The only necessary information now is that A used in Figures 3.7a

and 3.7b satisfies $A > A_{cl}$. Note that real part of the mode 1 solution is not on the $\bar{k} = \beta_r \sin \Psi$ line which represents a solution corresponding to the velocity of light. As $\bar{k}$ is increased from $\bar{k}_{cl}$ it is seen that β_i increases very fast as a function of $\bar{k}$. The imaginary part of β for mode 3 is larger than the corresponding solution for mode 1. A wave with this attenuation would decay rapidly. Consider the results for $A = 1.0$ shown in Figures 3.2a and 3.2b.

The solutions with zero imaginary parts, mode 2 and mode 1 with $\bar{k} < \bar{k}_{cl}$, are similar to the corresponding solutions where $A = 3.0$. This similarity, however, is not found for the solutions with non-zero imaginary parts. The behavior is considerably different than when $A > A_{cl}$. The fact that there is a considerable difference in behavior of the solutions for $A < A_{cl}$ and $A > A_{cl}$ leads to the obvious definition for A_{cl}. The value A_{cl} is that value of the parameter A in Equation (3.2) that separates the values of A into two sets, one set, $A > A_{cl}$, such that the solutions have the character similar to that shown in Figures 3.7a and 3.7b and the other set, $A < A_{cl}$, such that the solutions have the character similar to that shown in Figures 3.2a and 3.2b. The outstanding difference in the behavior for $A < A_{cl}$ and $A > A_{cl}$ may be observed by inspecting the imaginary part of the phase constant corresponding to mode 1. If $A > A_{cl}$ then $\beta_i > 0$ for all $\bar{k} > \bar{k}_{cl}$. If $A < A_{cl}$ then there exist regions where there exists no mode 1 solution for $\bar{k} > \bar{k}_{cl}$. The value $A = A_{cl}$ corresponds to a value $2A_o$ which, in turn, corresponds to a tape width δ that is larger than tape widths consistent with the narrow tape approximation. Therefore, no solutions of the determinantal equation in the region β_r near unity will correspond to the solutions given in Figures 3.2a and 3.2b. They are given

to assist in the understanding of this kind of equation. The strangest property of the solutions in Figures 3.2a and 3.2b is that in order to have a continuous solution, β as a function of $\bar{k}$, it is necessary to change branches of the argument at $\bar{k} = .273$ and $\bar{k} = .358$. These values of $\bar{k}$ correspond to values of $\beta_i = 0$.

The argument for the mode 1 solution corresponding to $\bar{k} = .372^-$ is $pe^{i\pi/2}$ where p is real. The argument for the mode 2 solution corresponding to $\bar{k} = .273^+$ is $pe^{i(\pi/2 - \pi)}$. The arguments are discontinuous by the amount π but the value of the right hand side of Equation (3.2) is the same for both arguments. The reason for this equality is not at first obvious. Now

$$I_o(ip)K_o(ip)+I_2(ip)K_2(ip)-2I_1(ip)K_1(ip)$$

is the complex conjugate of

$$I_o(-ip)K_o(-ip)+I_2(-ip)K_2(-ip)-2I_1(-ip)K_1(-ip)$$

for p real. In addition, the sum of the imaginary parts is zero for the value $\bar{k} = .273$. This may be seen easily from the fact that for $\bar{k} = .273$, $\beta_i = 0$, and therefore, the left hand side of Equation (3.2) has zero imaginary part. The right hand side also has zero imaginary part. The right hand sides for $\bar{k} = .273^-$ and $.273^+$ are complex conjugates and have zero imaginary parts, and therefore the right hand sides are equal. A similar situation occurs for $\bar{k} = .358$. Figures 3.6a and 3.6b show the results for a value of A near A_{c1}, A = 1.5.

Note that the difference in behavior of the solution for A = 1.0 and A = 1.5. Both A = 1.0 and A = 1.5 are less than A_{c1} since there exists a region of $\bar{k} > \bar{k}_{c1}$ where no solution for mode 1 exists. The real parts of the mode 1 solution are connected by a continuous solution of the other determination of the square root compared to the mode 1 solution for A = 1.5. However, for A = 1.0 the real parts of the mode 1 solution are not connected by a continuous solution. If Figures 3.2a through 3.6b are studied, it is seen that the change from connecting the real parts of the mode 1 solution by a continuous solution to not connecting the real parts takes place in a continuous manner. There is no question of discontinuity of the arguments since all the solutions have the same determination for the square roots. It is reiterated that this particular behavior will not be found in the determinantal equation since $A < A_{c1}$ corresponds to tapes which are too wide for the narrow tape approximation.

Figure 3.1a and 3.1b show the results for A = .9 and it is observed that the behavior of the solutions as a function of A is in a continuous manner.

Consider some of the general properties of the solutions for $A > A_{c1}$. (Inspect Figures 3.7a through 3.10b) Note that $\bar{k}_{c1}$ the lowest value of $\bar{k}$ for which mode 1 has a non-zero imaginary part, becomes greater as A is increased. Also for $\bar{k} > \bar{k}_{c1}$ the real part of β follows more closely to the $\bar{k} = \beta_r \sin \Psi$ line and follows for a greater range of $\bar{k}$ values. For the imaginary part the local maximum near $\bar{k}$ = .2 and the local minimum near $\bar{k}$ = .25 decrease as A increases. The values of β_1 for $.4 < \bar{k} < .5$ increase as A increases. For mode 2, the imaginary part increases as A

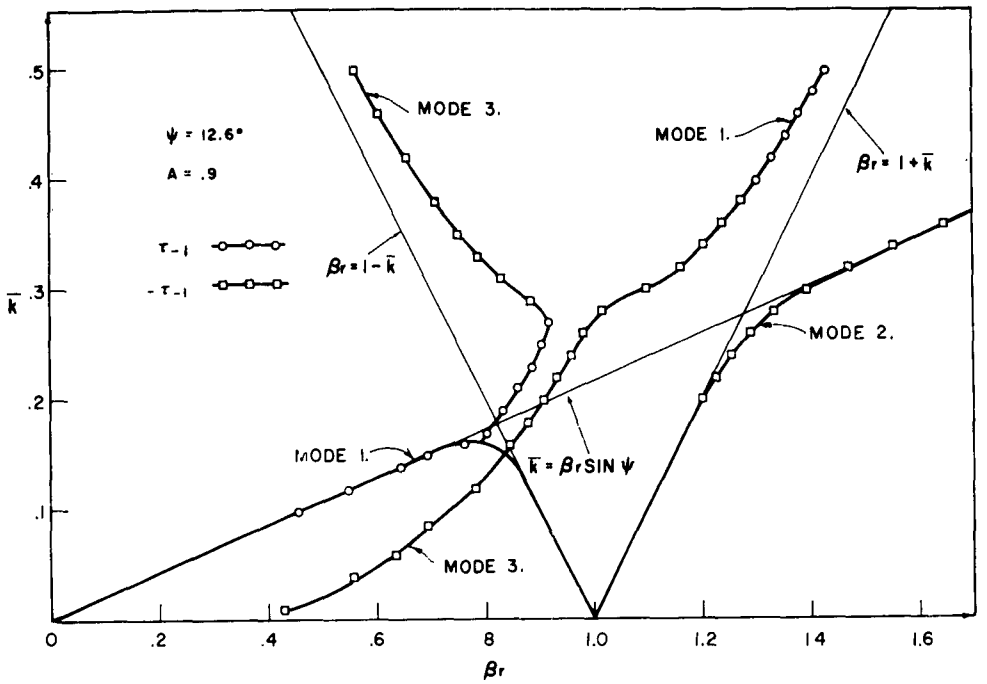

Figure 3.1a. The k - β_r diagram for simplified equation one; A = .9, $\psi^r = 12.6^o$.

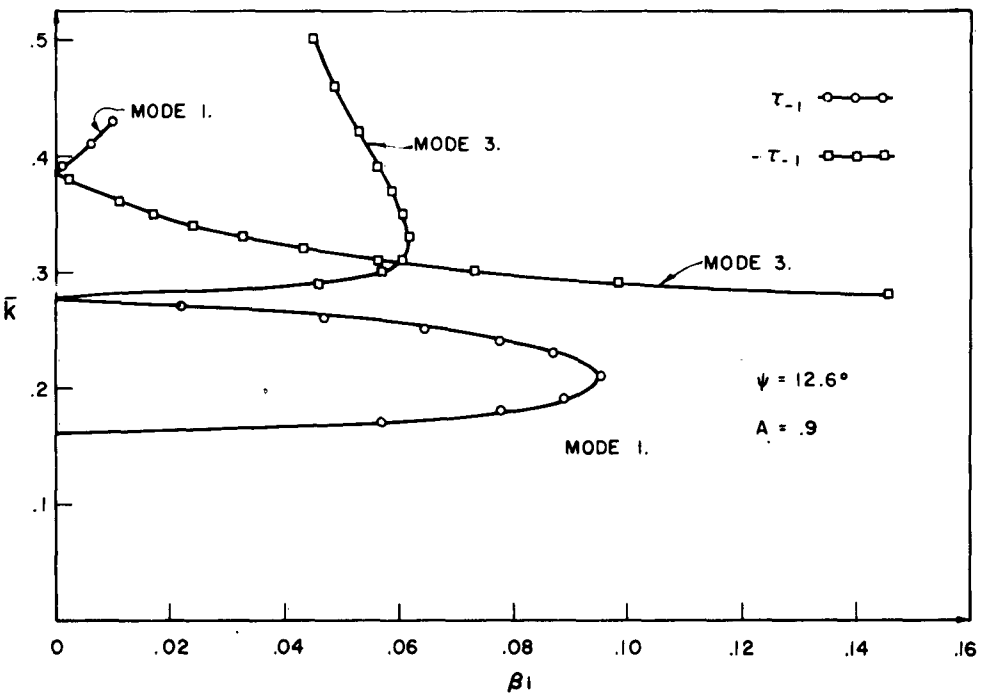

Figure 3.1b. The k - β_i diagram for simplified equation one; A = .9, $\psi^i = 12.6^o$.

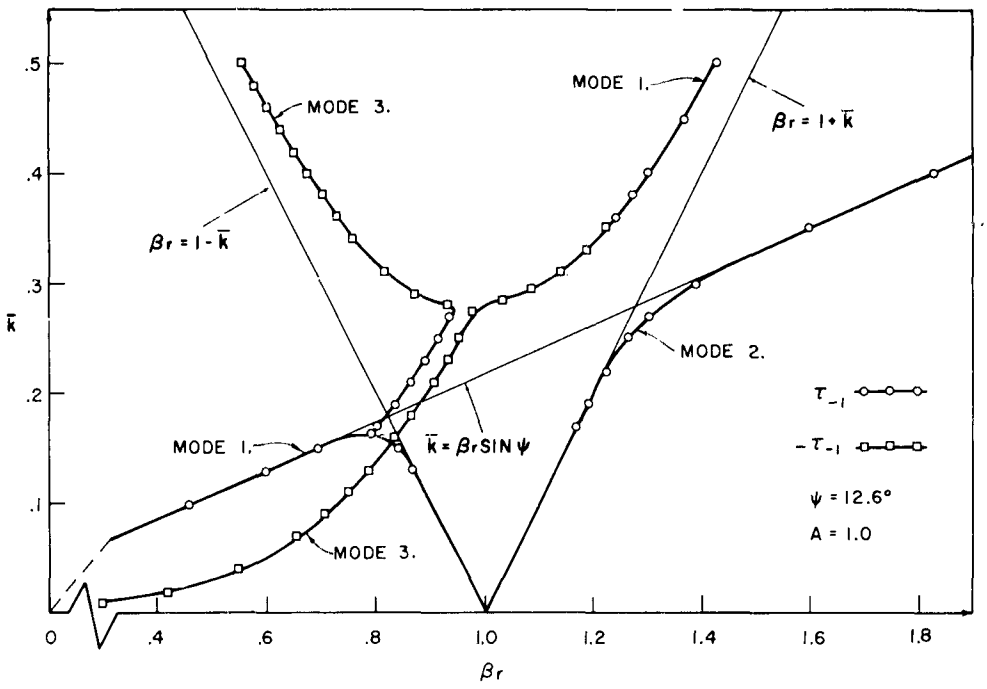

Figure 3.2a. The k - β_r diagram for simplified equation one; A = 1.0, ψ = 12.6°.

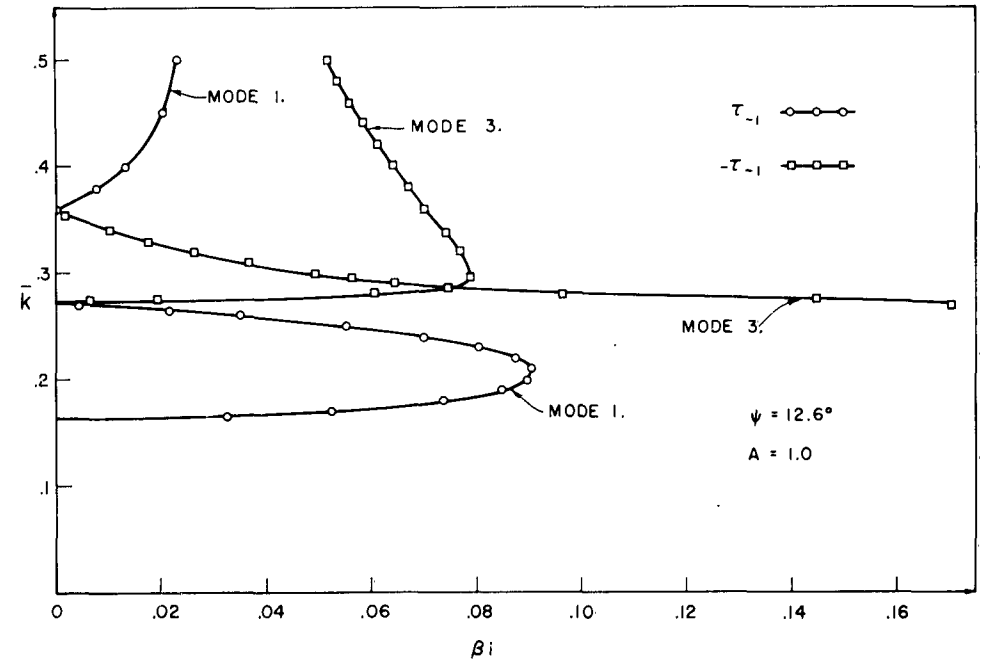

Figure 3.2b. The k - β_i diagram for simplified equation one; A = 1.0, ψ = 12.6°.

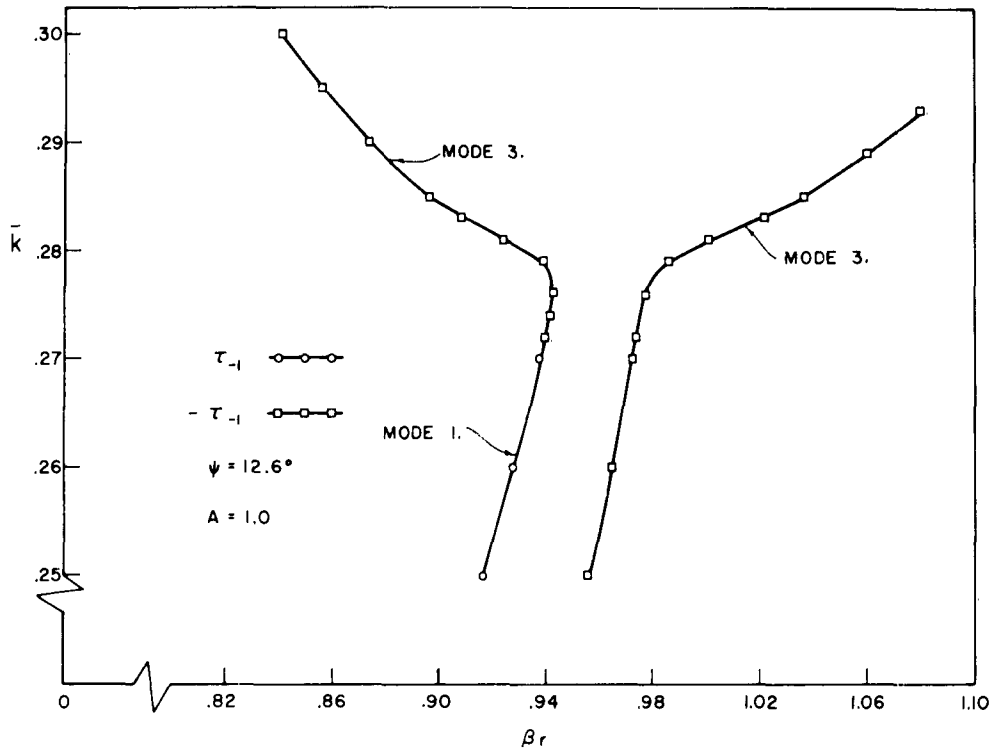

Figure 3.3a. The $\bar{k} - \beta_r$ diagram for simplified equation one expanded near $\bar{k} = .25$; $A = 1.0$, $\psi = 12.6^{\circ}$.

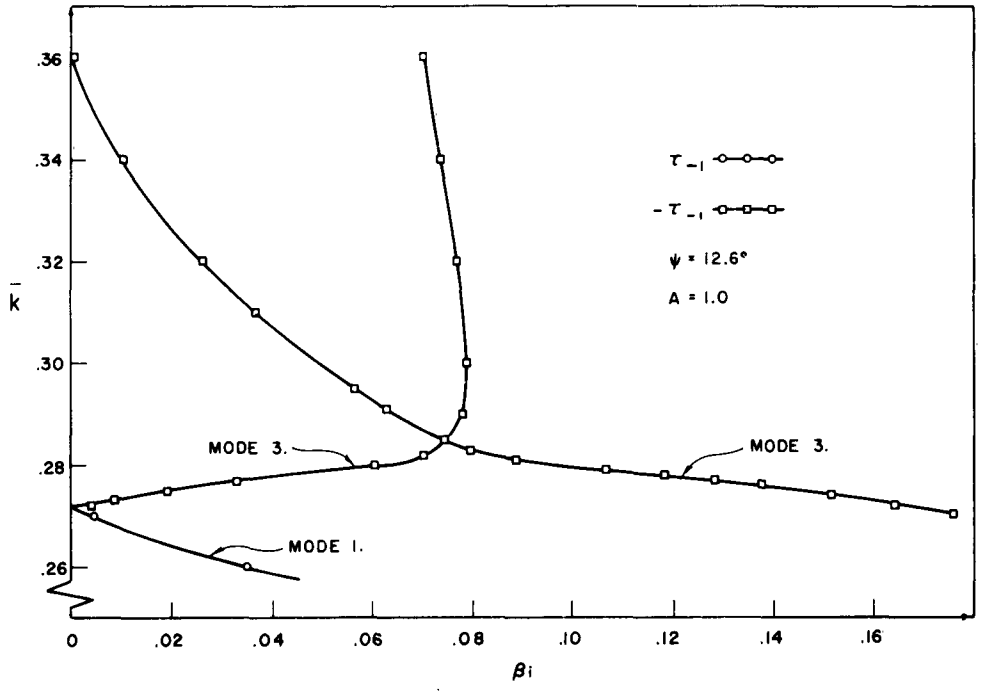

Figure 3.3b. The $\bar{k} - \beta_i$ diagram for simplified equation one expanded near $\bar{k} = .25$; $A = 1.0$, $\psi = 12.6^{\circ}$.

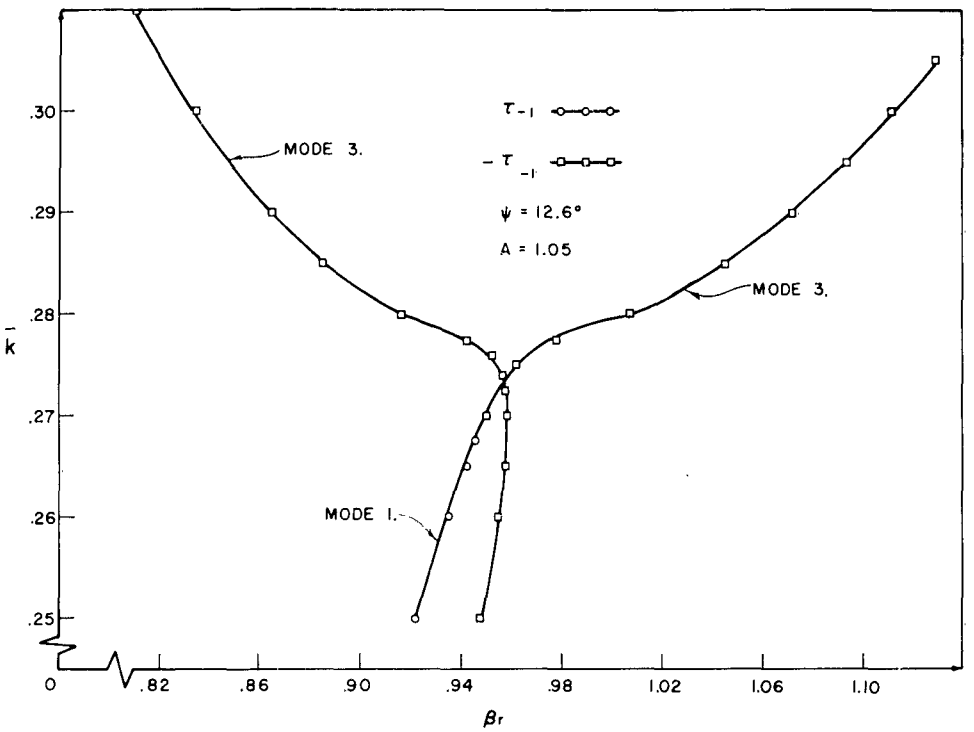

Figure 3.4a. The k - β_r diagram for simplified equation one expanded near k = .25, A = 1.05, $\Psi = 12.6^{\circ}$.

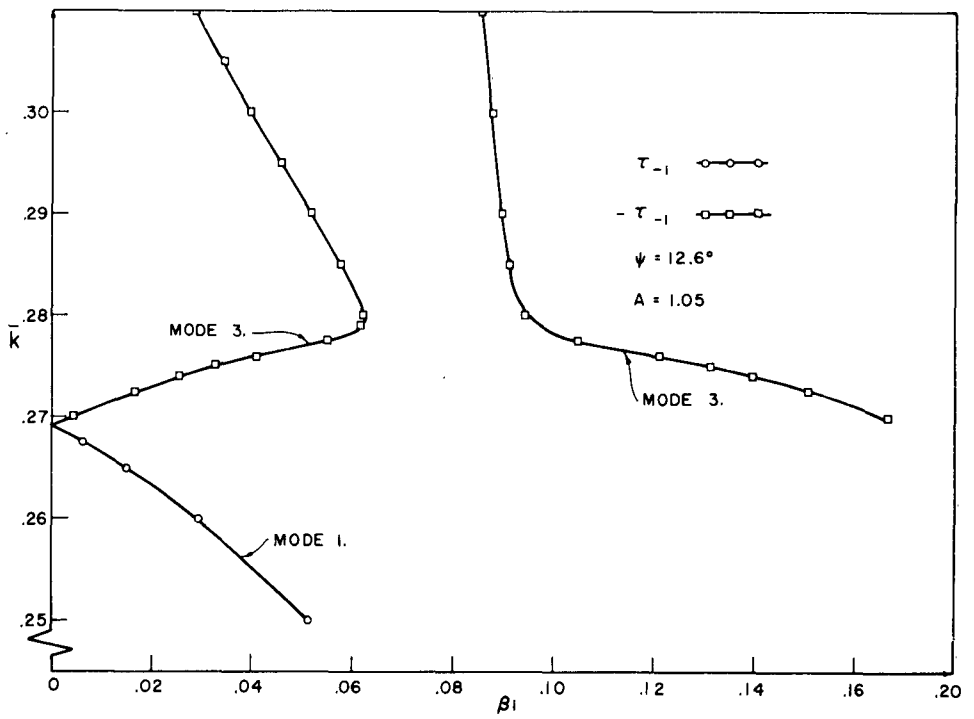

Figure 3.4b. The k - β_I diagram for simplified equation one expanded near k = .25; A = 1.05, $\Psi = 12.6^{\circ}$.

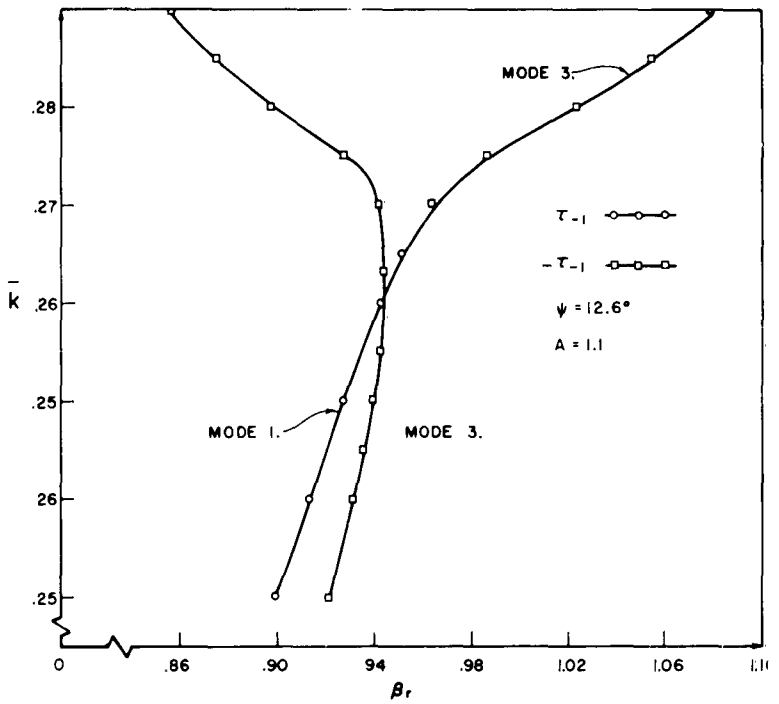

Figure 3.5a. The k - β_r diagram for simplified equation one expanded near $\bar{k}$ = .25; A = 1.1; Ψ = 12.6°.

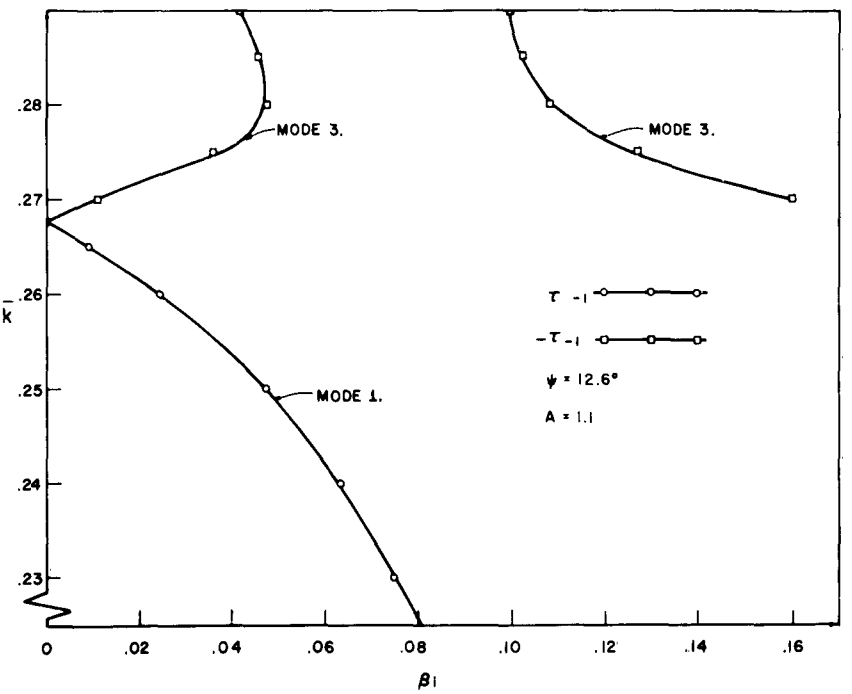

Figure 3.5b. The k - β_i diagram for simplified equation one expanded near $\bar{k}$ = .25; A = 1.1, Ψ = 12.6°.

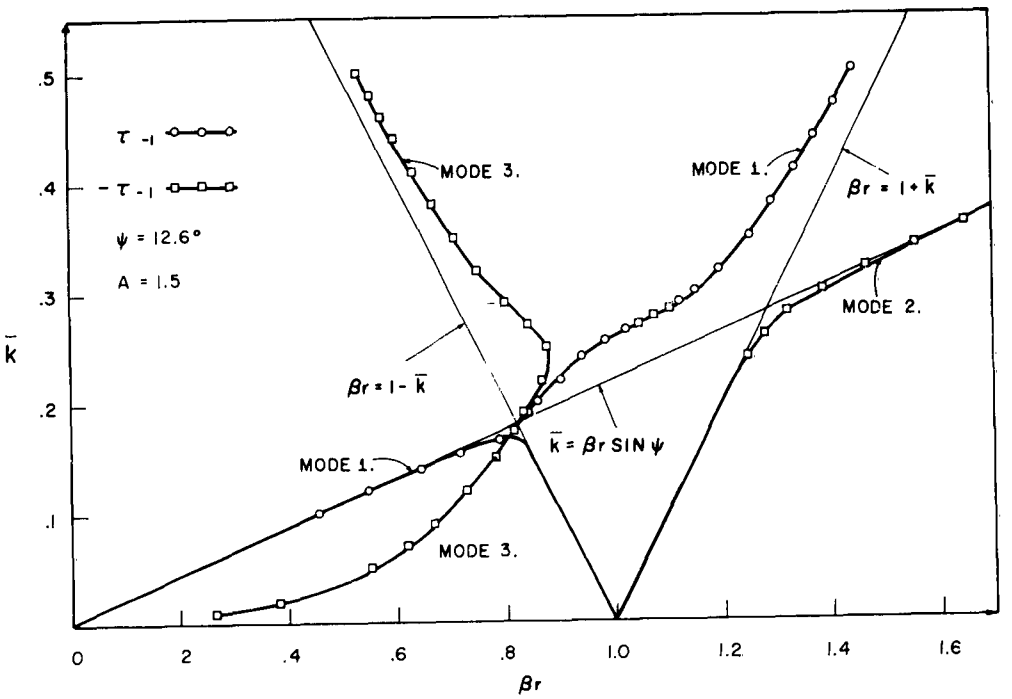

Figure 3.6a. The k - β_r diagram for simplified equation one, A = 1.5, $\psi = 12.6^{\circ}$.

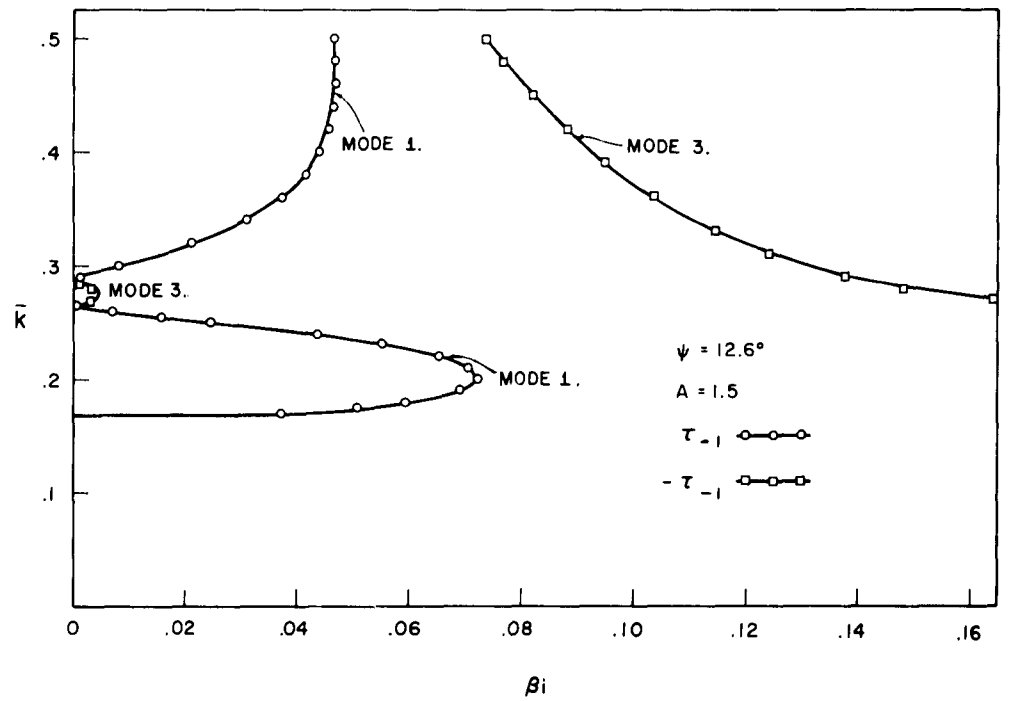

Figure 3.6b. The k - β_i diagram for simplified equation one, A = 1.5, $\psi = 12.6^{\circ}$.

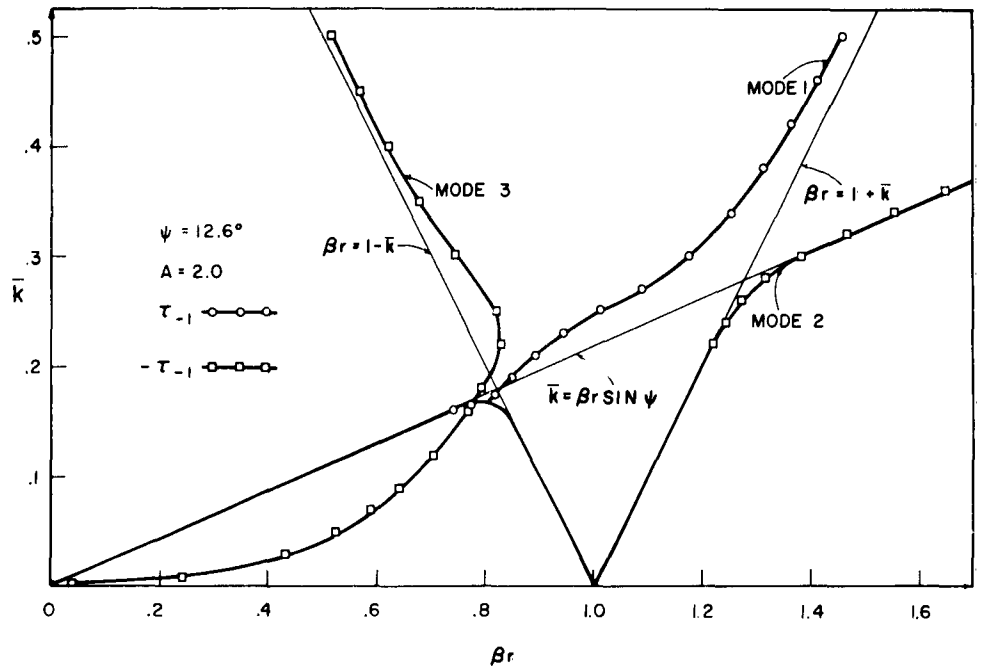

Figure 3.7a. The k - β_r diagram for simplified equation one; A = 2.0, $\psi = 12.6^{\circ}$.

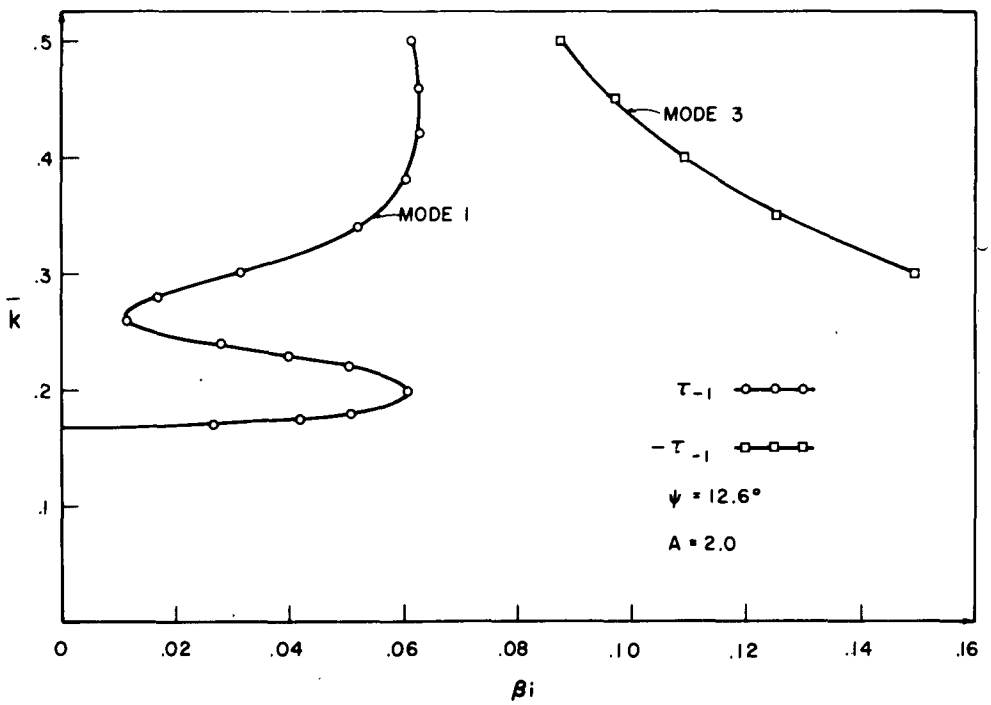

Figure 3.7b. The k - β_i diagram for simplified equation one; A = 2.0, $\psi = 12.6^{\circ}$.

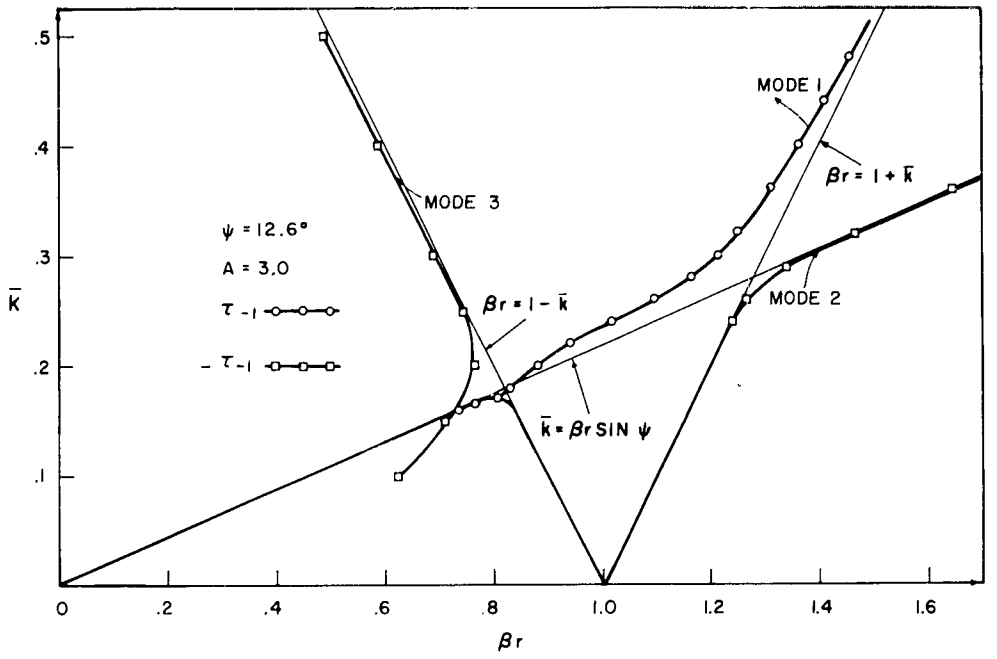

Figure 3.8a. The k - β_r diagram for simplified equation one; A = 3.0, $\psi = 12.6^{\circ}$.

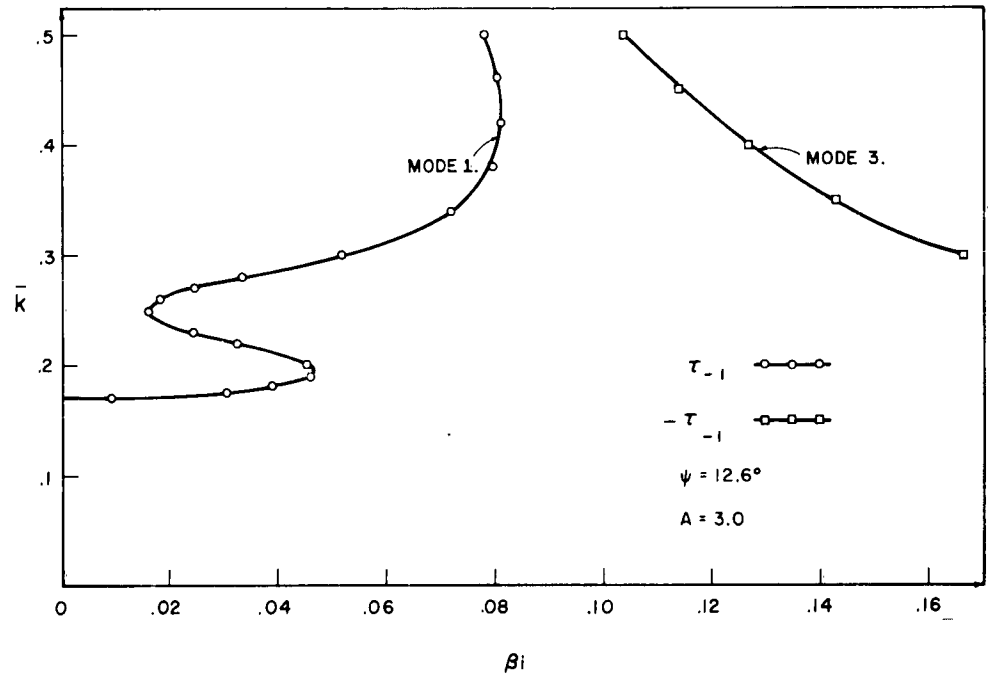

Figure 3.8b. The k - β_i diagram for simplified equation one; A = 3.0, $\psi = 12.6^{\circ}$.

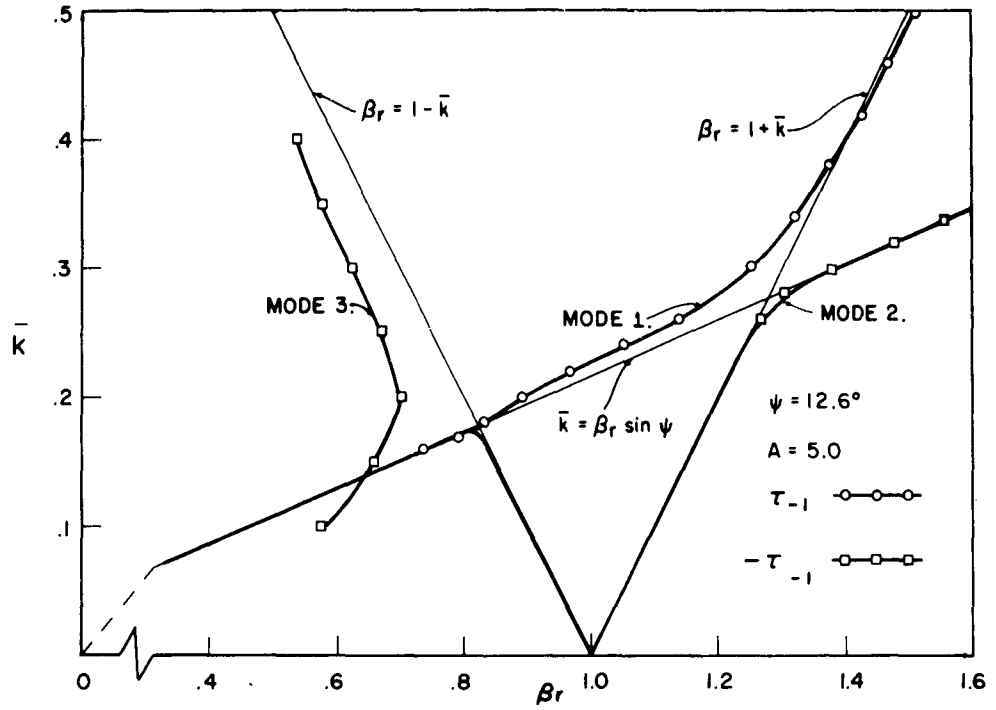

Figure 3.9a. The k - β_r diagram for simplified equation one; A = 5.0, ψ = 12.6°.

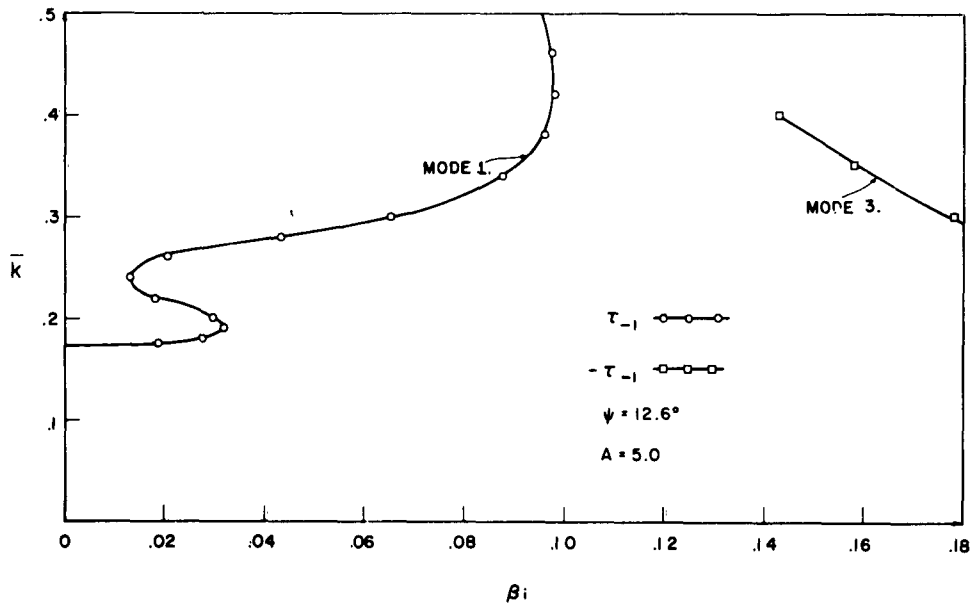

Figure 3.9b. The k - β_i diagram for simplified equation one; A = 5.0, ψ = 12.6°.

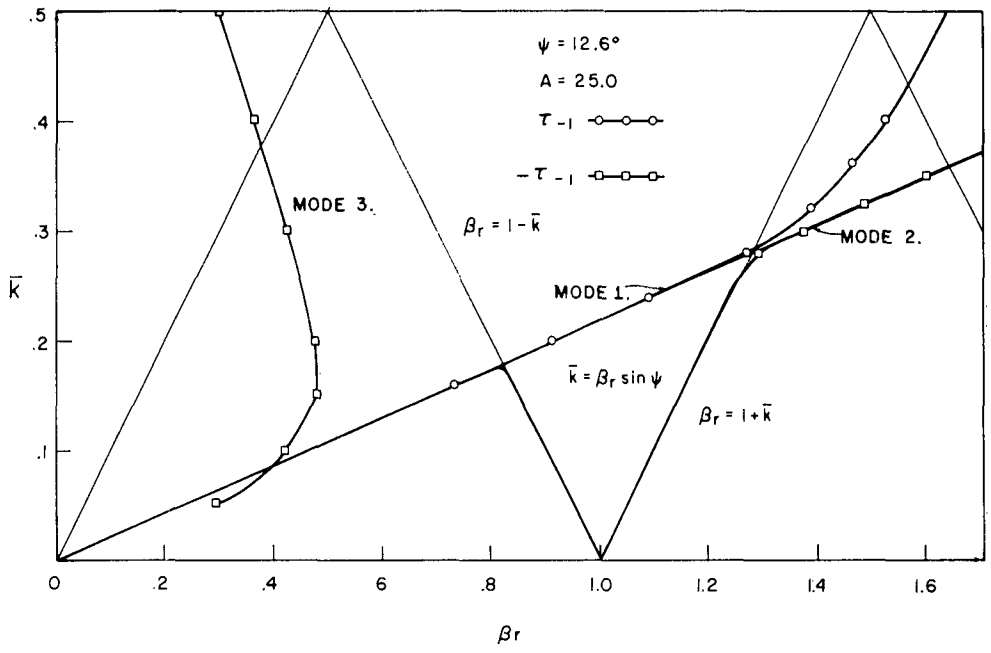

Figure 3.10a. The k - β_r diagram for simplified equation one; A = 25.0, $\Psi = 12.6^{\circ}$.

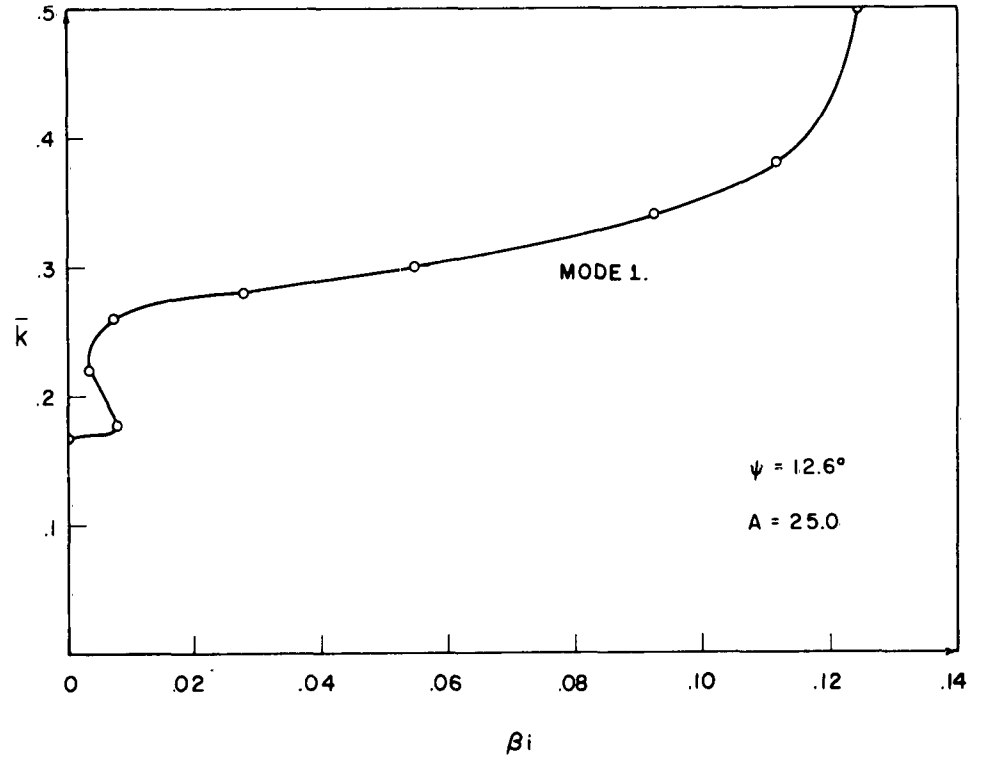

Figure 3.10b. The k - β_i diagram for simplified equation one; A = 25.0, $\Psi = 12.6^{\circ}$.

increases.

One could study this simplified equation in more detail, e.g., as a function of pitch angle ψ. This kind of study will be delayed until the complete determinantal equation is studied. At that time the physical significance of the increasing or decreasing of solutions will be discussed.

The reason for studying the simplified equation was to show the existence of the various modal solutions of the determinantal equation and show how the arguments of the IK products could be treated so that the solutions would be continuous functions of $\bar{k}$.

3.3 The Second Simplified Equation

It will be instructive to study another simplified equation. This equation will approximate the behavior of the determinantal equation in the region β_r near 2. Since for $\beta_r \simeq 2$,

$$\tau_{-2} = [(\beta_r-2)^2 - (\bar{k}^2+\beta_i^2)+2i\beta_i(\beta_r-2)]^{1/2}\operatorname{ctn}\psi$$

changes rapidly, only those terms in the numerator of the determinantal equation, Equation (3.1), will be used for the simplified equation. Also, as stated in the last section, the denominator, $2A_o$, is a slowly varying function of $\bar{k}$ and β. Again $2A_o$ is replaced by a constant, A. Simplified equation two is

$$\frac{\beta^2 - \dfrac{\bar{k}^2}{\sin^2\psi}}{\bar{k}^2\operatorname{ctn}^2\psi} = \frac{I_1K_1(\tau_{-2}) + I_3K_3(\tau_{-2}) - 2\,I_2K_2(\tau_{-2})}{A} \qquad (3.3)$$

The solutions are shown in the following figures.

The line $\bar{k} = \beta_r \sin\psi$ is shown on the $\bar{k} - \beta_r$ planes. The lines $\beta_r = 2 \pm \bar{k}$ are shown on the $\bar{k} - \beta_r$ planes. Inside the "v" shaped region formed by the lines $\beta_r = 2 \pm \bar{k}$ the argument τ_{-2} has non-zero imaginary part. Outside the "v" shaped region formed by the lines $\beta_r = 2 \pm \bar{k}$ the argument τ_{-2} may have zero imaginary part.

If one examines Figures 3.11 and 3.12 the immediate observation is that for a given $\bar{k}$ there exists more than one solution for β. The different modes do not all have the same determination of the square root for agrument of the IK products. Modes 2 and 5 have the positive determination for the argument of the IK products, whereas modes 4 and 6 have the negative determination.

Let $\bar{k}_{c2}$ be the lowest value of $\bar{k}$ such that the solution for mode 2 will have a non-zero imaginary part. The mode 2 solution for $\beta_r < 2-\bar{k}$ and $\bar{k} < \bar{k}_{c2}$ is similar to the solution found by Sensiper[7] The mode 4 solution also corresponds to Sensiper's results. The mode 2 solution for $\bar{k} > \bar{k}_{c2}$ has an imaginary part which is similar to the mode one solution to the simplified equation of the previous section.

Consider the results shown in Figure 3.16 which is an expanded view of a section of Figure 3.11a. Note that to have the real part of the phase constant continuous across the line $\beta_r = 2-\bar{k}$, for $\bar{k} < \bar{k}_{c2}$, it is necessary to change the determination of the square root. This difference in the determination of the arguments causes a discontinuity in the arguments by the amount π. However the value of the right hand side of Equation 3.3 is the same for either determination of the τ_{-2} argument at $\beta_r = 2-\bar{k}$. This equality is true because when $\beta_r = 2-\bar{k}$

and $\beta_i = 0$, $\tau_{-2} = 0$ and further

$$\lim_{\tau_{-2} \to 0} I_n(\tau_{-2})\, K_n(\tau_{-2}) = \frac{1}{2n}, \quad n \neq 0$$

which is independent of which branch was chosen.

The results shown in Figure 3.18 which is an expanded view of a section of Figure 3.11a are to be studied. Again the same type of discontinuity occurs. The line $\beta_r = 2 + \bar{k}$ separates modes 4 and 5 which have a continuous real part. The argument has a discontinuity equal to π for modes 4 and 5 at $\beta_r = 2 + \bar{k}$. The right hand side of Equation 3.3 is the same for either determination of the argument. The reason for this equality is similar to that given above.

In Figure 3.21a the behavior of the solutions for modes 2 and 5 should be observed. This behavior is typical for values of the parameter A less than A_{c2}, where A_{c2} will be defined later. In Figure 3.19 the behavior of the solutions for modes 2 and 5 for A = 10 should be studied. Note the behavior of the solutions is different for A = 10.0 than for A = 7.0. This behavior for A = 10.0 is typical for values of the parameter $A > A_{c2}$. The number A_{c2} is now easily defined. The number A_{c2} divides the set A into two classes, one, $A < A_{c2}$, where the mode 2 solutions corresponding to these values of A are not continuous with the solutions for mode 4 and the other, $A > A_{c2}$, where the mode 2 solutions corresponding to these values of A are continuous with the solutions for mode 4.

If one examines Figures 3.22a, 3.22b, 3.23a, 3.23b, 3.24a, and 3.24b it is seen how these solutions take on the different character as the

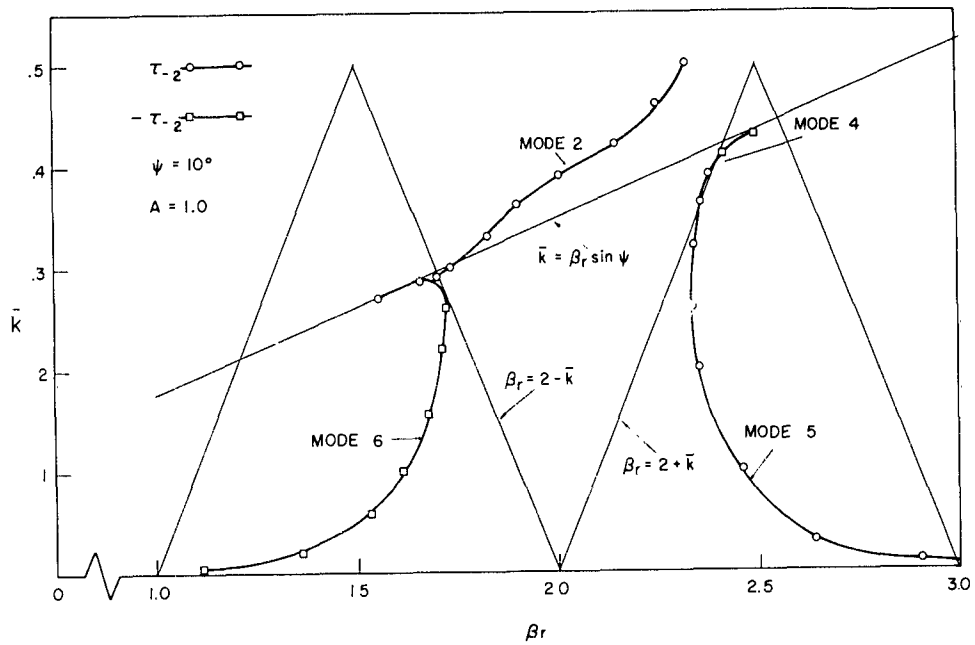

Figure 3.11a. The k - β_r diagram for simplified equation two; A = 1.0, $\psi = 10^{o}$.

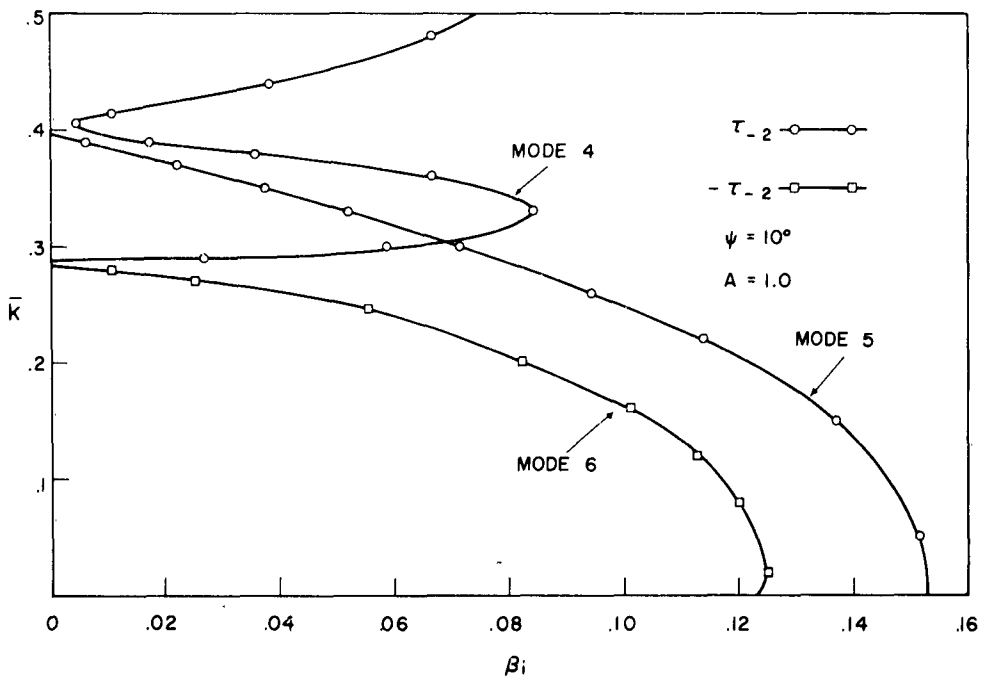

Figure 3.11b. The k - β_i diagram for simplified equation two; A = 1.0, $\psi = 10^{o}$.

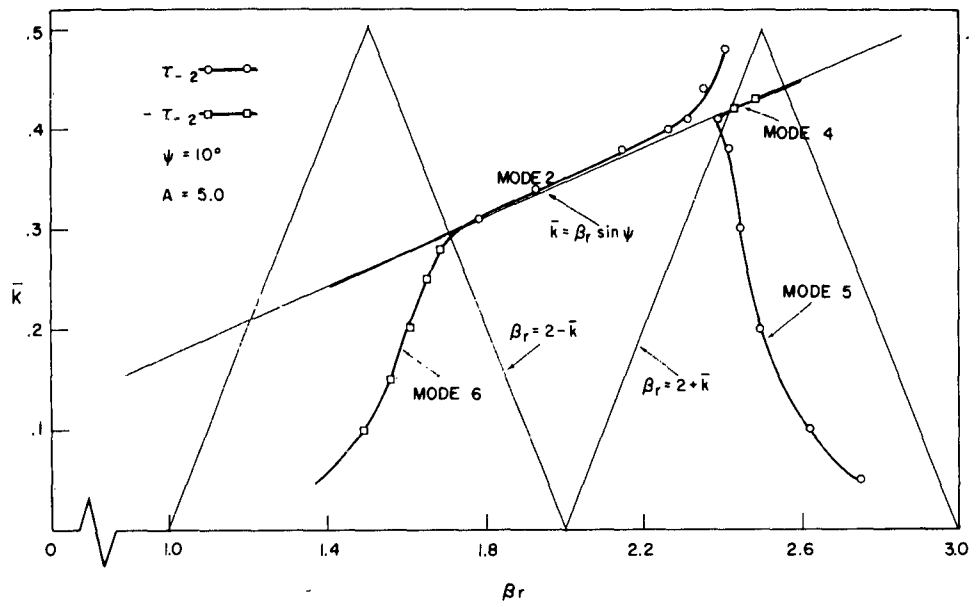

Figure 3.12a. The k - β_r diagram for simplified equation two; A = 5.0, $\psi = 10^{o}$.

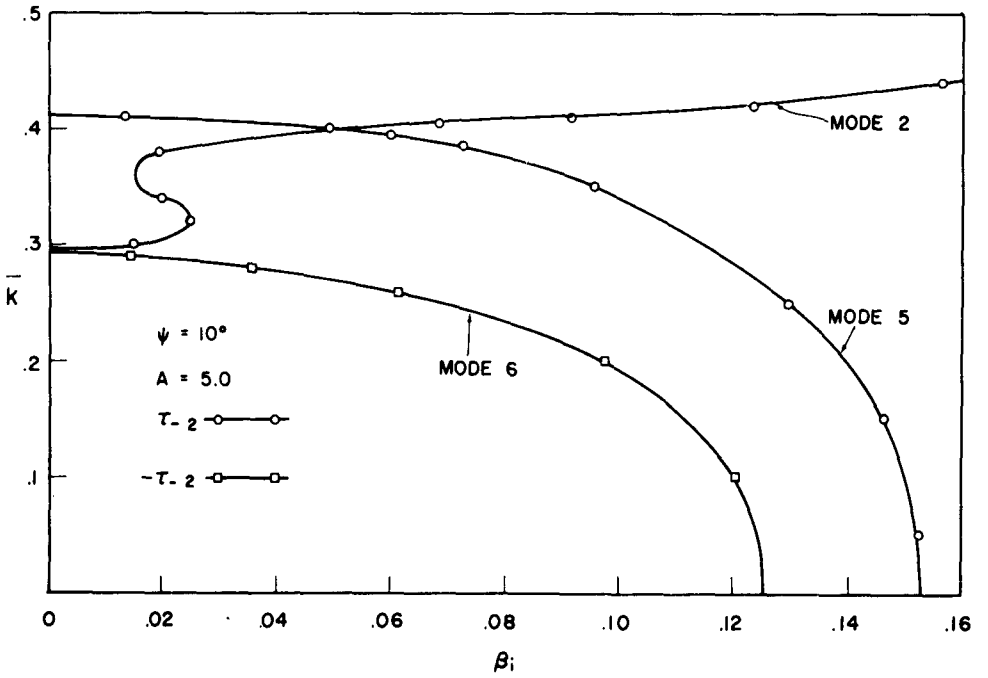

Figure 3.12b. The k - β_i diagram for simplified equation two; A = 5.0, $\psi = 10^{o}$.

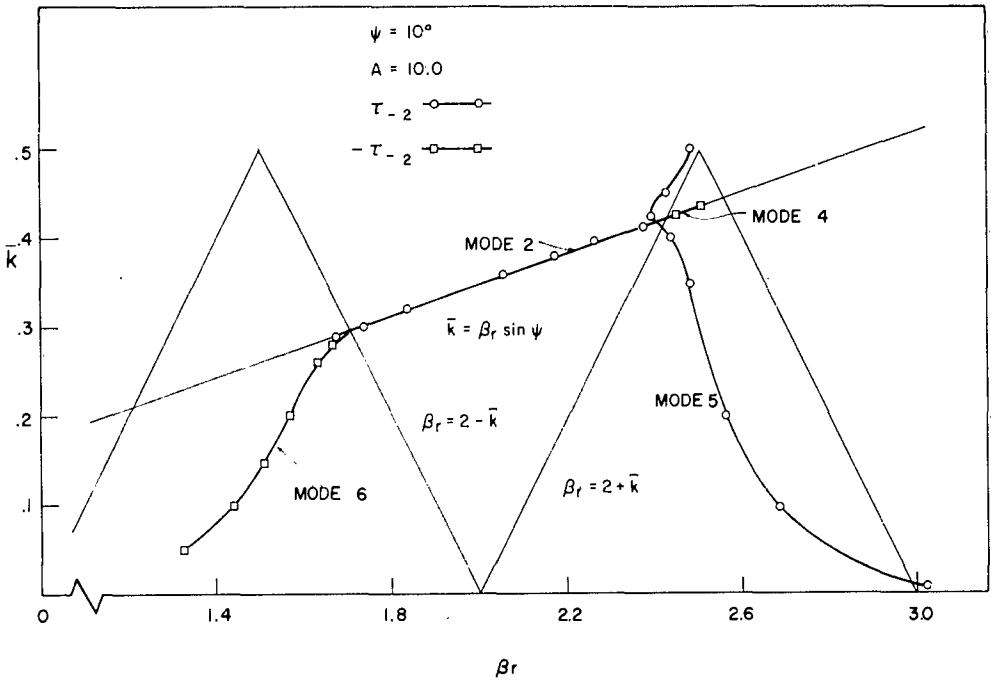

Figure 3.13a. The k - β_r diagram for simplified equation two; A = 10.0, $\psi = 10^{o}$.

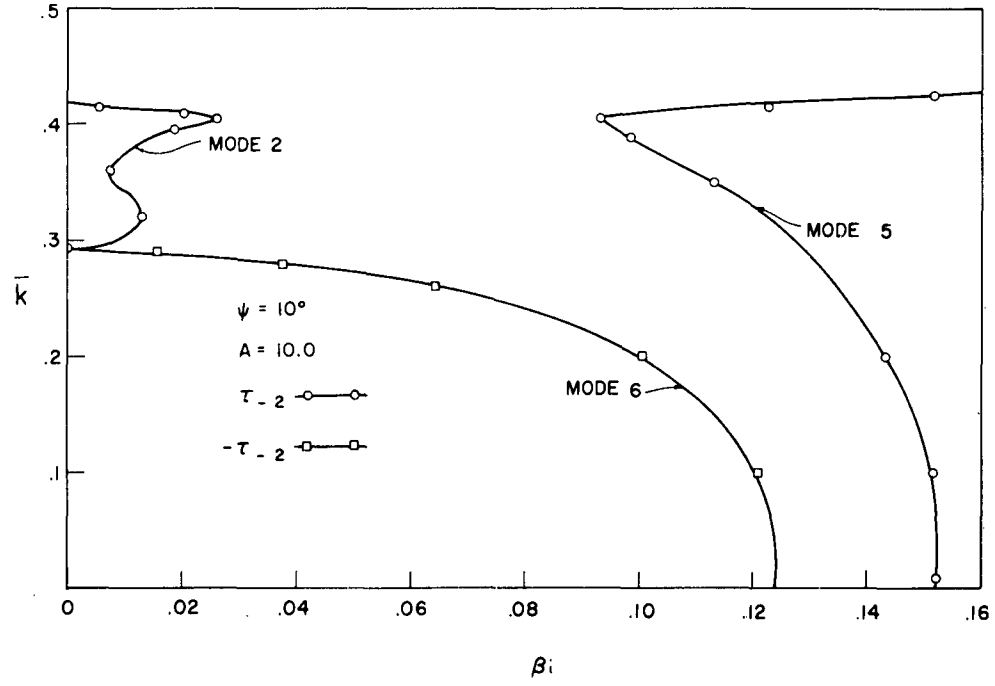

Figure 3.13b. The k - β_i diagram for simplified equation two; A = 10.0, $\psi = 10^{o}$.

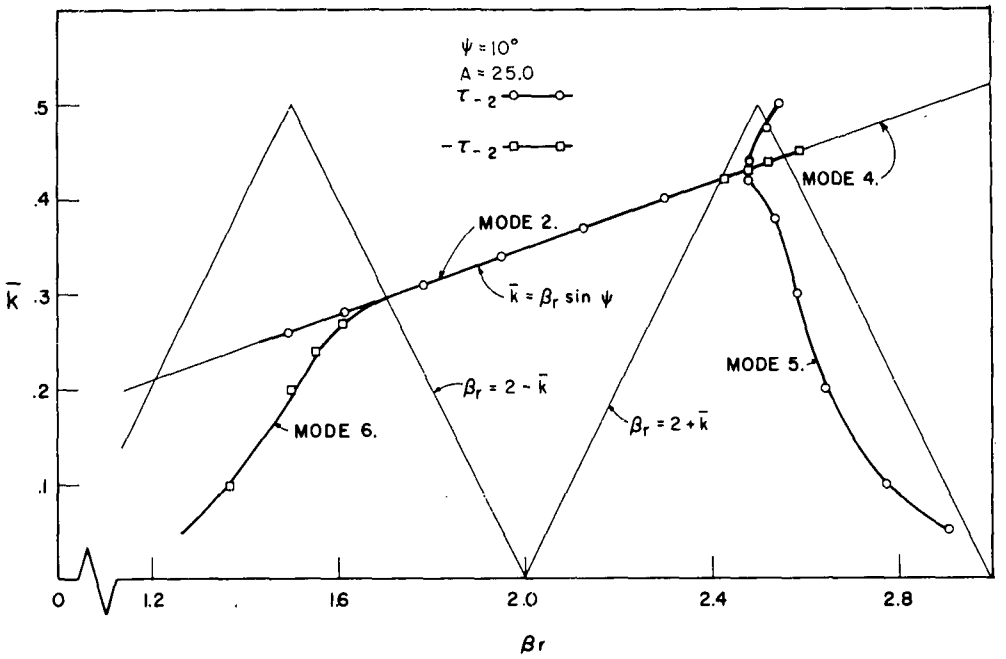

Figure 3.14a. The k - β_r diagram for simplified equation two; A = 25.0, $\psi = 10^{o}$.

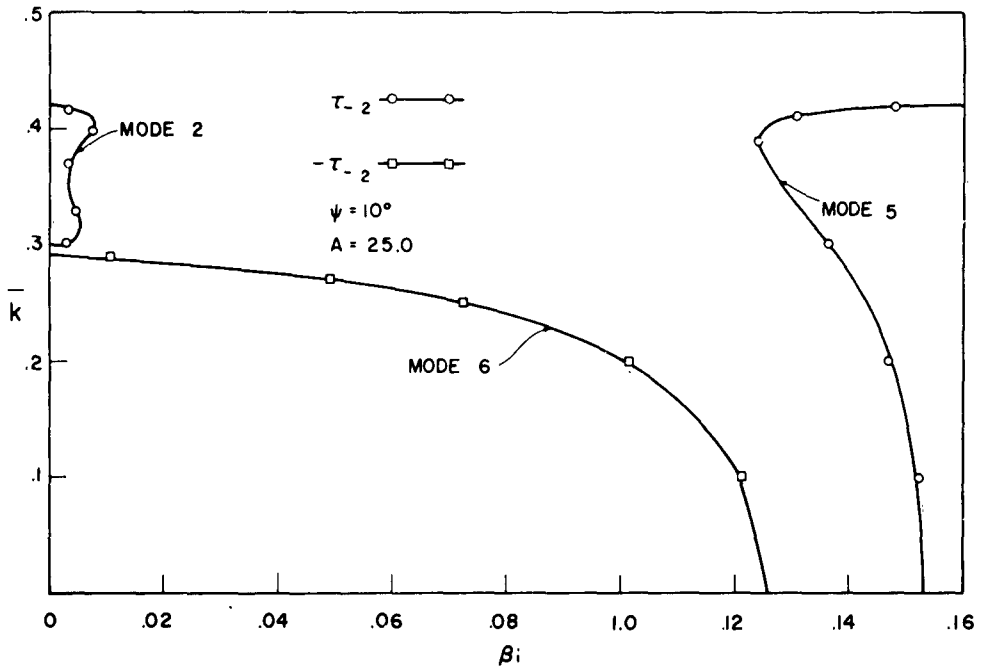

Figure 3.14b. The k - β_r diagram for simplified equation two; A = 25.0, $\psi = 10^{o}$.

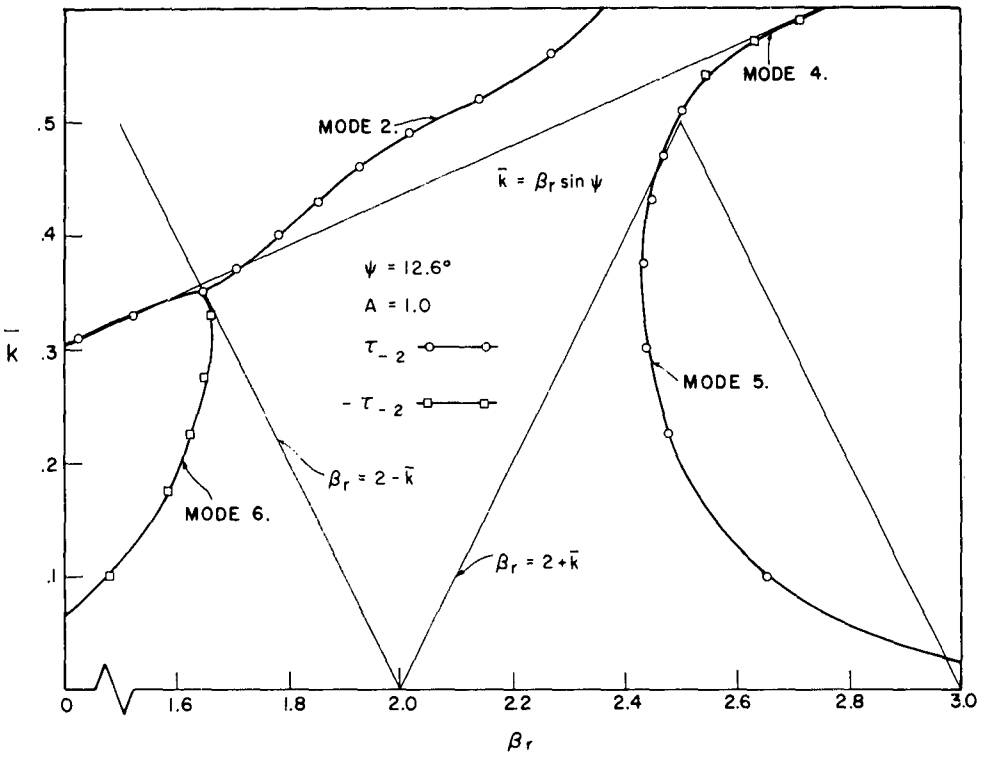

Figure 3.15a. The k - β_r diagram for simplified equation two; A = 1.0, $\psi = 12.6°$.

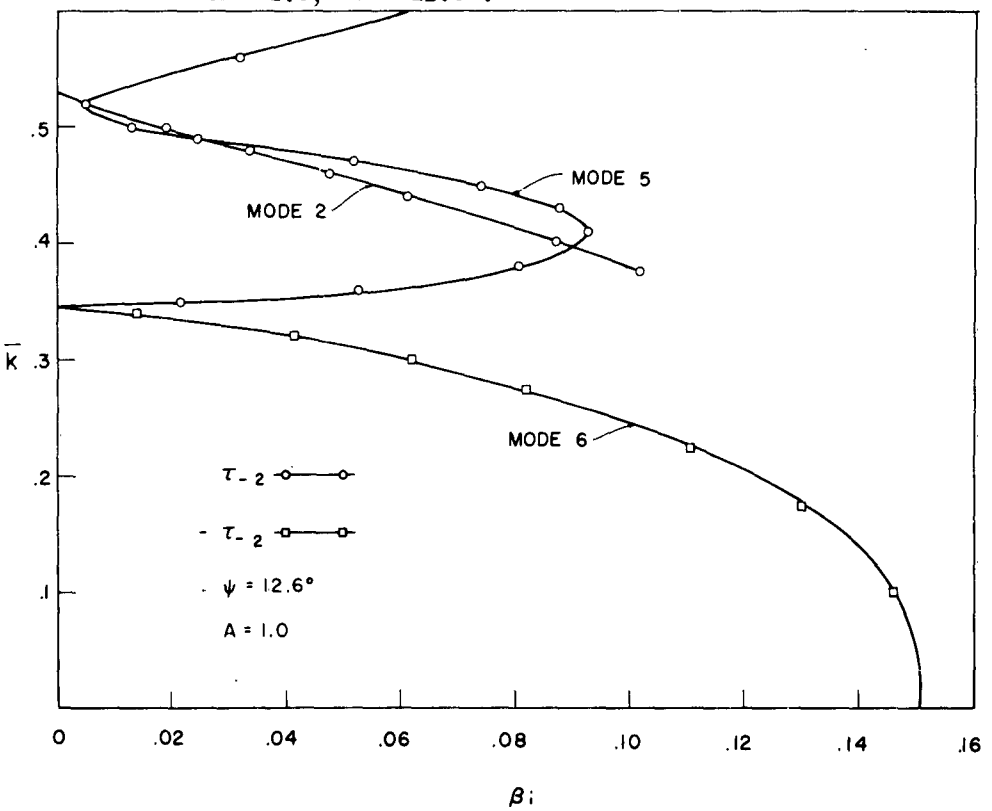

Figure 3.15b. The k - β_i diagram for simplified equation two; A = 1.0, $\psi = 12.6°$.

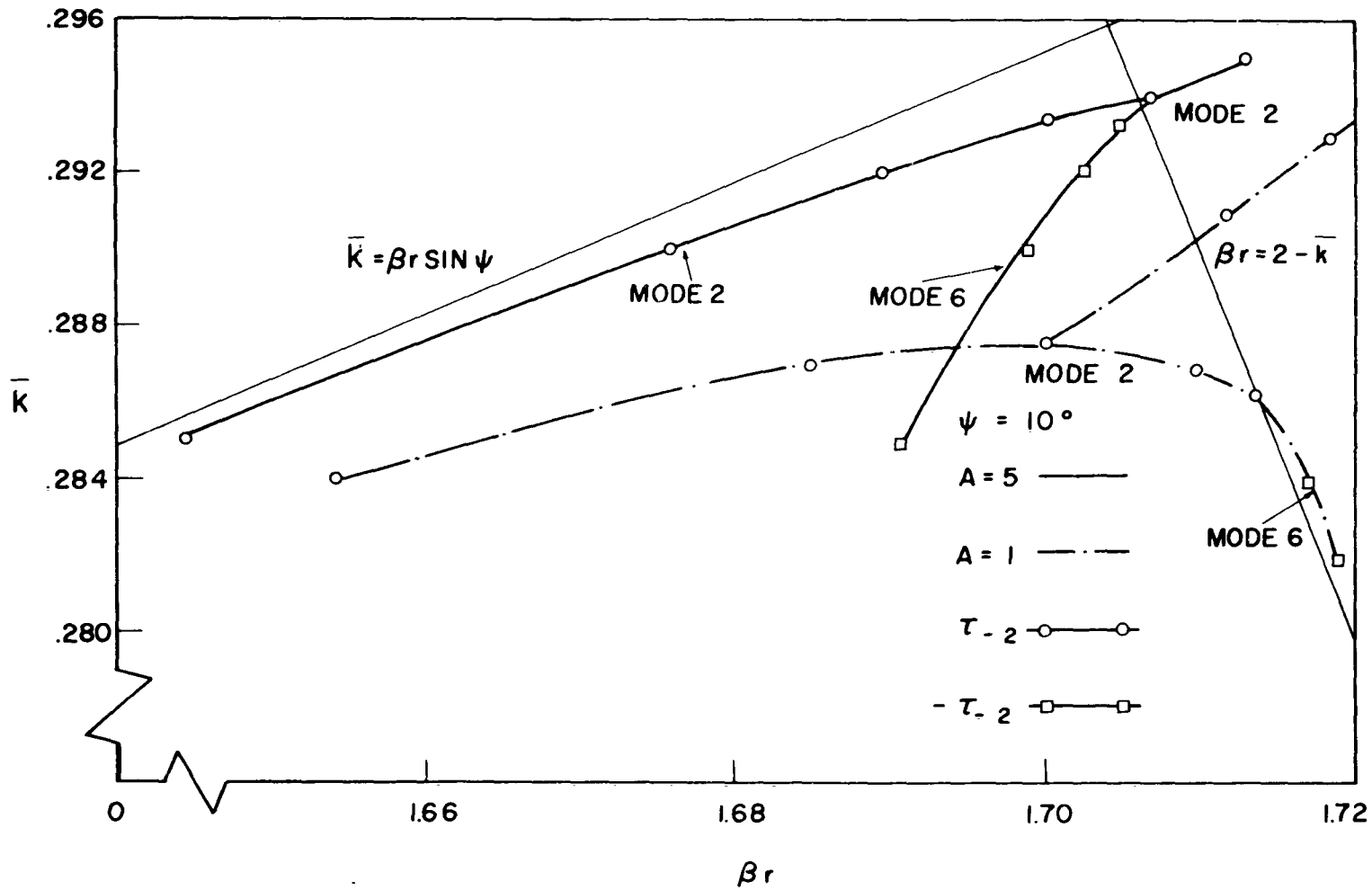

Figure 3.16. The $\bar{k} - \beta_r$ diagram for simplified equation two near $\bar{k}_{c2}$; A = 1.0 and 5.0, $\psi = 10^{\circ}$.

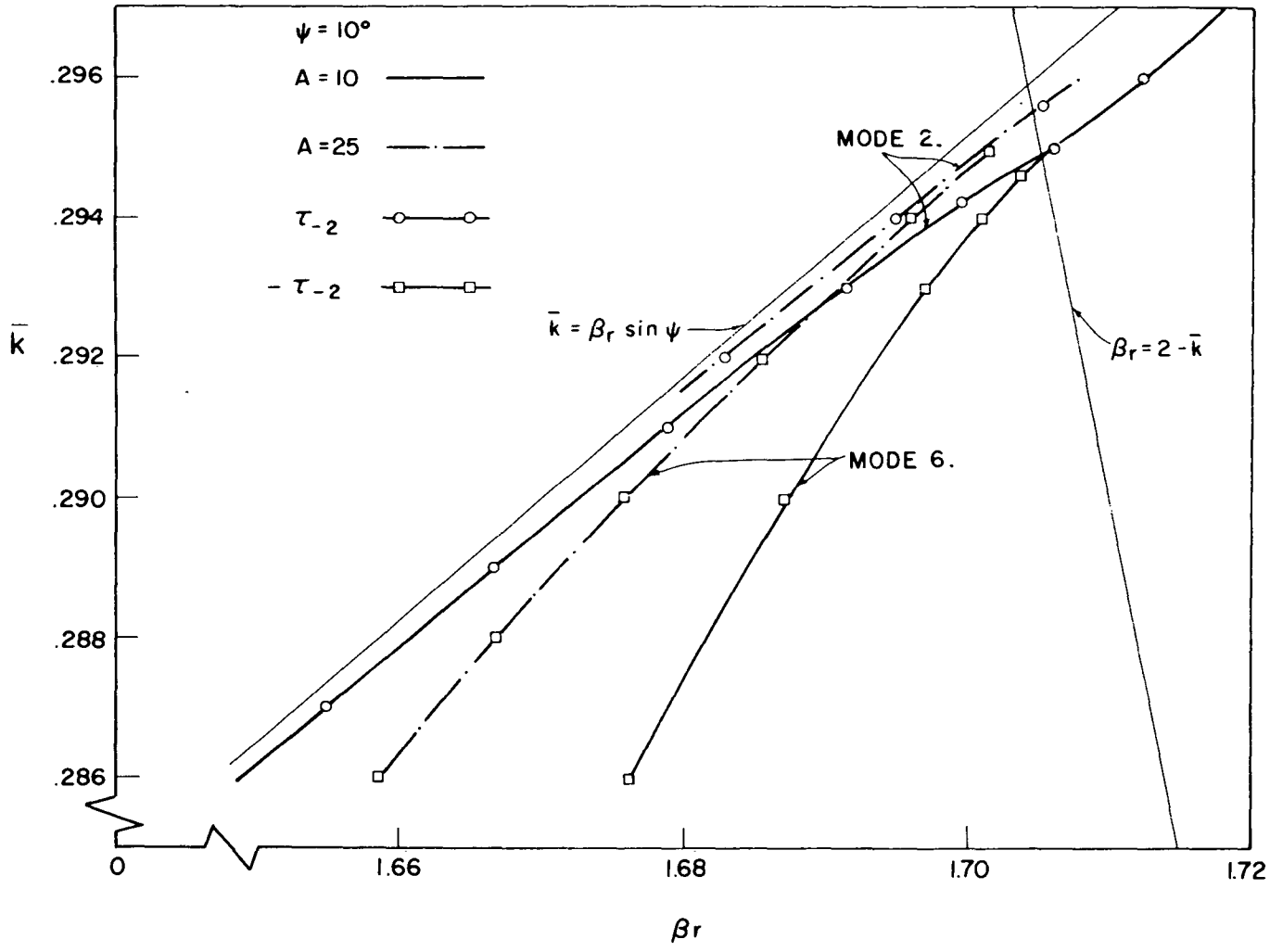

Figure 3.17. The k - β_r diagram for simplified equation two near $\bar{k}_{c2}$, A = 10.0 and 25.0, $\Psi = 10^{o}$.

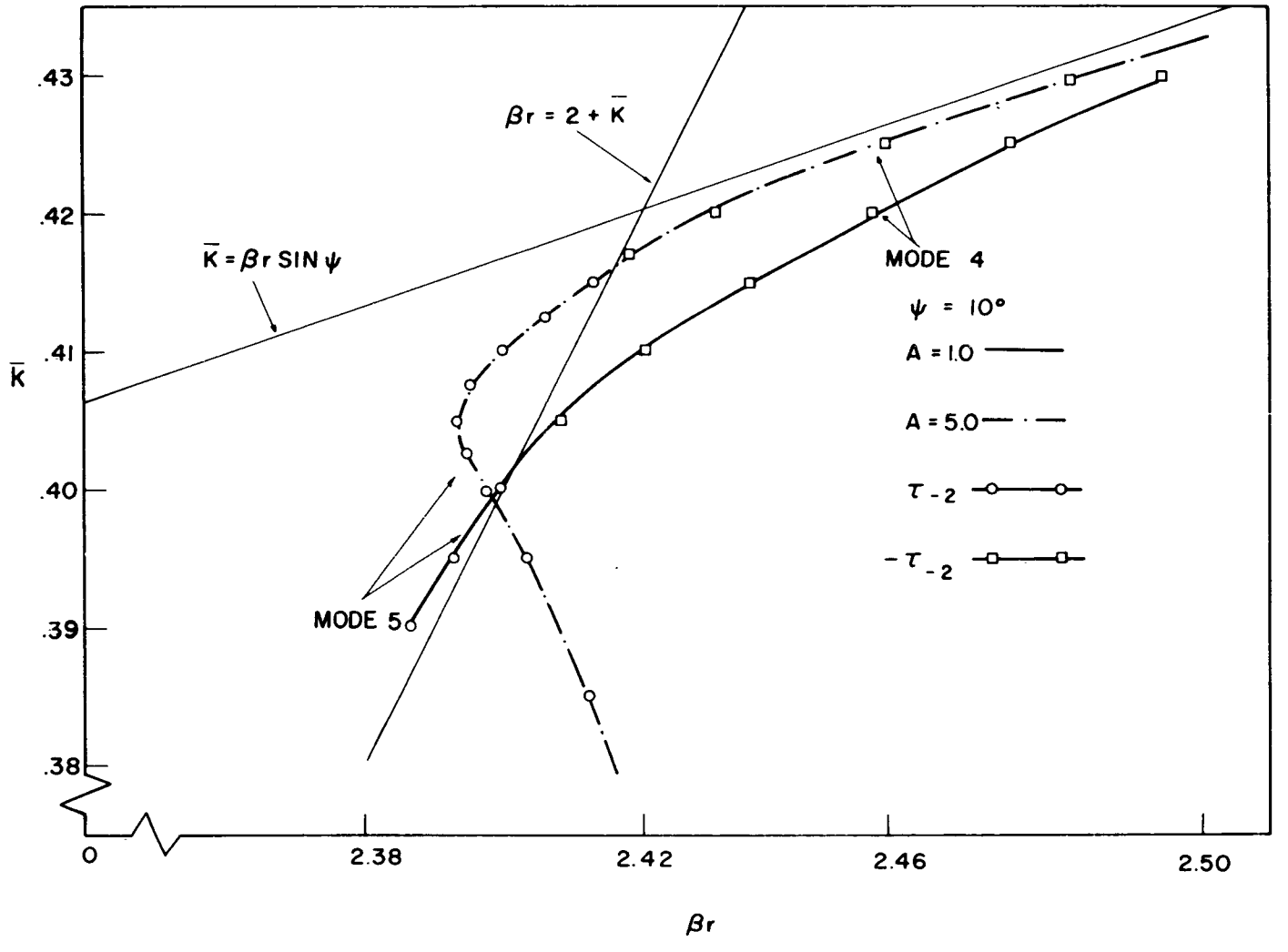

Figure 3.18. The k - β_r diagram for simplified equation two near $\bar{k}^{-1}_{c4}$; A = 1.0 and 5.0, $\psi = 10^{o}$.

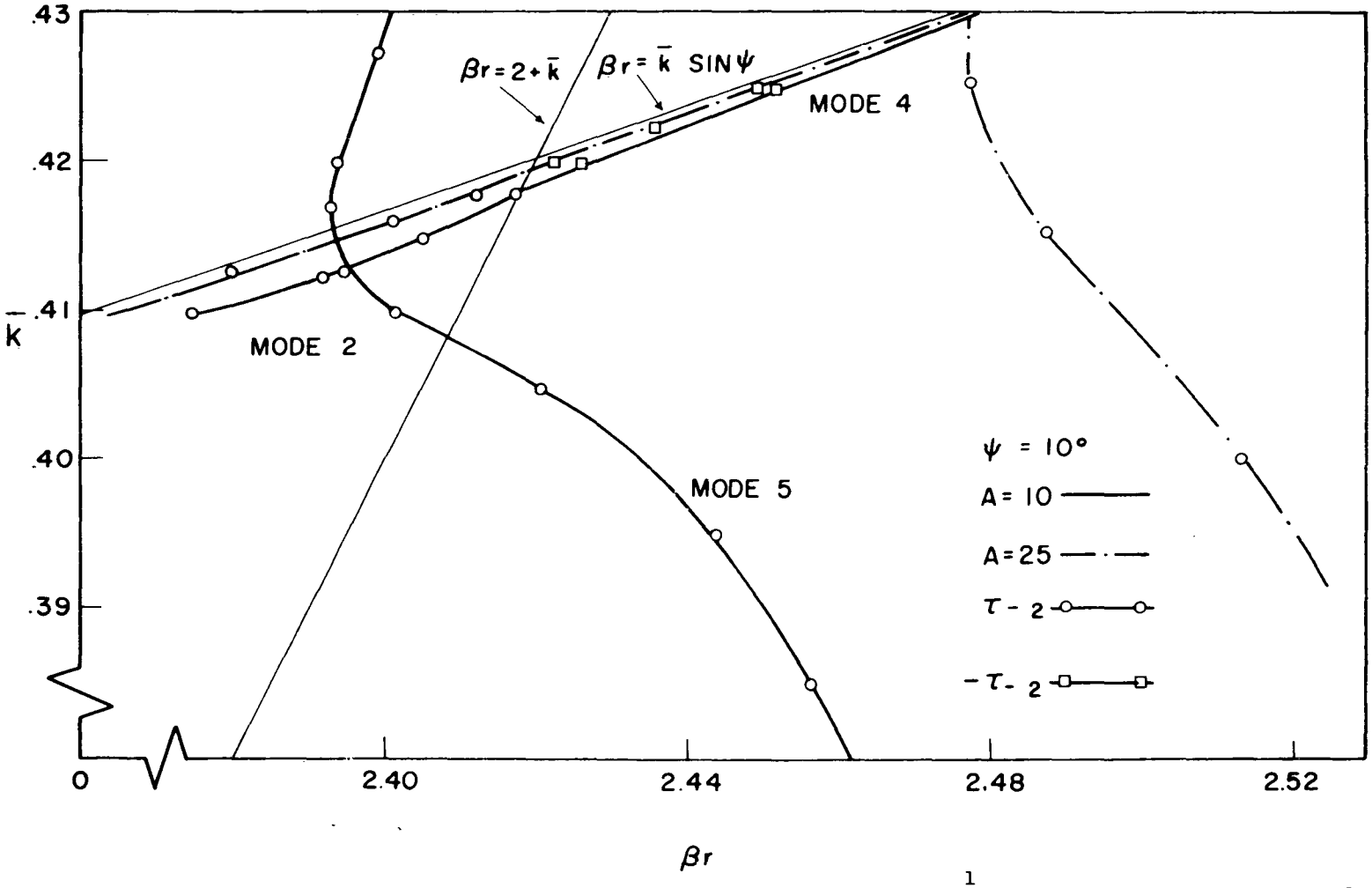

Figure 3.19. The k - β_r diagram for simplified equation two near $\bar{k}^1_{c4}$; A = 10.0 and 25.0, $\psi = 10^o$.

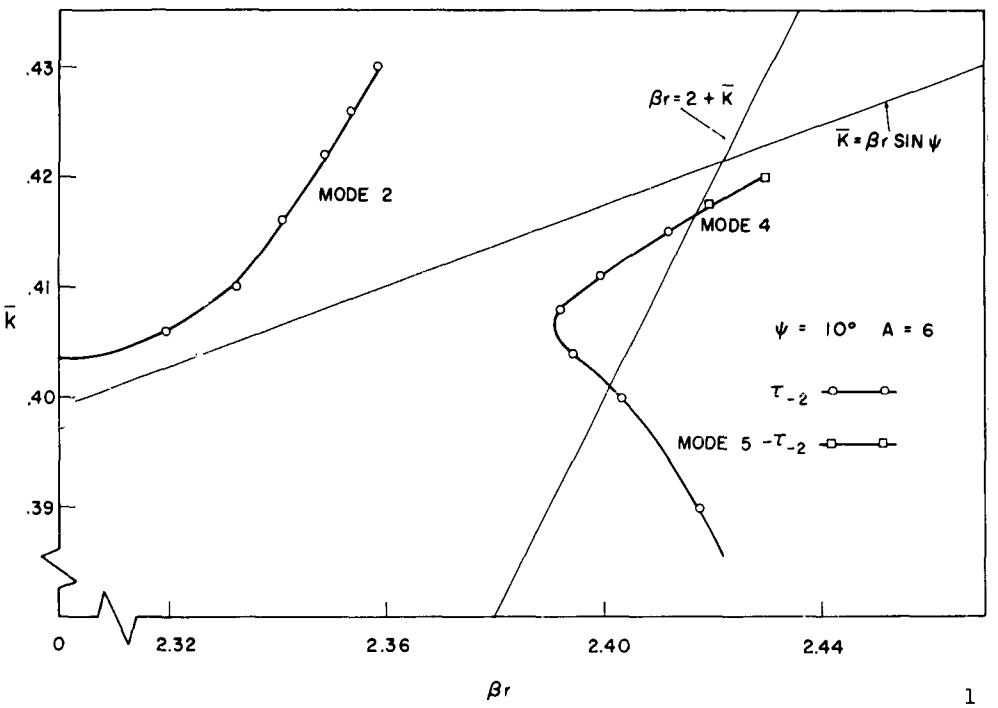

Figure 3.20a. The k - β_r diagram for simplified equation two near $\bar{k}^1_{c4}$; A = 6.0, $\psi = 10^o$.

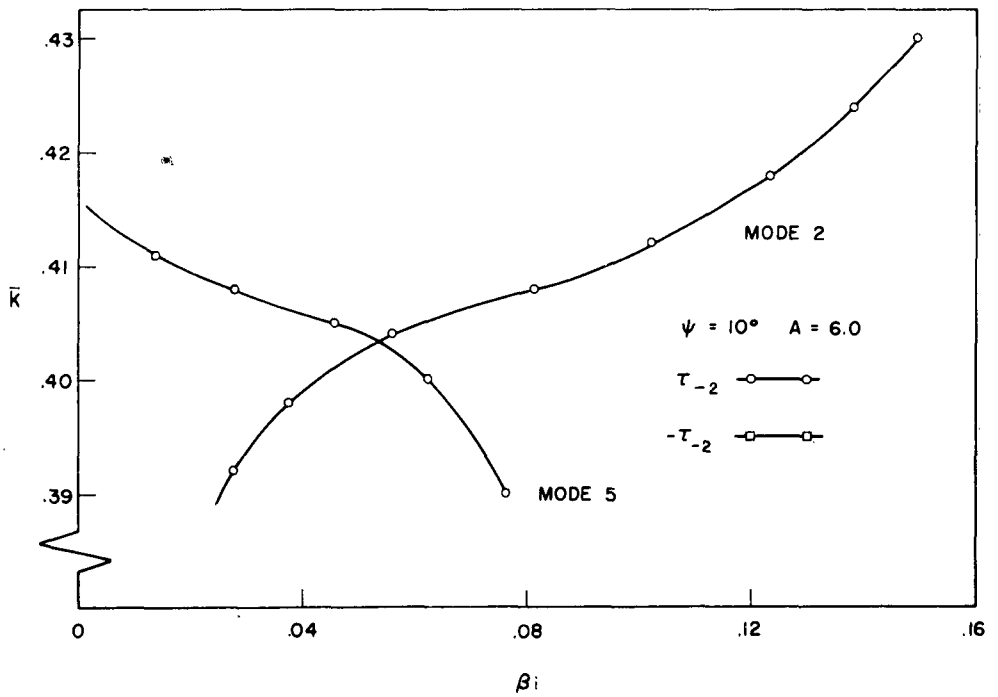

Figure 3.20b. The k - β_i diagram for simplified equation two near $\bar{k}^1_{c4}$ A = 6.0, $\psi = 10^o$.

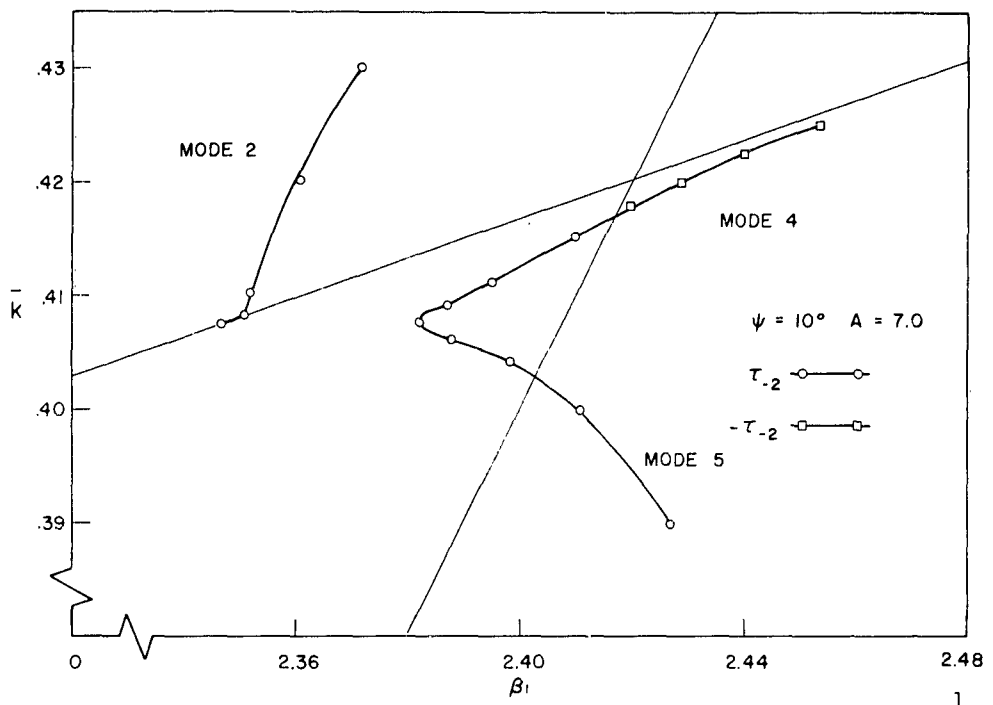

Figure 3.21a. The $k - \beta_r$ diagram for simplified equation two near $\bar{k}_{c4}^{1}$; $A = 7.0$, $\psi = 10^{o}$.

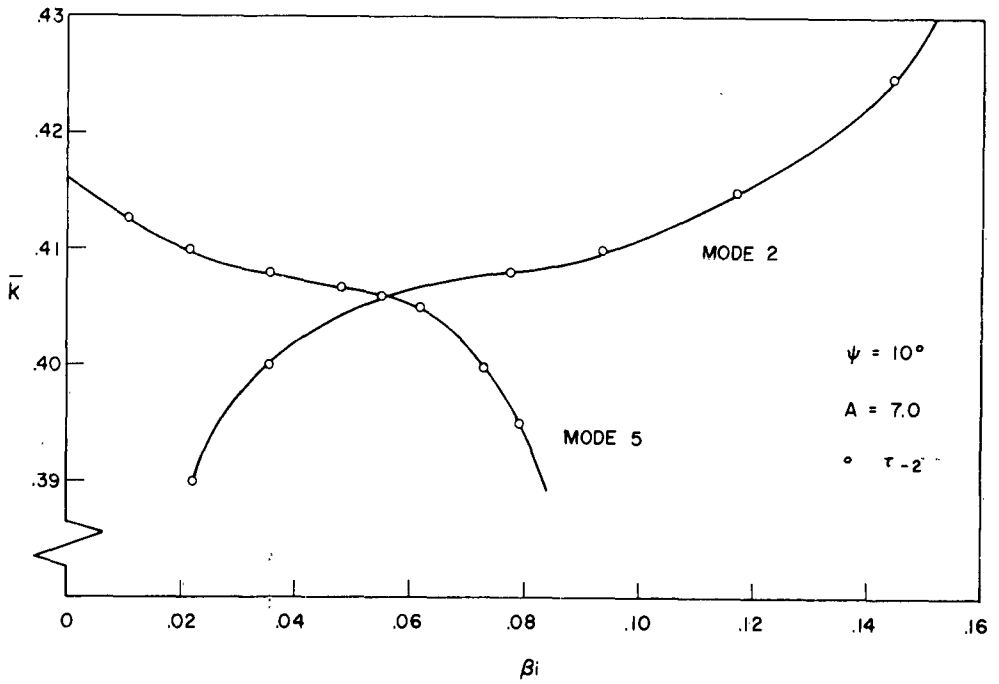

Figure 3.21b. The $k - \beta_i$ diagram for simplified equation two near $\bar{k}_{c4}^{1}$; $A = 7.0$, $\psi = 10^{o}$.

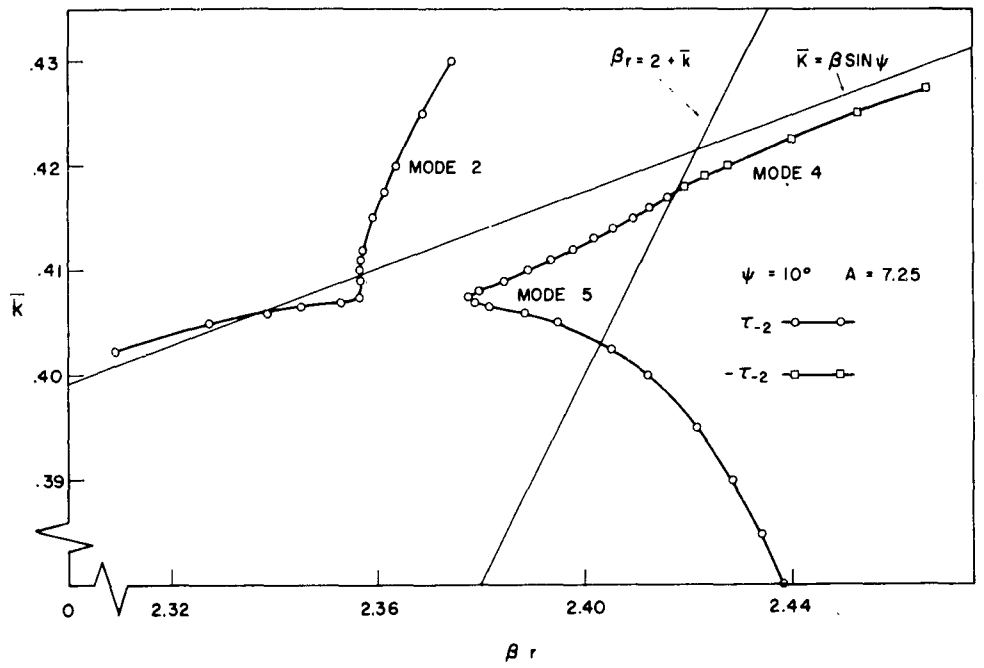

Figure 3.22a. The $k - \beta_r$ diagram for simplified equation two near $\bar{k}_{c4}^{1}$; $A = 7.25$, $\psi = 10^{o}$.

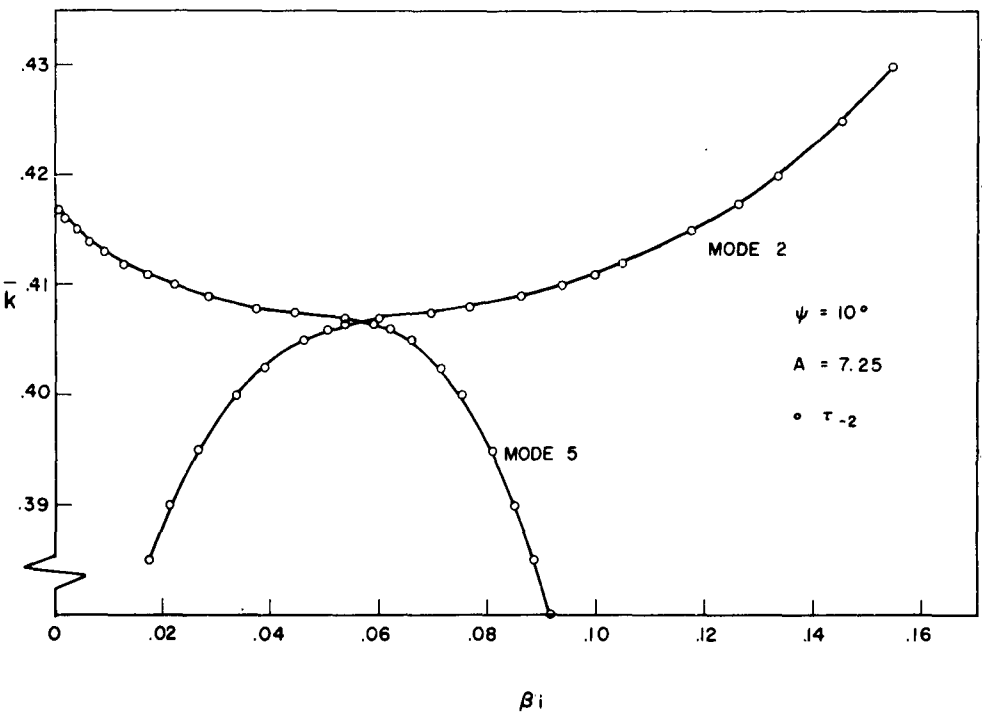

Figure 3.22b. The $k - \beta_i$ diagram for simplified equation two near $\bar{k}_{c4}^{1}$ $A = 7.25$, $\psi = 10^{o}$.

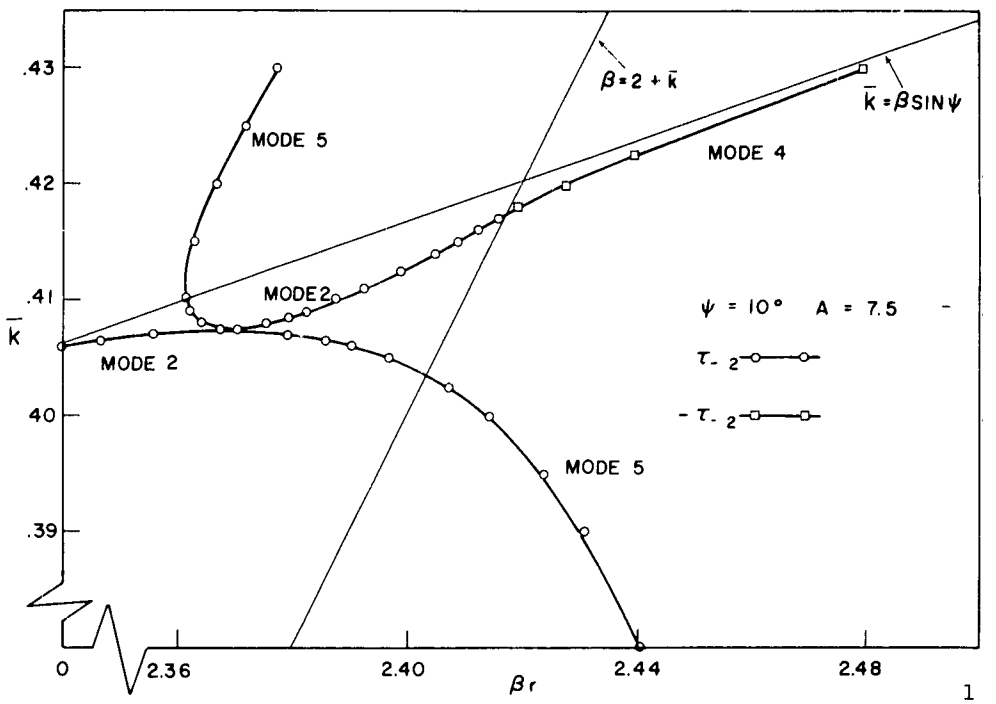

Figure 3.23a. The k - β_r diagram for simplified equation two near $\bar{k}_{c4}^{1}$; A = 7.5, $\psi = 10^{o}$.

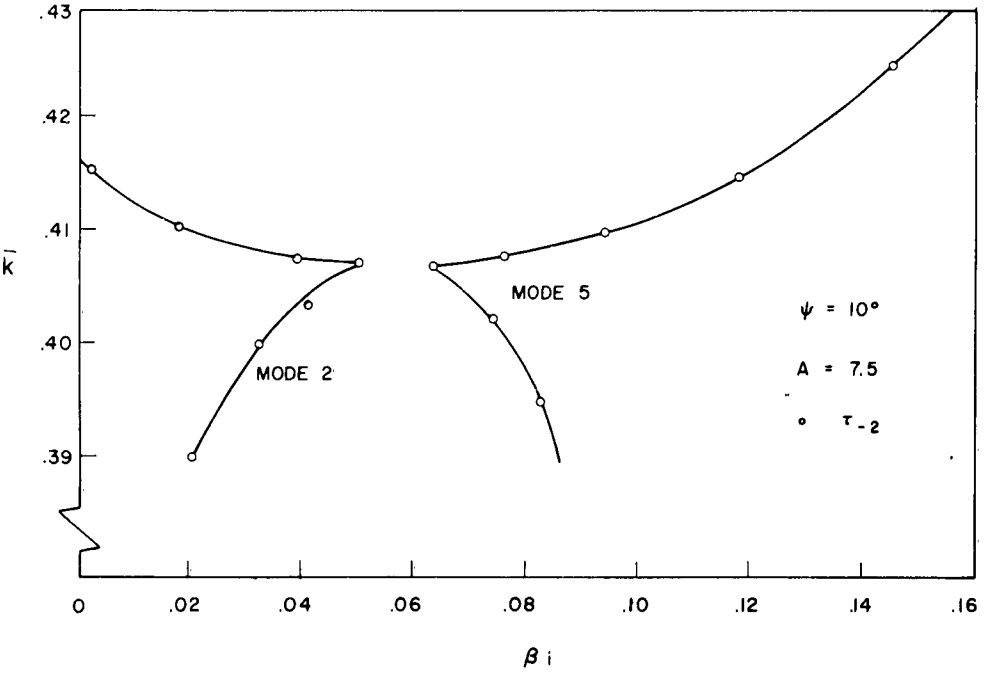

Figure 3.23b. The k - β_i diagram for simplified equation two near $\bar{k}_{c4}^{1}$; A = 7.5, $\psi = 10^{o}$.

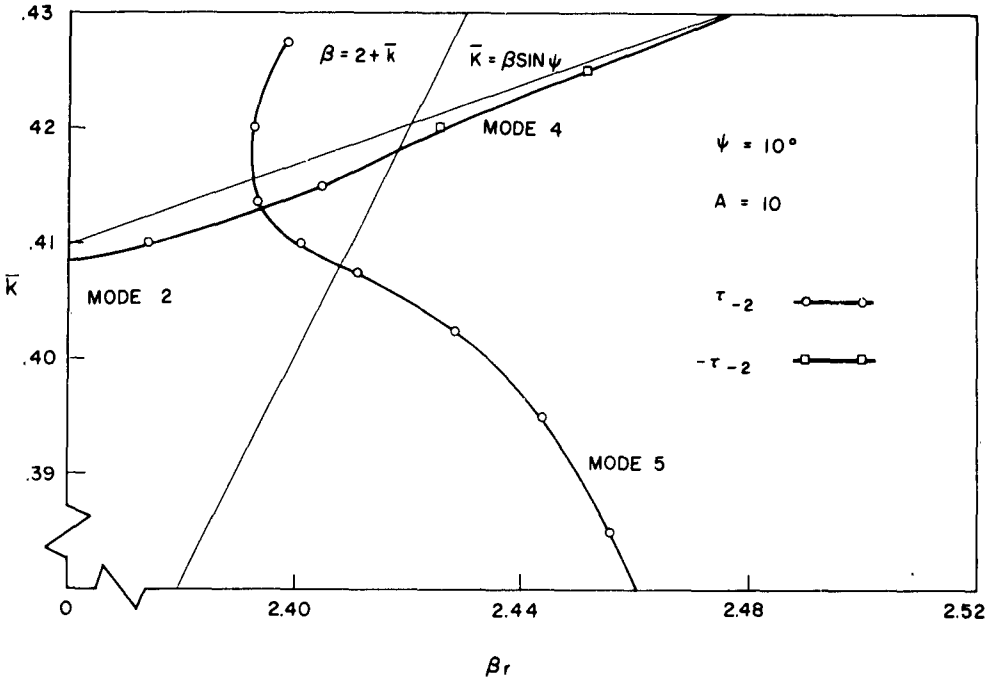

Figure 3.24a. The k - β_r diagram for simplified equation two near $\bar{k}^1_{c4}$; A = 8.0, $\psi = 10^o$.

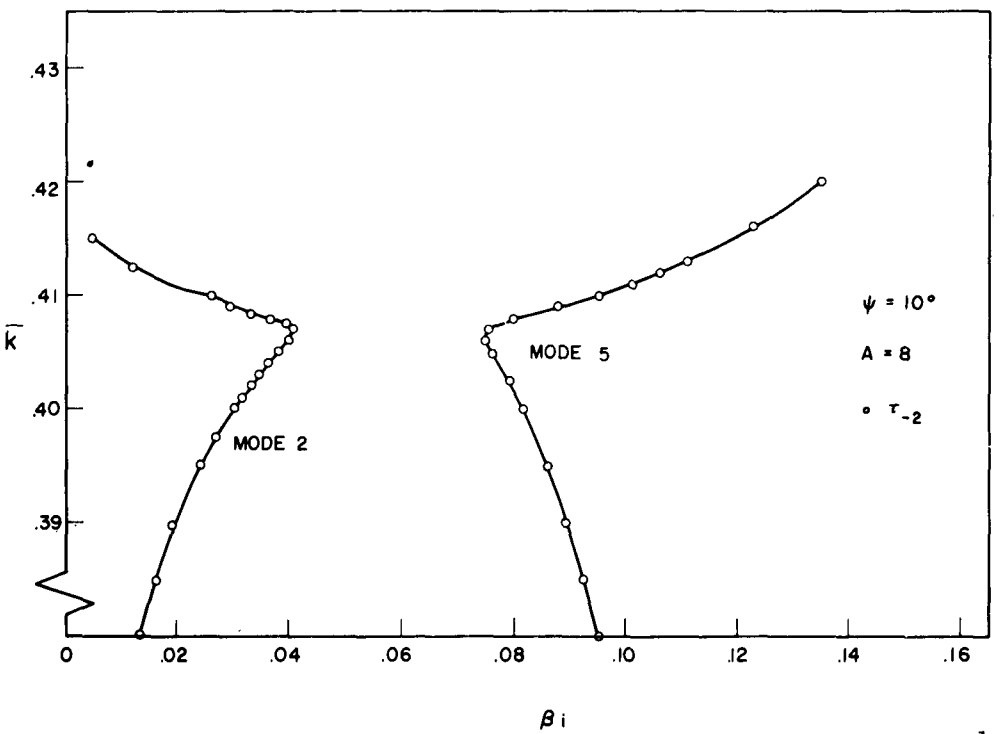

Figure 3.24b. The k - β_i diagram for simplified equation two near $\bar{k}^1_{c4}$; A = 8.0, $\psi = 10^o$.

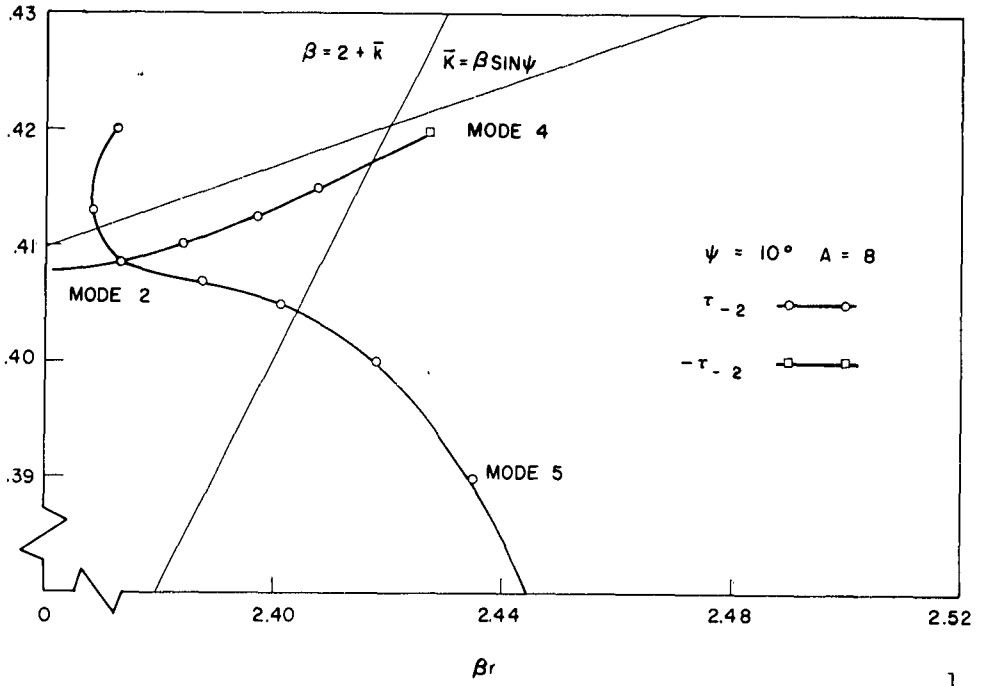

Figure 3.25a. The k - β_r diagram for simplified equation two near $\bar{k}_{c4}^{1}$; A = 10.0, $\Psi = 10^{o}$.

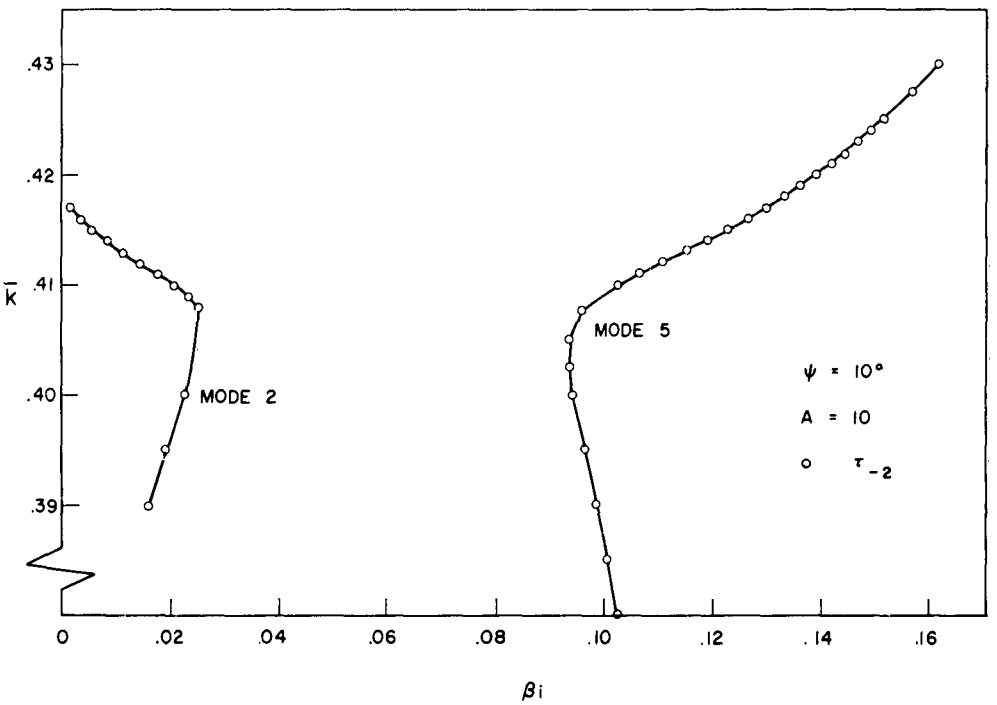

Figure 3.25b. The k - β_i diagram for simplified equation two near $\bar{k}_{c4}^{1}$ A = 10.0, $\Psi = 10^{o}$.

value of A is increased through the value A_{c2}. There is no question of discontinuity in the argument here since all arguments are of the same determination. Note that the character of the solutions changes in a continuous manner as a function of the parameter A. This type of behavior, as well as the behavior exhibited at the $\beta_r = 2 \pm \bar{k}$ lines, will be seen in the determinantal equation.

3.4 Summary

Two equations which are relatively simple compared to the determinantal equation and which, furthermore, exhibited some of the character of the determinantal equation were studied in this chapter. It was shown how discontinuities in the argument of IK product could result in solutions which would be continuous. If the discontinuities of the arguments are not introduced there is no continuation of the solutions. Further it was seen that the solutions for modes 2 and 4 changed character as a function of the parameter A.

The parameter A was chosen to be approximately equal to $2A_o$. As the tape width δ is made more narrow A_o increases. Consequently, the larger values of the parameter A correspond to the narrower tape widths.

Solutions for β which are complex valued have been found for both simplified equations. The use of complex roots will be discussed later.

The behavior of the solution of simplified equation one, Equation (3.2), for A = 1.0 is reminiscent of Pierce's coupled mode theory for the helix as discussed by Watkins[25]. However, as was pointed out in the discussion of equation one, the values of the parameter $A < A_{c1}$ correspond to tapes which are not narrow, i.e. too wide for the determinantal equation to be valid. The fact that the solutions for $A > A_{c1}$, which correspond to

narrow tapes, do not exhibit the character needed for Pierce's coupled mode theory inhibits the use of Pierce's simple theory.

Simplified equations one and two, Equation (3.2) and (3.3), are related to the determinantal equation for the sheath helix for sheath helix modes -1 and -2 respectively. The complex-valued solutions for the sheath helix and a discussion of their relation to the solutions for the tape helix are given by Klock and Mittra[29].

With the background obtained from studying the solutions of the two simplified equations one is now ready for the determinantal equation.

4. SOLUTION OF THE DETERMINANTAL EQUATION

4.1 Introduction

The determinantal equation

$$\frac{\beta^2 - \dfrac{\bar{k}^2}{\sin^2\psi}}{\bar{k}^2 \operatorname{ctn}^2 \psi} = \frac{A_{+1} + A_{-1} - 2A_o}{2A_o} \tag{4.1}$$

$$A_j = \sum_{n=-\infty}^{\infty} I_{n+j}(\tau_n)\, K_{n+j}(\tau_n)\, D_n$$

$$\tau_n = \left[(\beta + n)^2 - \bar{k}^2\right]^{1/2} \frac{a}{\bar{p}}$$

$$D_n = \frac{\sin\,(\beta+n)\,\dfrac{\delta}{2\bar{p}}}{(\beta+n)\,\dfrac{\delta}{2\bar{p}}}, \qquad \bar{k} = k\,\bar{p}$$

derived in Chapter 2 which is a complex-valued equation if β is complex-valued, was solved with the aid of a digital computer.

The determinantal equation can be written such that the complex-valued phase constant, β, is a function only of the parameters, normalized tape width, pitch angle, and normalized frequency. Symbolically, this is written as $\beta(\delta, \psi, \bar{k})$. The tape width is normalized with respect to the radius, i.e. $\delta = \frac{\delta}{a}$. The ratio $\frac{a}{\bar{p}}$ is replaced by its equal, $\operatorname{ctn}\psi$, so that Equation (4.1) reads

$$\frac{\beta^2 - \dfrac{\bar{k}^2}{\sin^2\psi}}{\bar{k}^2 \operatorname{ctn}^2 \psi} = \frac{A_{+1} + A_{-1} - 2A_o}{2A_o} \tag{4.2}$$

$$A_j = \sum_{n=-\infty}^{\infty} I_{n+j}(\tau_n)\, K_{n+j}(\tau_n)\, D_n$$

$$\tau_n = \left[(\beta+n)^2 - \bar{k}^2 \right]^{1/2} \operatorname{ctn} \psi$$

$$D_n = \frac{\sin\left[(\beta+n) \frac{\delta}{2} \operatorname{ctn} \psi \right]}{(\beta+n) \frac{\delta}{2} \operatorname{ctn} \psi}$$

Define $\alpha = \frac{\delta}{2} \operatorname{ctn} \psi$

The normalized frequency is $\bar{k} = \frac{ka}{\operatorname{ctn} \psi}$ where k is the free space wave number. By normalizing with respect to the radius one is able to reduce the study of the determinantal equation to the solution for the complex valued phase constant as a function of only normalized tape width, normalized frequency and pitch angle.

All of the coefficients in Equation (4.2) are real. Therefore, if $\beta = \beta_r + i\beta_i$ is a solution, then $\beta = \beta_r - i\beta_i$ is a solution. If the solution for the phase constant is $\beta = \beta_r - i\beta_i$, then the ϕ dependent fields are of the form $e^{-i\beta_r \phi}\, e^{-\beta_i \phi}$.

The real part of the phase constant, β_r, is a measure of the phase delay as the wave travels in the $+\phi$ direction and has units of radians per radian. The imaginary part of the phase constant, β_i, is a measure of the attenuation as the wave travels in the $+\phi$ direction and has units of nepers per radian.

The line $\bar{k} = \beta_r \sin \psi$ is shown on all the curves for β_i. This line separates the $\bar{k} - \beta_r$ diagram into two regions:

1) Points above the line represent waves which are traveling down the tape with a phase velocity greater than the velocity of light i.e. fast waves and

2) Points below the line represent waves which are traveling down the tape with a phase velocity less than the velocity of light, i.e. slow waves.

The lines $\beta_r = 1 \pm \bar{k}$ and $\beta_r = 2 \pm \bar{k}$ are shown. Between the lines $\beta_r = 1 \pm \bar{k}$ and between the lines $\beta_r = 2 \pm \bar{k}$ the arguments τ_{-1} and τ_{-2} respectively have non-zero real parts. Recall $\tau_n = [(\beta+n)^2 - \bar{k}^2]^{1/2} \frac{a}{\bar{p}}$.

4.2 Solutions

4.2.1 The $\bar{k}$ - β diagram. $\psi = 10^\circ$, $\bar{\delta} = .035$

Figures 4.1a, b, c, d and e is the $\bar{k}$ - β diagram for pitch angle 10° and $\bar{\delta} = .035$. The immediate observation is that for a value of $\bar{k}$ there exist more than one solution for β. The various solutions or modes each correspond to a different determination of a square root argument for the IK products.

The determination of the square roots was discussed in Section 2.4. Note that mode 1 has positive determination for both τ_{-1} and τ_{-2}. All the other modes have the negative determination for τ_{-1}. Modes 2,3, and 5 have the positive determination and modes 4 and 6 have the negative determination for τ_{-2}.

In the regions $\beta_r \simeq 1$ and $\beta_r \simeq 2$ the solution behaves similarly to the solution of the simplified equations studied in Sections 4.2 and 4.3 respectively.

The constants $\bar{k}_{c1}$ and $\bar{k}_{c2}$ are defined as in Section 4.2 and 4.3 respectively.

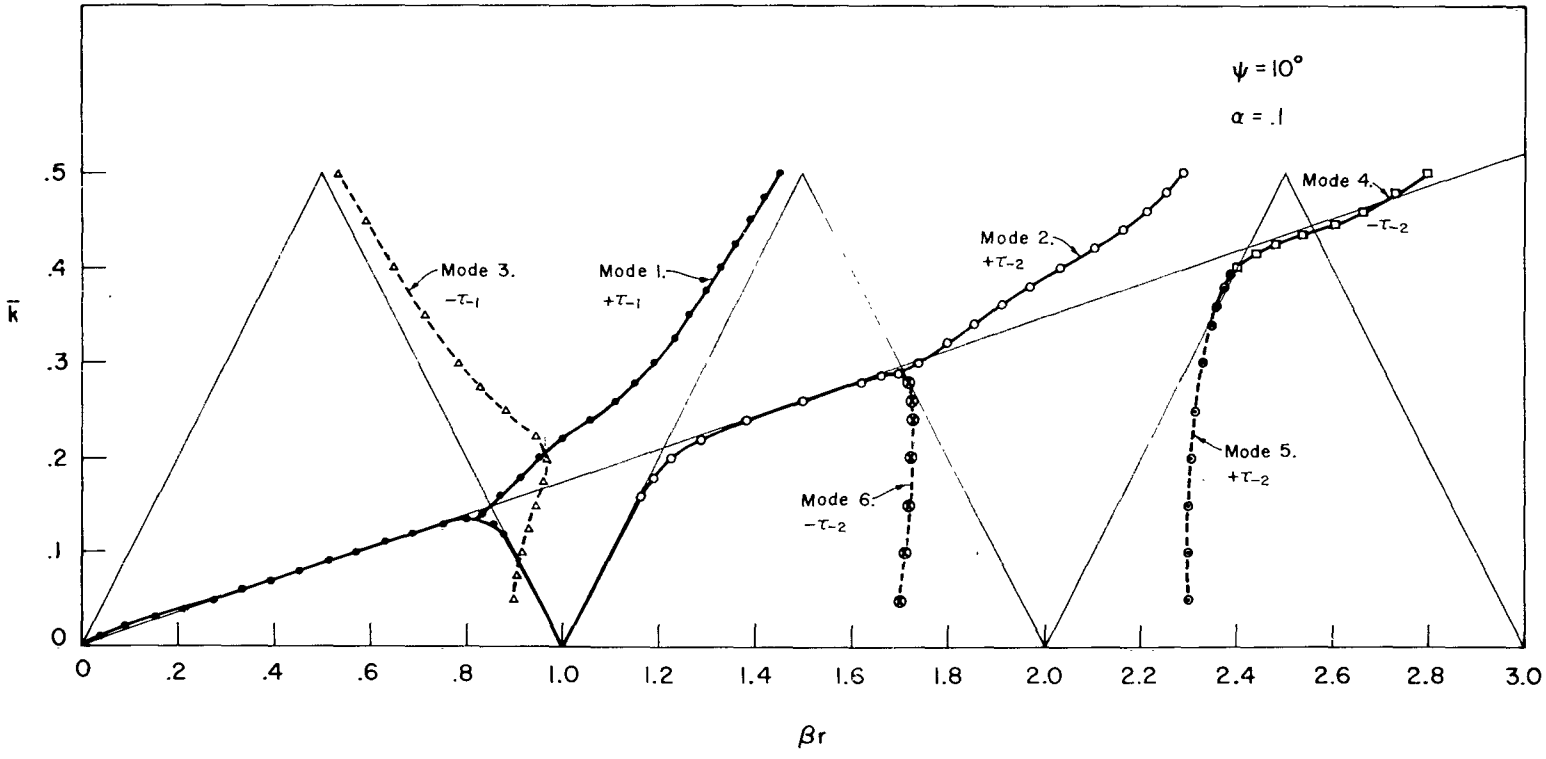

Figure 4.1a. The complete $k - \beta_r$ diagram for the tape helix: $\psi = 10$, $\alpha = .1$.

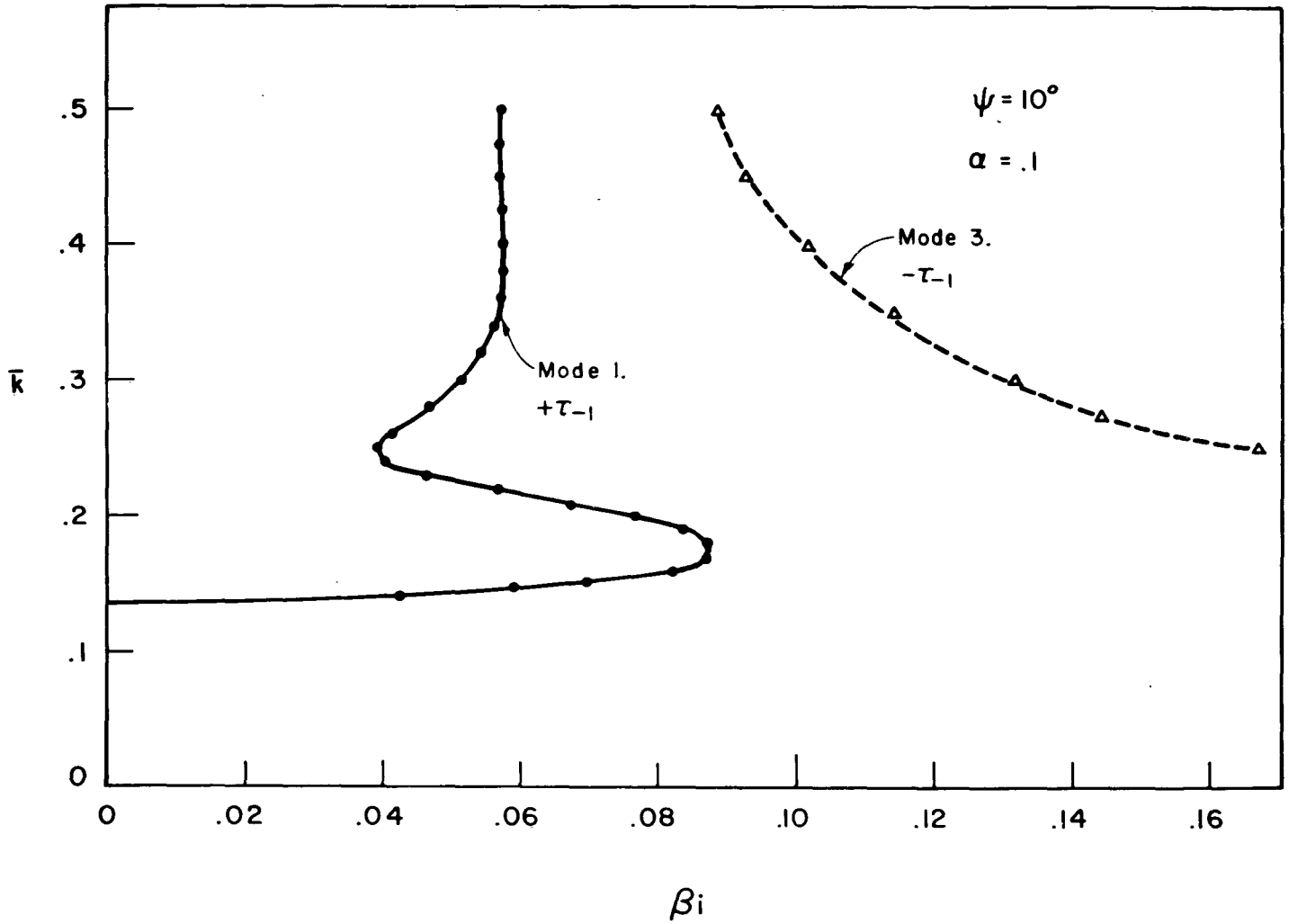

Figure 4.1b. The $k - \beta_i$ diagram for the tape helix: Modes 2 and 3; $\Psi = 10$, $\alpha = .1$.

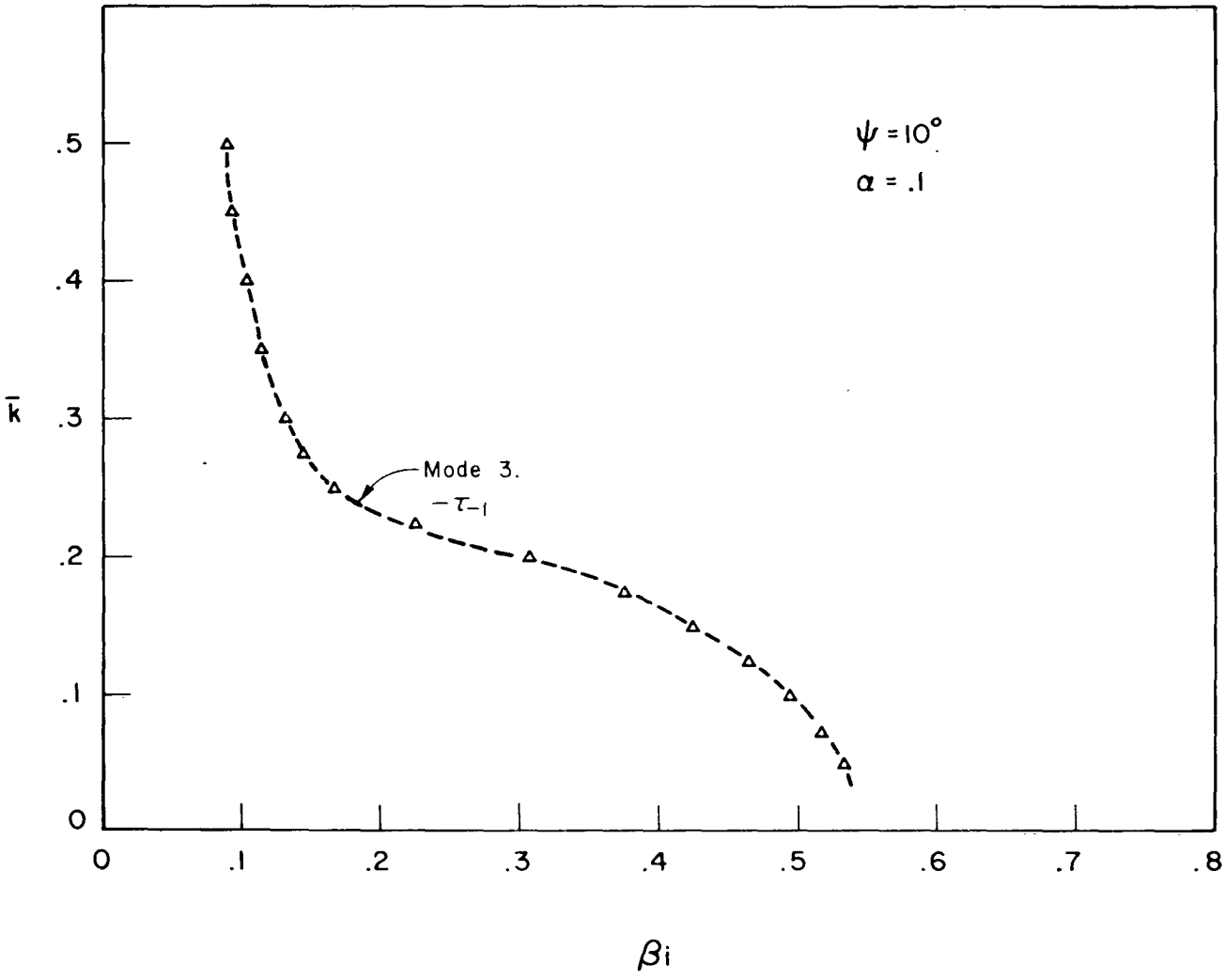

Figure 4.1c. The $k - \beta_1$ diagram for the tape helix. Mode 3; $\psi = 10$, $\alpha = .1$.

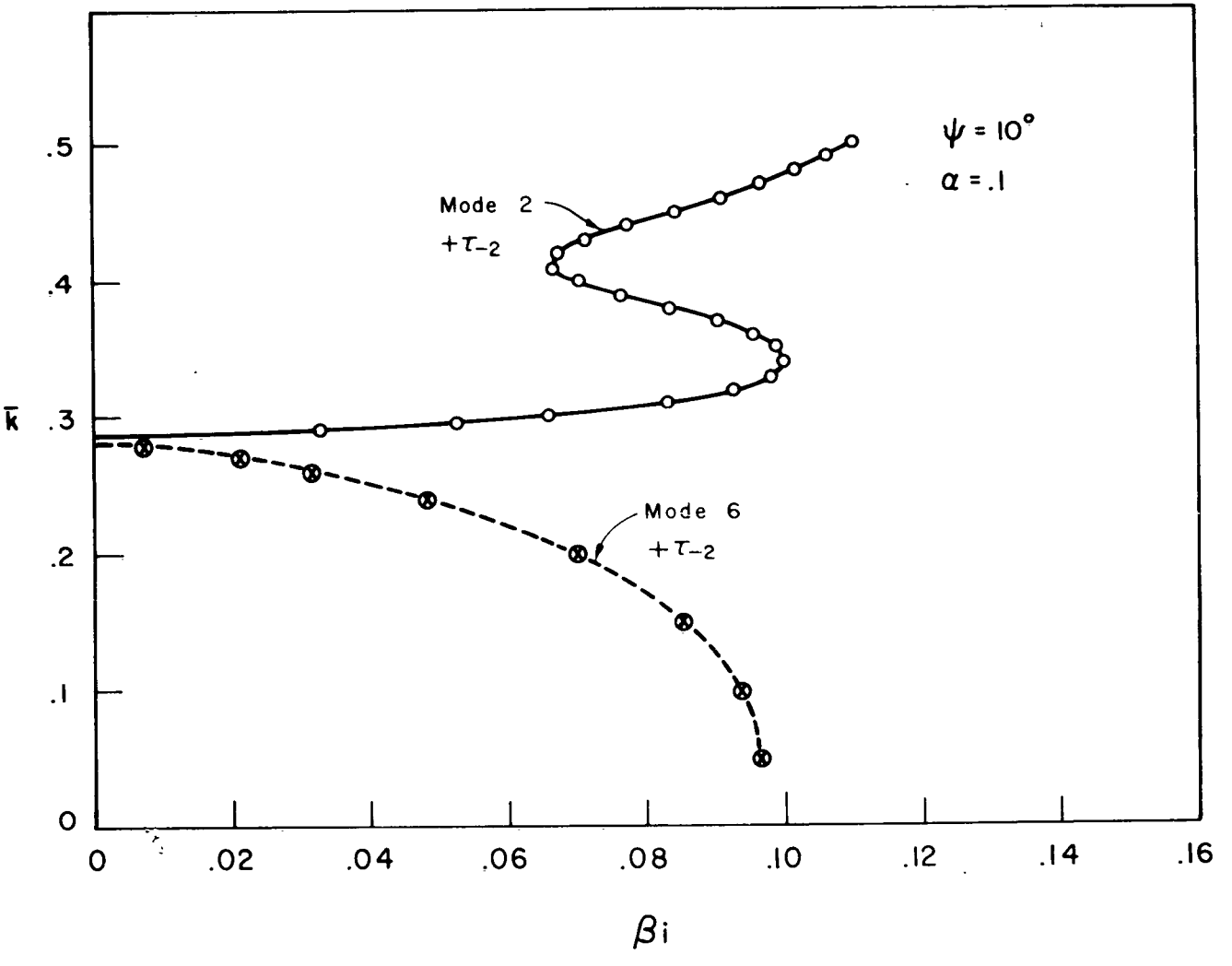

Figure 4.1d. The k - β_i diagram for the tape helix: Modes 2 and 6; Ψ = 10, α = .1.

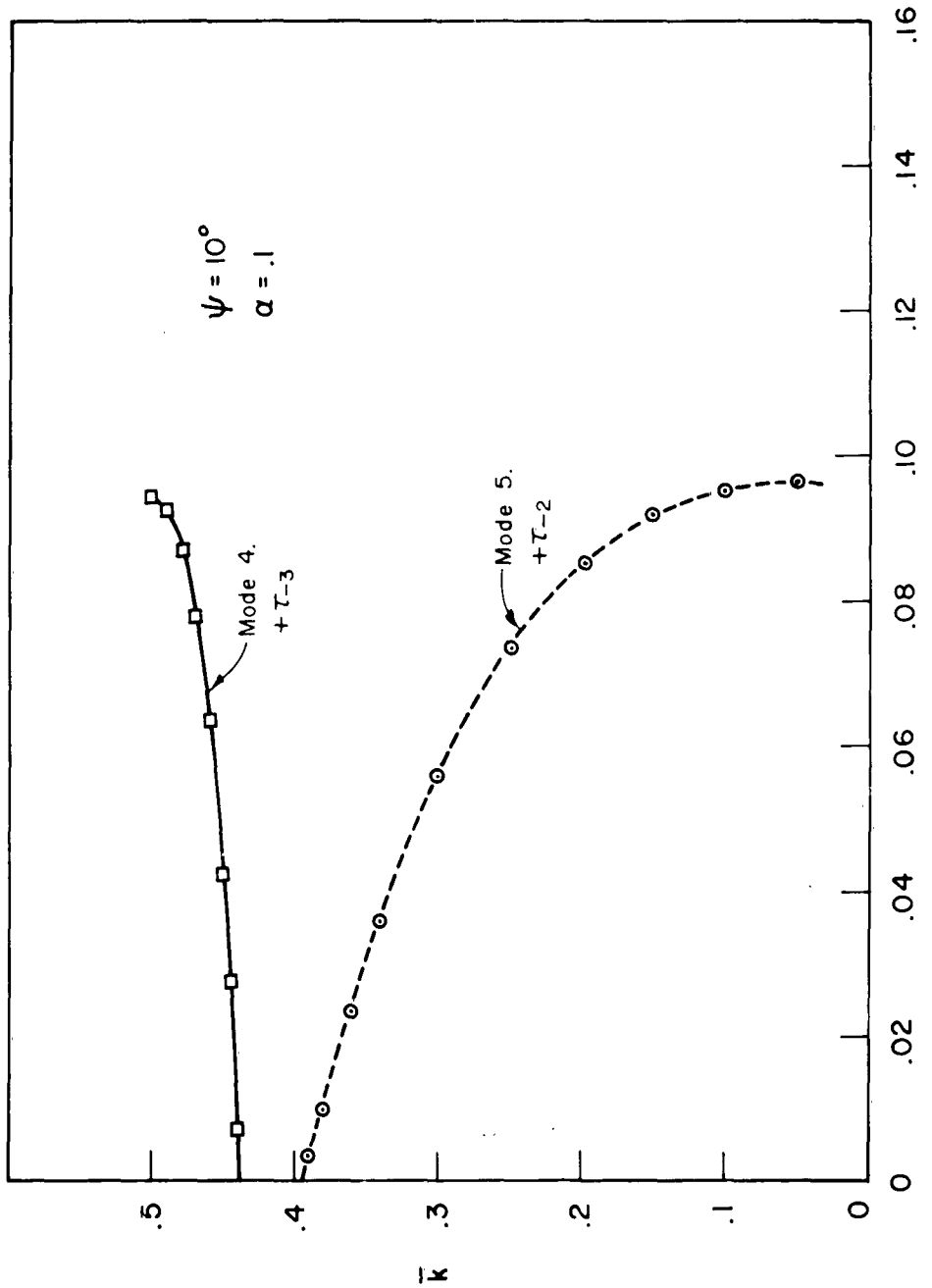

Figure 4.1e. The $\bar{k}$ - β_1 diagram for the tape helix. Modes 4 and 5; $\psi = 10°$, $\alpha = .1$.

The solutions for mode 1, $\bar{k} < \bar{k}_{c1}$, mode 2, $\bar{k} < \bar{k}_{c2}$; and mode 4, $\bar{k} < \bar{k}_{c4}$; correspond and agree with the results obtained by Sensiper. All other solutions have non-zero imaginary parts.

4.2.2 Mode 1 Solution. $\Psi = 12.6^{o}$, $\alpha = 10^{-308}, .0001, .1, .4$,

The solutions for mode 1 as a function of $\bar{\delta}$ are shown in Figures 4.2a and b. As the tape is made more narrow the real part of the phase constant tends toward the $\bar{k} = \beta_r \sin\Psi$ line as would be predicted for an infinitesimally narrow tape or filament. The maximum value of the imaginary part of the phase constant increases as the tape is made wider. The imaginary part of the phase constant increases rapidly as $\bar{k}$ is increased from $\bar{k}_{c1}$. The behavior of the solution changes quite fast for a small change in normalized frequency.

Expanded views for a range of $\bar{k}$ near $\bar{k}_{c1}$ are shown in Figures 4.3a and b. As the tape is made more narrow, $\bar{k}_{c1}$ increases with $\bar{k}_{c1}$ approaching $\frac{\sin\Psi}{1+\sin\Psi}$ as $\bar{\delta}$ tends toward zero.

4.2.3 Mode 1 Solution. $\bar{\delta} = .035$, various pitch angles

The solutions for mode 1 for various pitch angles for fixed tape width, $\bar{\delta} = .035$, are shown in Figures 4.4a and b. As the pitch angle is increased the β_r locus deviates less from the $\bar{k} = \beta_r \sin\Psi$ line. This result seems reasonable physically since as the pitch angle is increased a section of unit length of the helix is becoming more nearly a straight wire. Also note that as pitch angle is increased the imaginary part of the phase constant decreases.

4.2.4 Mode 3 Solution. $\Psi = 12.6^{o}$, $\alpha = 10^{-308}, .0001, .1, .4$

Figures 4.6a and b shows the mode 3 solutions as a function of tape width. Note that the imaginary part of the phase constant is now to a

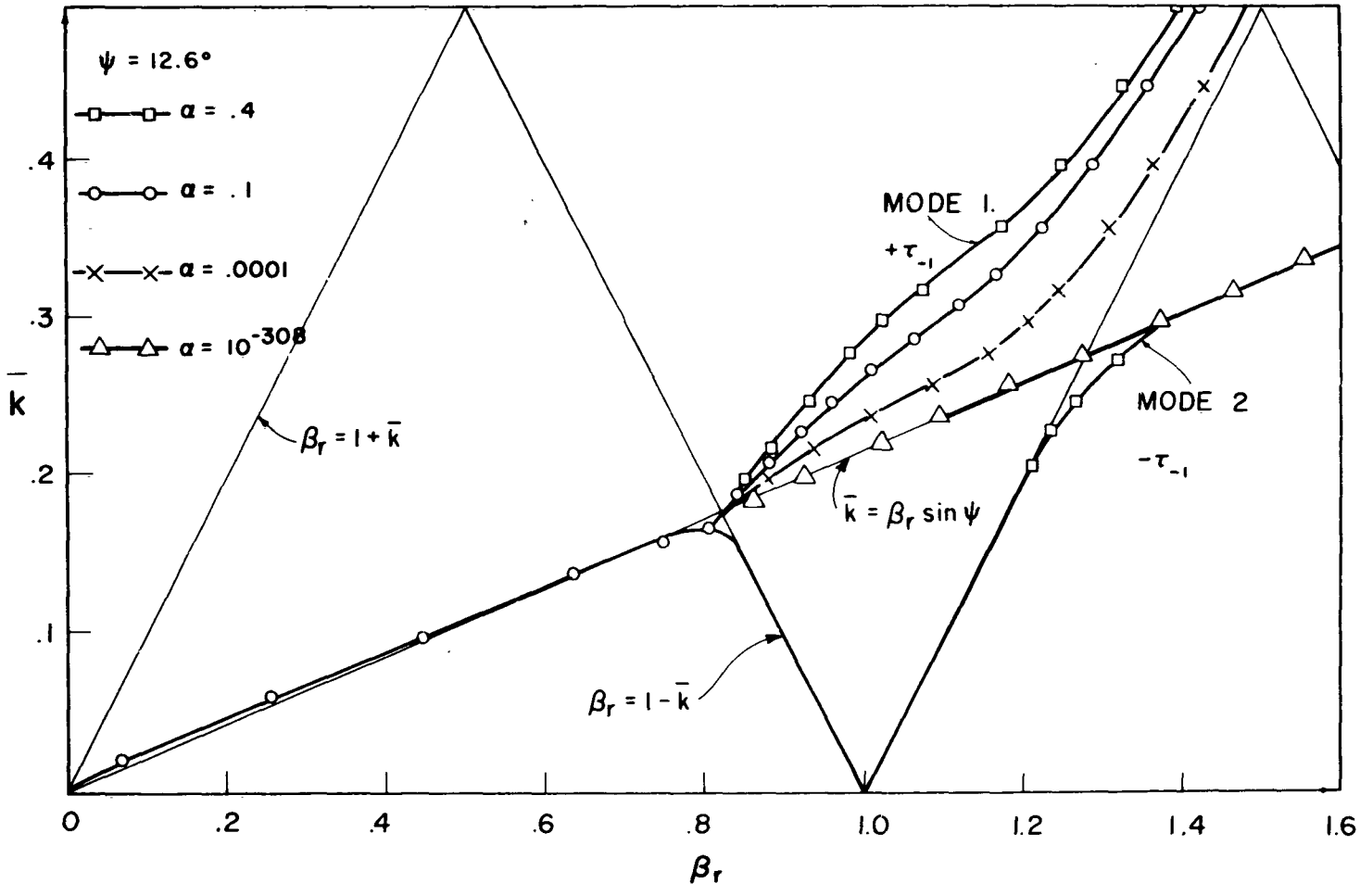

Figure 4.2a. The k - β_r diagram for the tape helix: Modes 1 and 2; $\psi = 12.6^{\circ}$, $\alpha = 10^{-308}$, .0001, .1, .4.

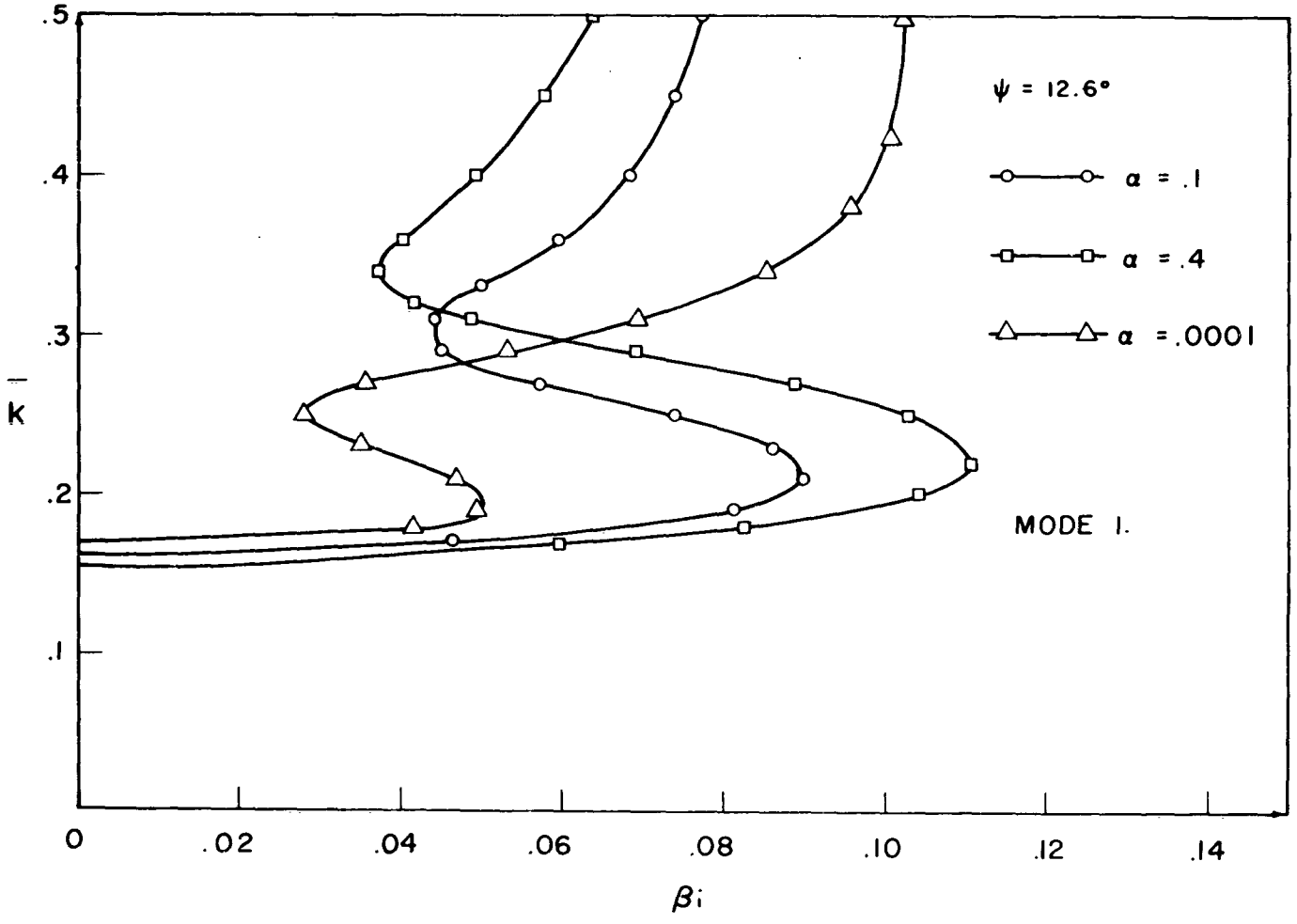

Figure 4.2b. The $k - \beta_i$ diagram for the tape helix: Mode 1; $\psi = 12.6^o$, $\alpha = 10^{-30}$, .0001, .1, .4.

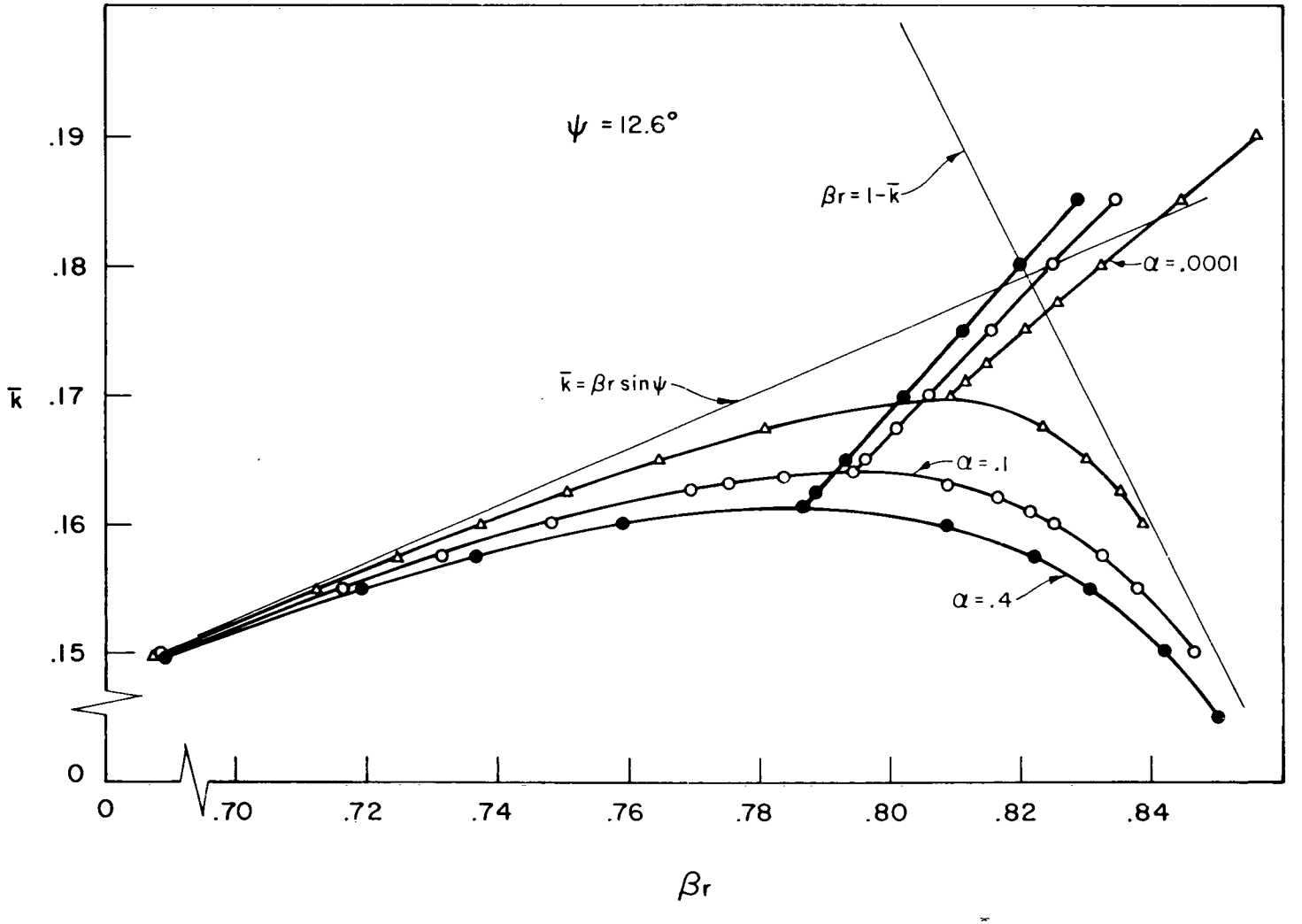

Figure 4.3a. The $k - \beta_r$ diagram for the tape helix near $\bar{k}_{cl}$; Mode 1; $\psi = 12.6^{\circ}$, $\alpha = 10^{-308}$, .0001, .1, .4.

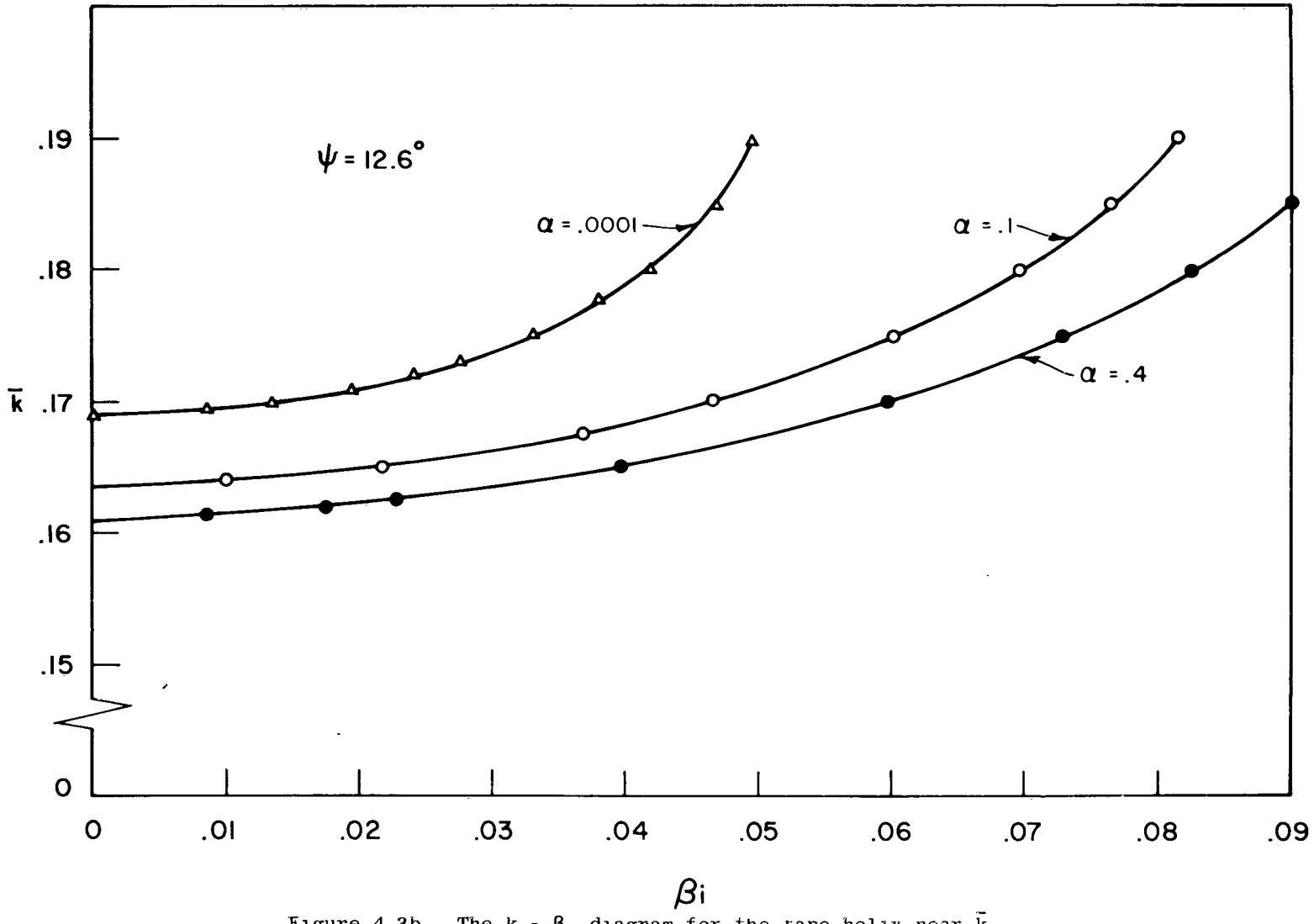

Figure 4.3b. The k - β_i diagram for the rape helix near $\bar{k}_{c1}$, Mode 1; $\psi^1 = 12.6^\circ$, $\alpha = 10^{-308}$, .0001, .1, .4.

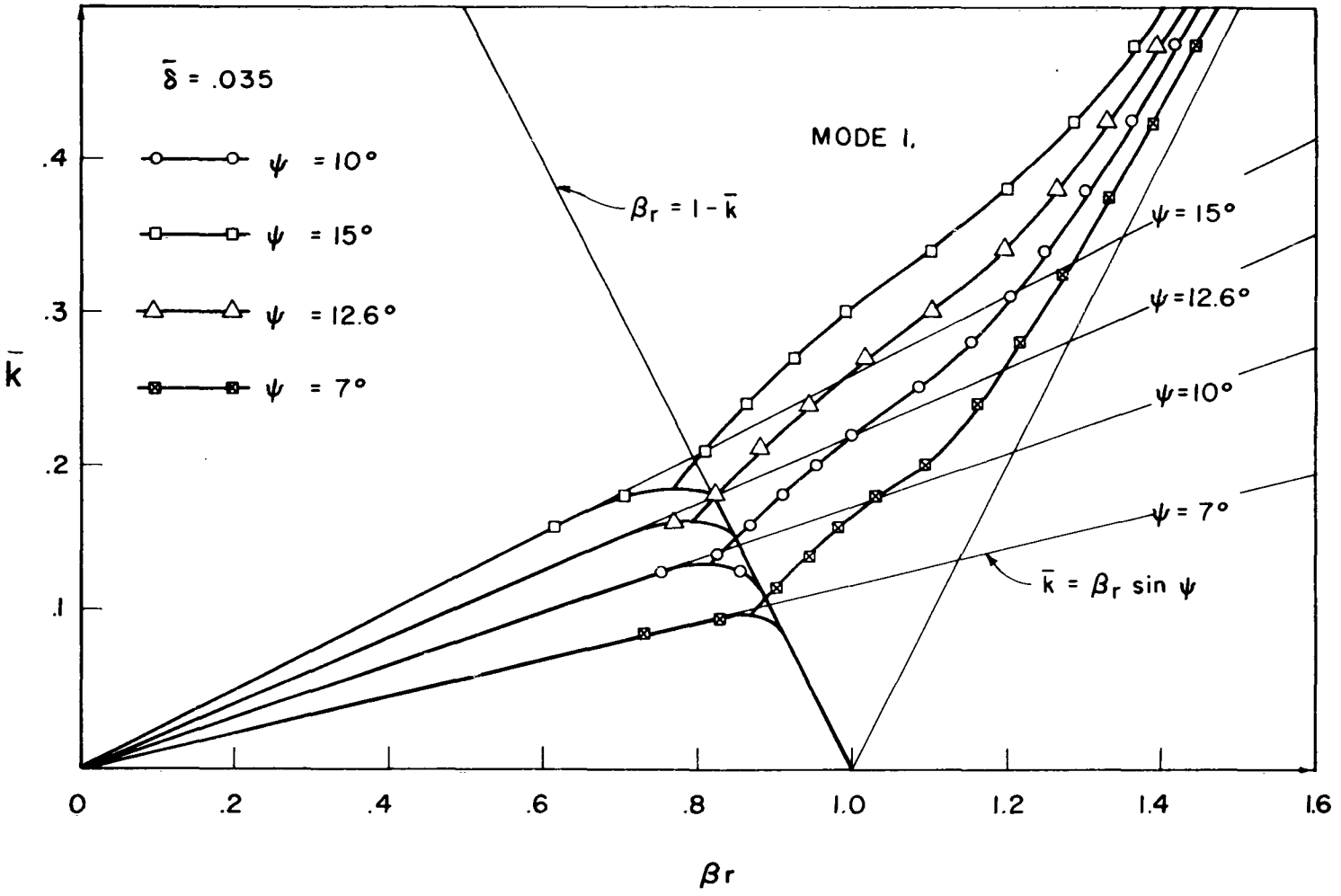

Figure 4.4a. The k - β_r diagram for the tape helix: Mode 1; $\bar{\delta}$ = .035, ψ = 7°, 10°, 12.6°, 15°.

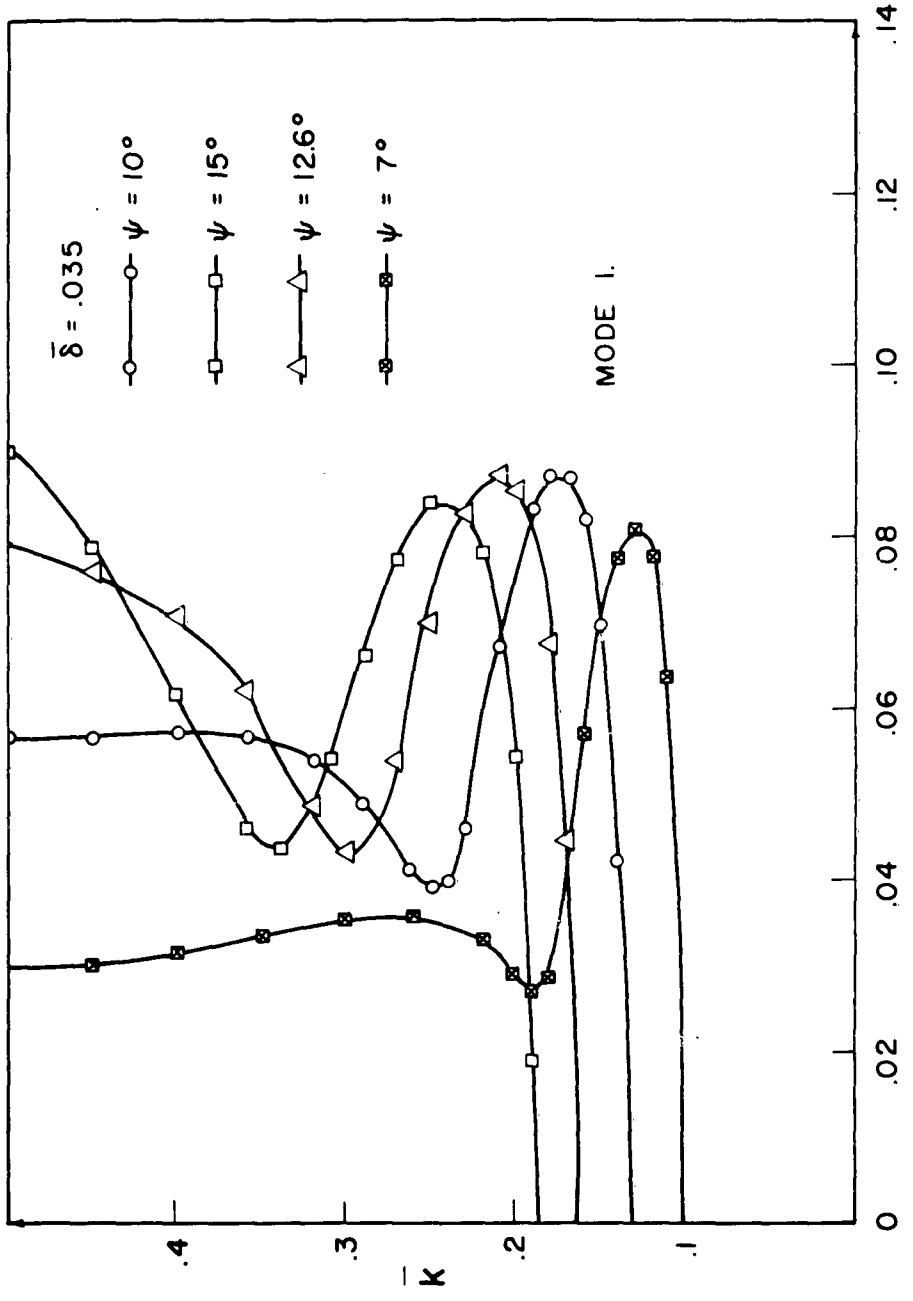

Figure 4.4b. The k - β_i diagram for the tape helix: Mode 1; $\bar{\delta}$ = .035, ψ = 7°, 10°, 12.6°, 15°.

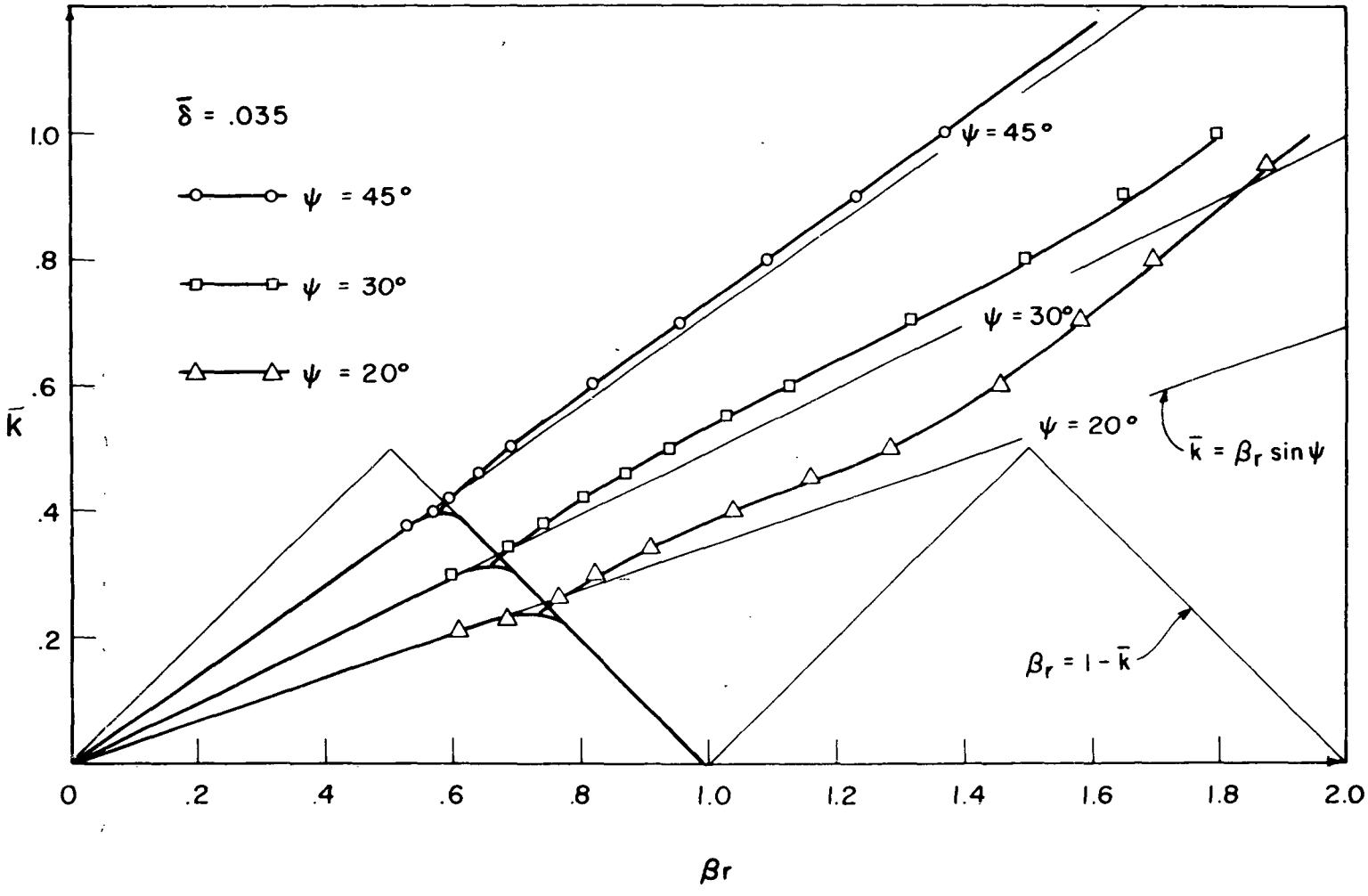

Figure 4.5a. The k - β_r diagram for the tape helix: Mode 1; $\bar{\delta}$ = .035, ψ = 20°, 30°, 45°.

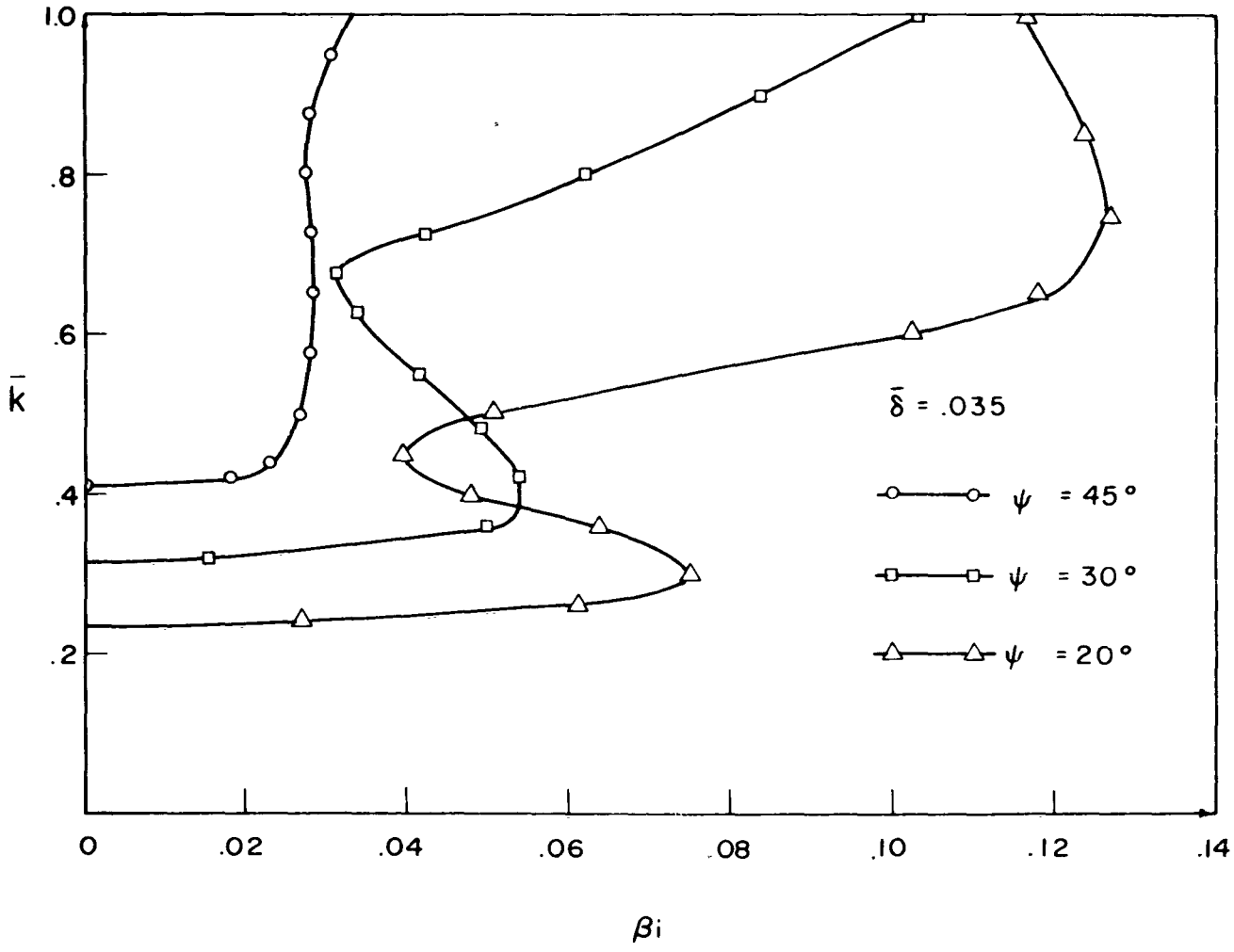

Figure 4.5b. The $k - \beta_i$ diagram for the tape helix: Mode 1; $\bar{\delta} = .035$, $\psi = 20^\circ$, 30°, 45°.

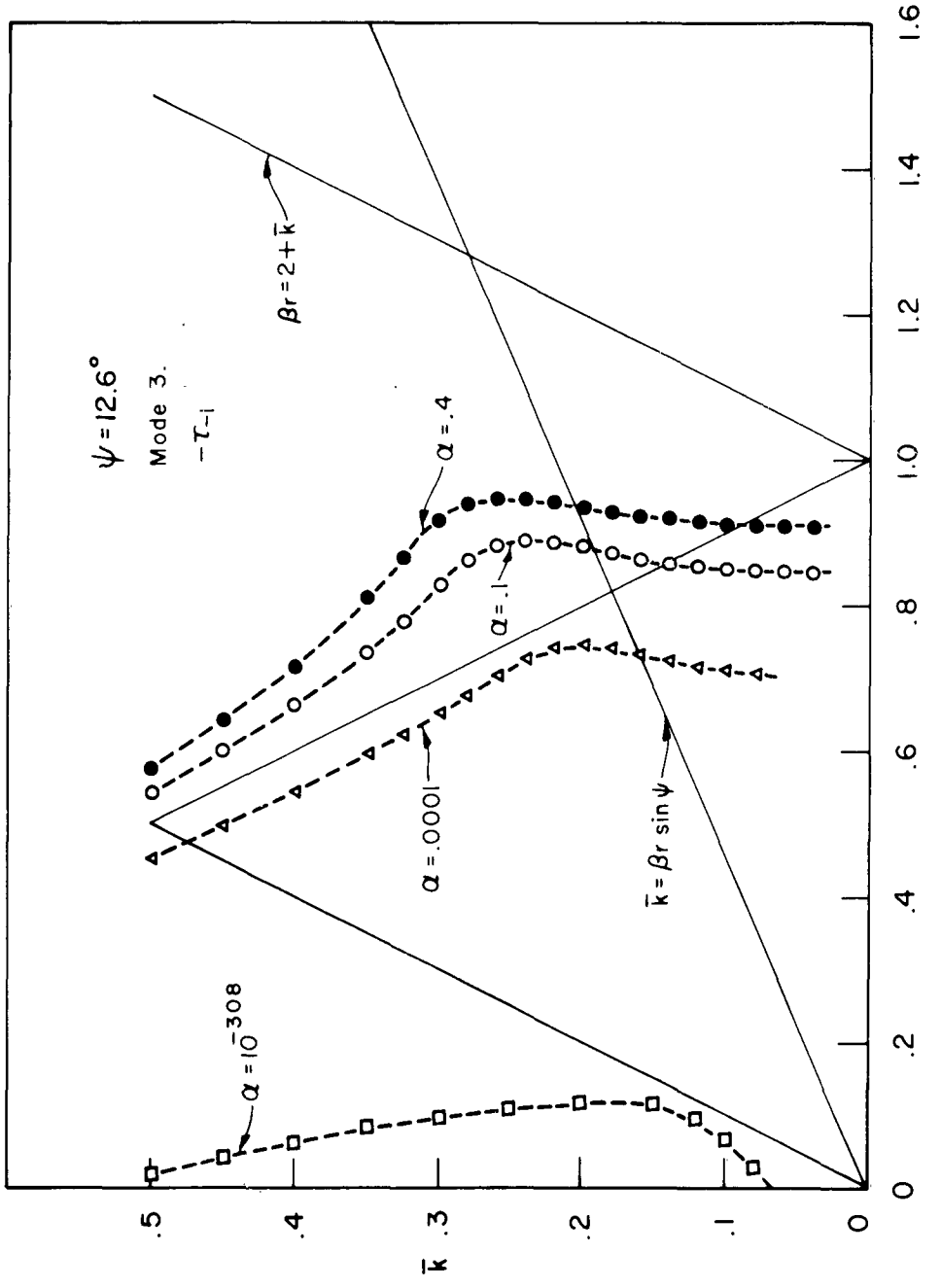

Figure 4.6a. The k β_r diagram for the tape helix Mode 3; $\psi = 12.6^0$, $\alpha = 10^{-308}$, .0001, .1, .4

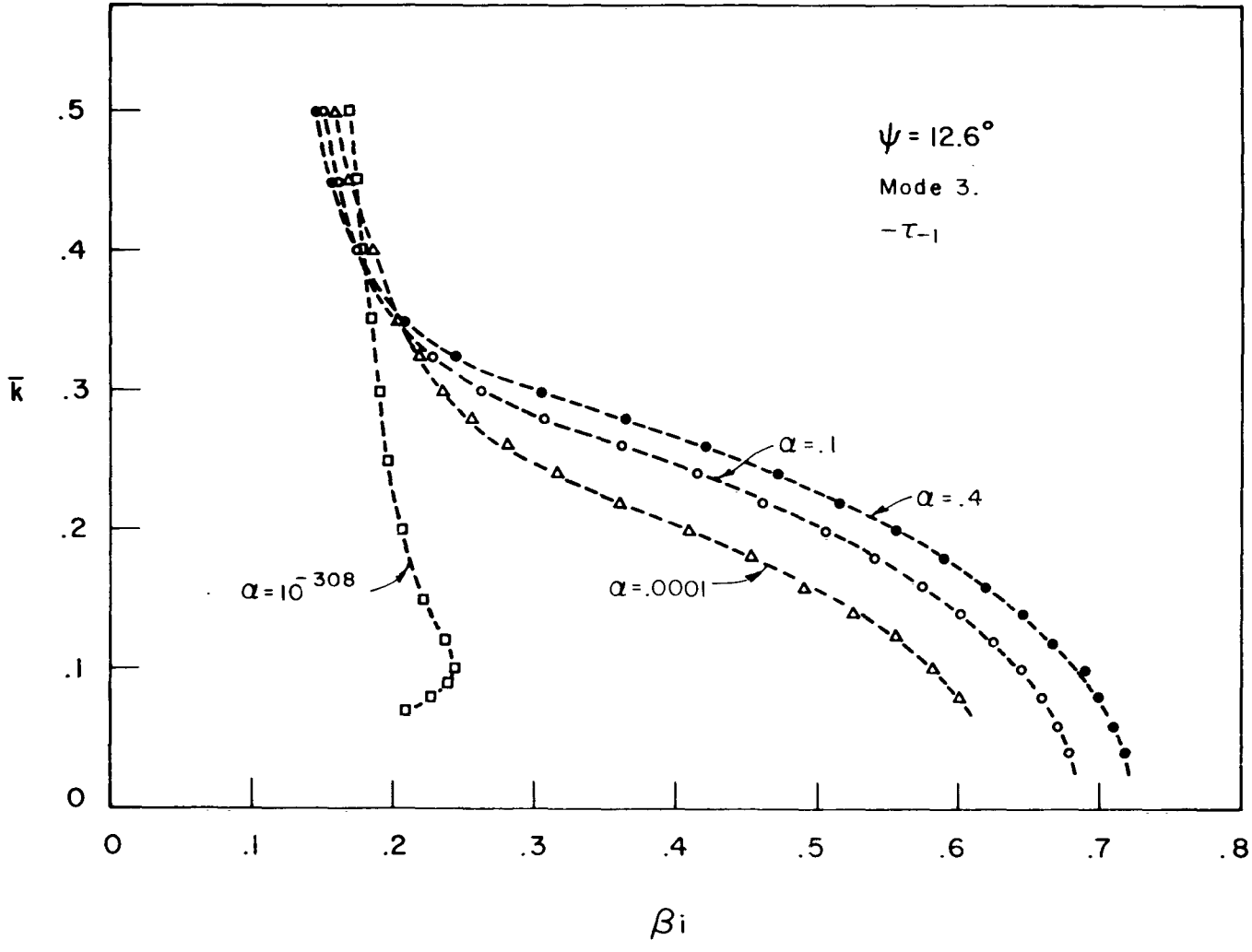

Figure 4.6b. The k - β diagram for the tape helix. Mode 3; $\Psi = 12.6^{o}1$, $\alpha = 10^{-308}$, .0001, .1, .4.

different scale since β_1 is larger than it is for any other mode.

4.2.5 Modes 2 and 6. $\Psi = 12.6$, $\alpha = 10^{-308}, .0001, .1, .4$

The solution for modes 2 and 6 are shown in Figures 4.7a and b. Figures 4.8a and b show an expanded view for a range of $\bar{k}$ values near $\bar{k}_{c2}$. The behavior for mode 2 above $\bar{k}_{c2}$ is similar to the behavior for mode 1 above $\bar{k}_{c1}$. In contrast to mode 1 behavior, the behavior of the solution with zero imaginary part does not approach the line $\beta = 2 - \bar{k}$ asymptotically but terminates at the line. To find a continuous solution, the determination of τ_{-2} must be changed. This type of behavior was exhibited by simplified equation two, Equation (3.3).

4.2.6 Modes 4 and 5: $\Psi = 10^{\circ}$, $\alpha = ,10^{-308}, .0001, .4$, $\Psi = 12.6^{\circ}$, $\alpha = .1$

Modes 4 and 5 exhibit behavior as shown in Figures 4.9a and b. The solution for mode 4 terminates on the line $\beta_r = 2+\bar{k}$. To have a continuous solution the determination of τ_{-2} must be changed as in simplified equation two, Equation (3.3.1). Figures 4.10a and b give the results for modes 4 and 5 for different parameters. The solution exhibits the same character as for the previous parameters.

4.2.7 Modes 2,4, and 5: $\Psi = 10^{\circ}$, $\beta_r \simeq 2.4$, $\alpha = 10^{-10}, 10^{-15}, 10^{-17}, 10^{-20}, 10^{-29}$

In Figure 4.11a through Figure 4.15b are shown the change of character of the solution that modes 2, 4, and 5 exhibit as the tape width is changed. If the tape is made sufficiently narrow, mode 2 terminates on the line $\beta = 2 + \bar{k}$ and connects in a continuous manner to mode 4. This is exactly the same behavior as was shown by simplified equation two, Equation (3.3).

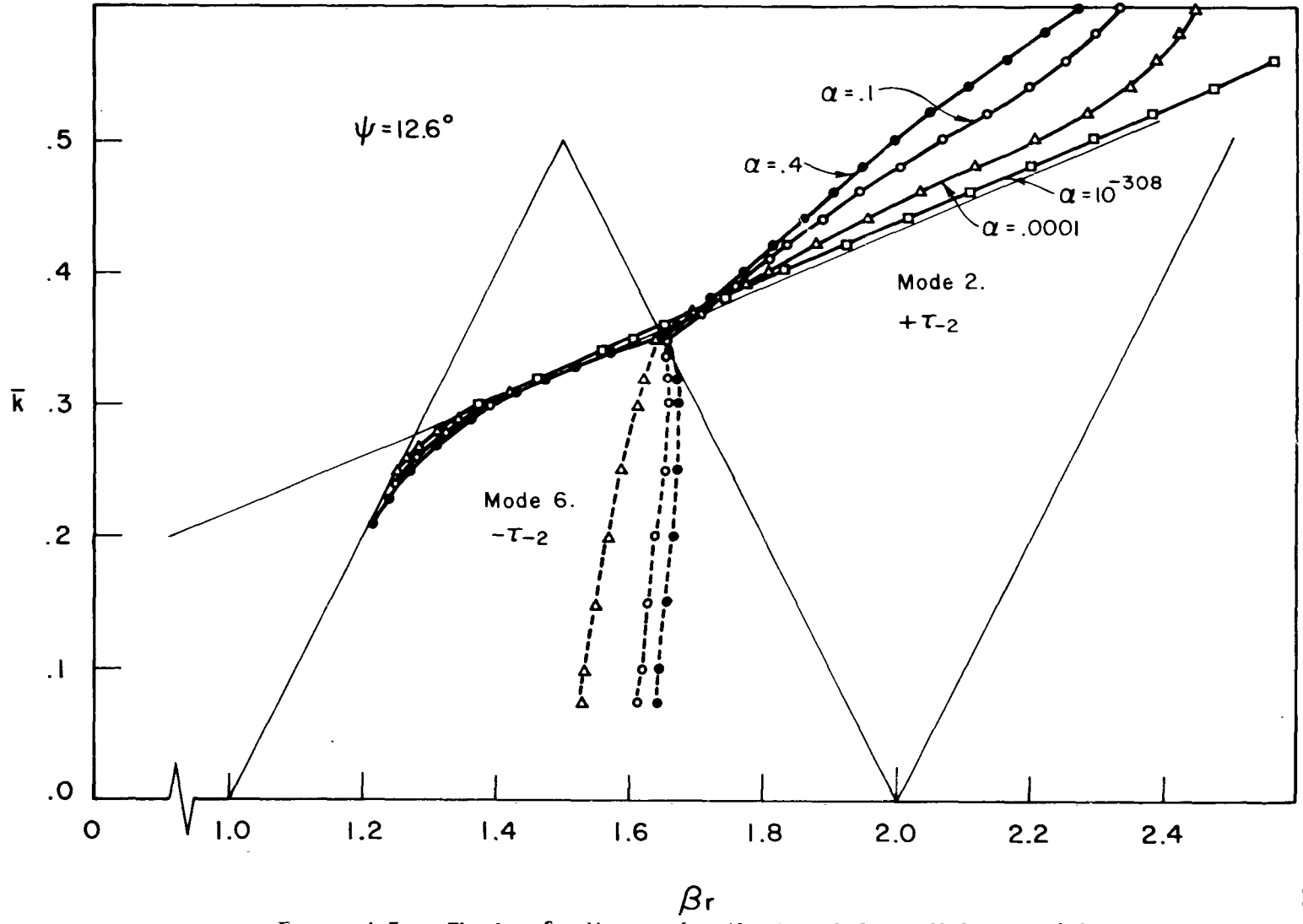

Figure 4.7a. The k - β_r diagram for the tape helix: Modes 2 and 6; $\psi = 12.6^o$, $\alpha = 10^{-308}$, .0001, .1, .4.

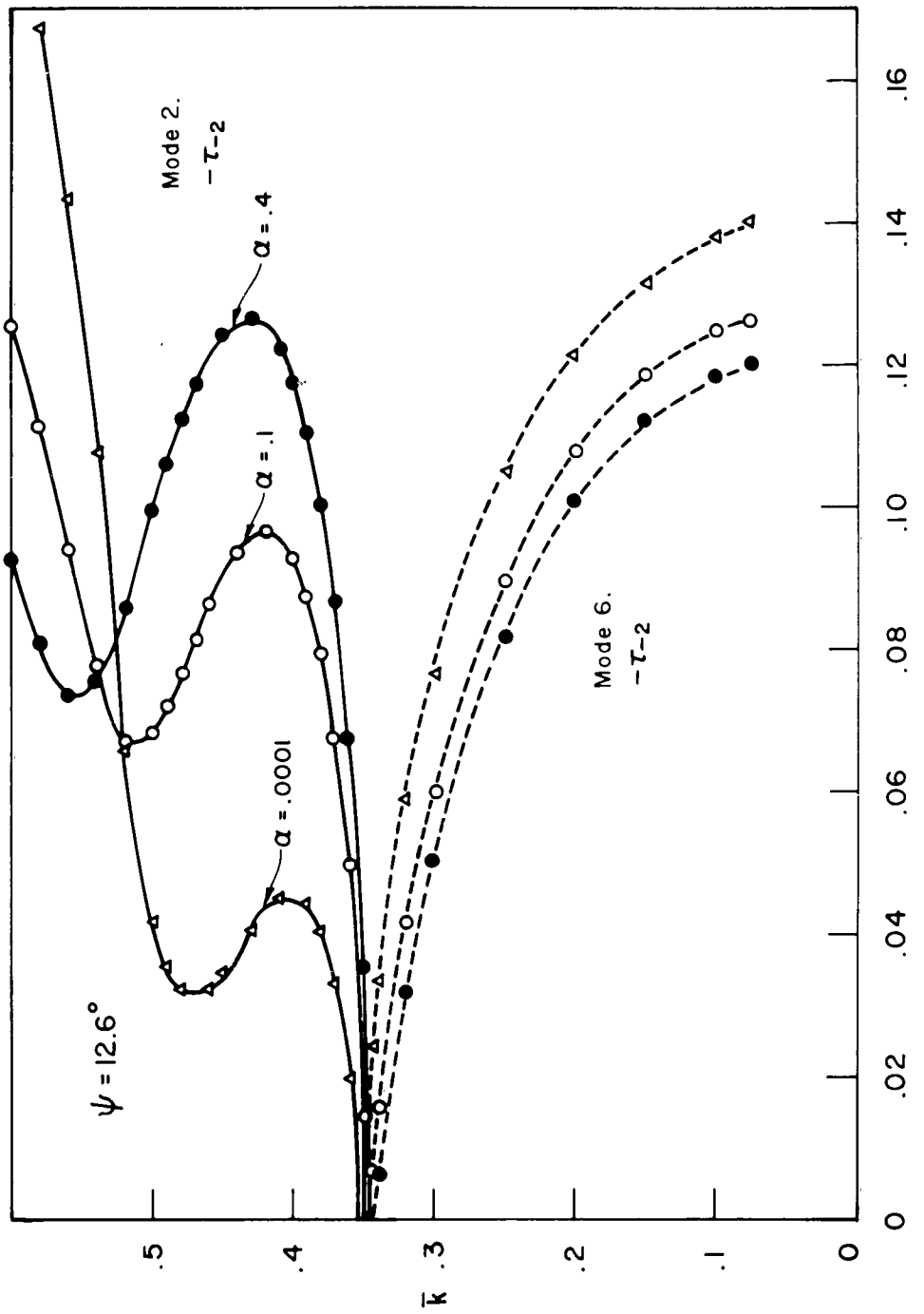

Figure 4.7b. The $k - \beta_i$ diagram for the tape helix: Modes 2 and 6; $\psi = 12.6°$, $\alpha = 10^{-308}$, .0001, .1, .4.

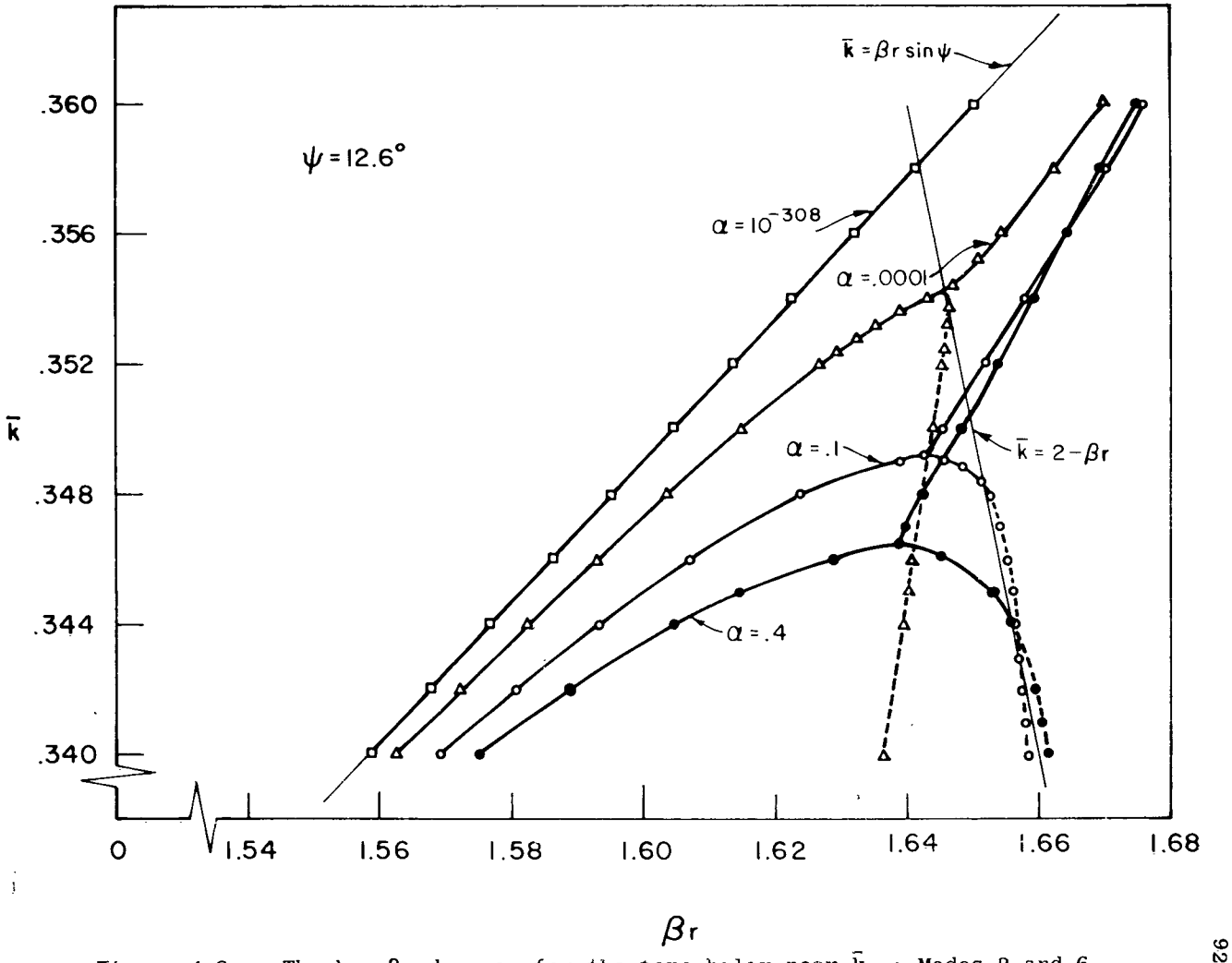

Figure 4.8a. The $k - \beta_r$ diagram for the tape helix near $\bar{k}_{c2}$: Modes 2 and 6, $\psi = 12.6°$, $\alpha = 10^{-308}$, .0001, 1, .4.

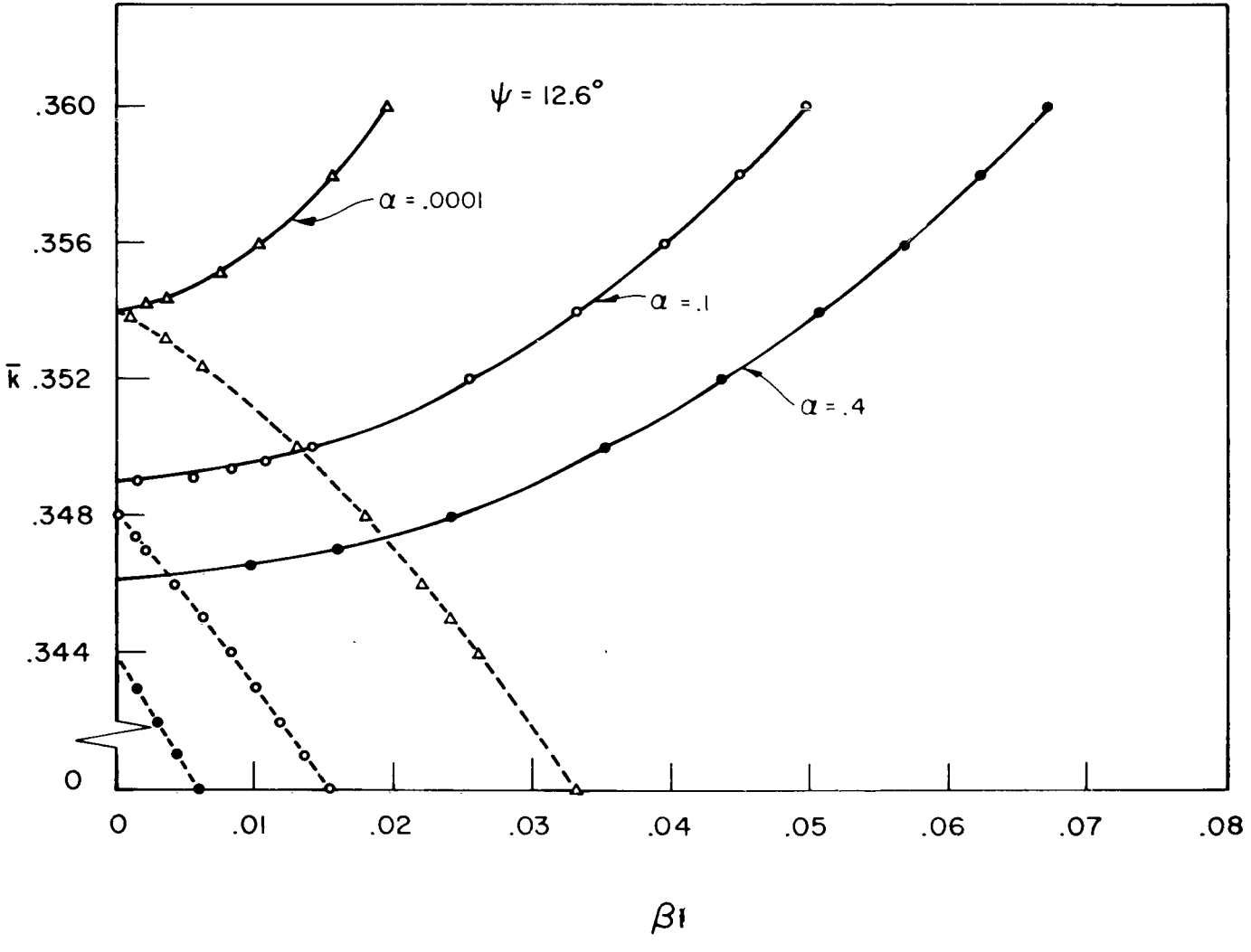

Figure 4.8b. The k - β_1 diagram for the tape helix near $\bar{k}_{c2}$ Modes 2 and 6; $\psi = 12.6^{o}$, $\alpha = 10^{-308}$, .0001, .1, 4

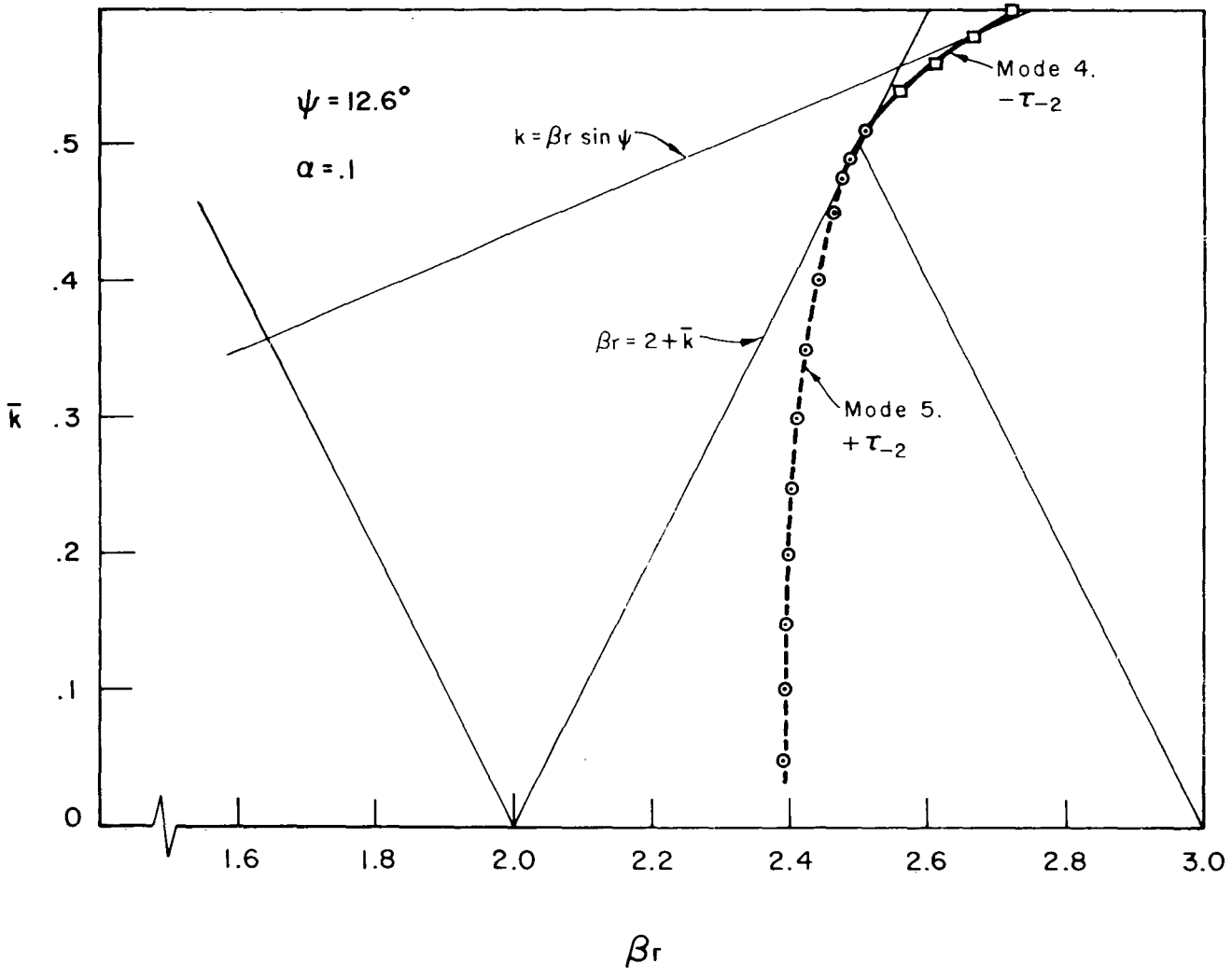

Figure 4.9a. The k - β_r diagram for the tape helix Modes 4 and 5; $\Psi = 12\ 6^{o}$, $\alpha = .1$.

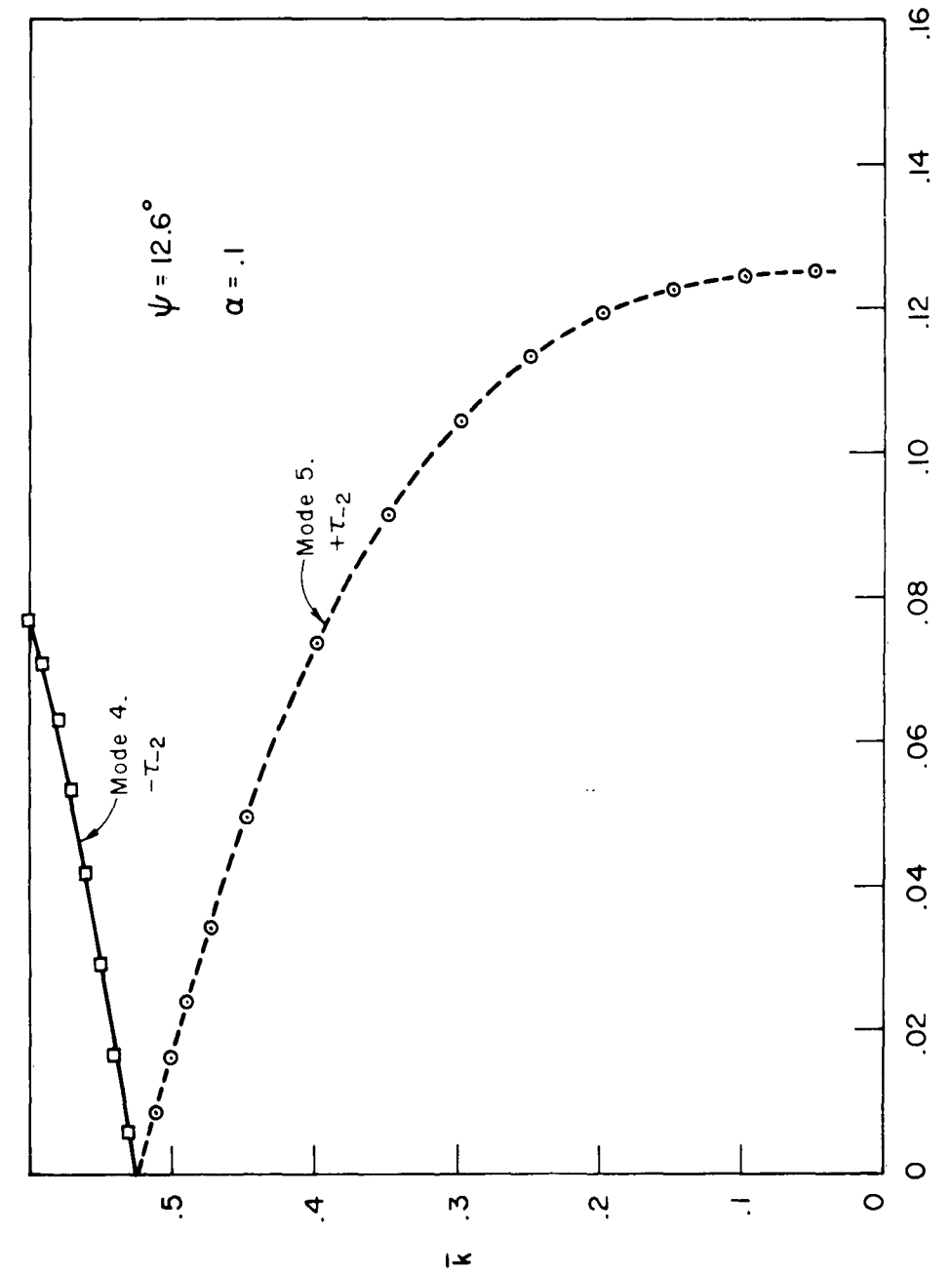

Figure 4.9b The k - β_1 diagram for the tape helix Modes 4 and 5; ψ = 12.6°, α = .1

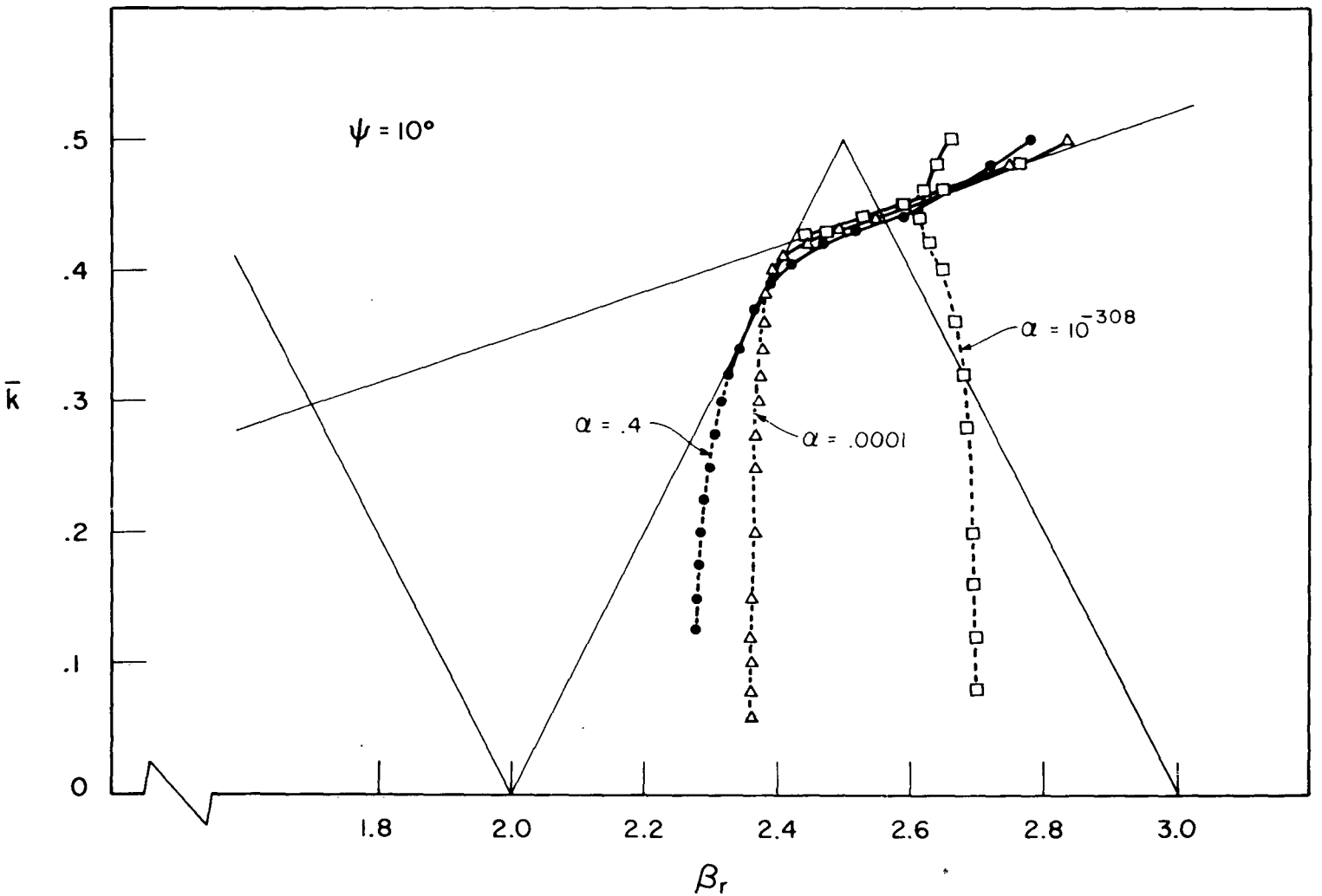

Figure 4.10a The k - β_r diagram for the tape helix. Modes 4 and 5; $\psi = 10^o$, $\alpha = 10^{-308}$, .0001, .4.

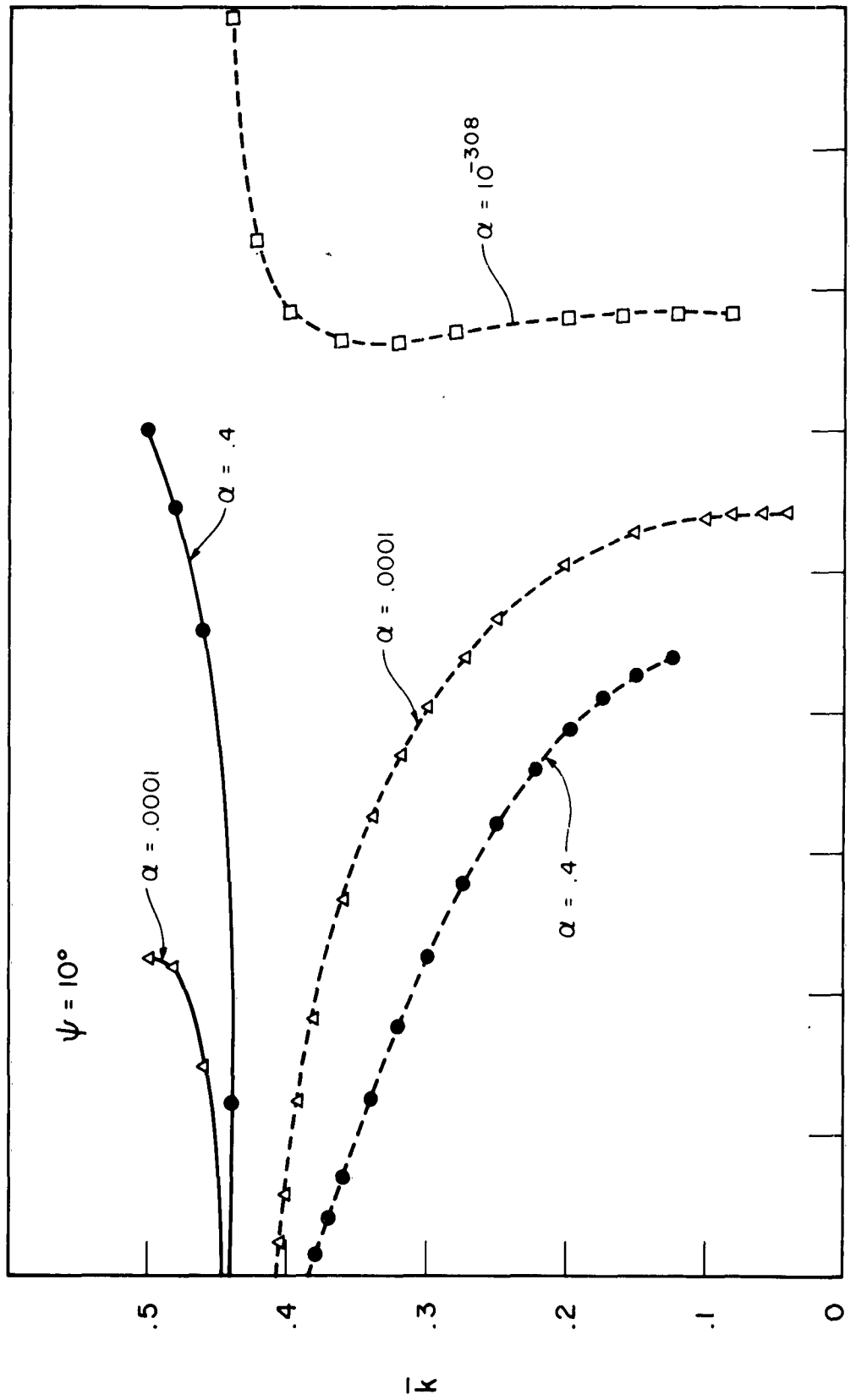

Figure 4.10b. The k - β_1 diagram for the tape helix Modes 4 and 5; $\psi = 10^{\circ}$, $\alpha = 10^{-308}$, .0001, .4.

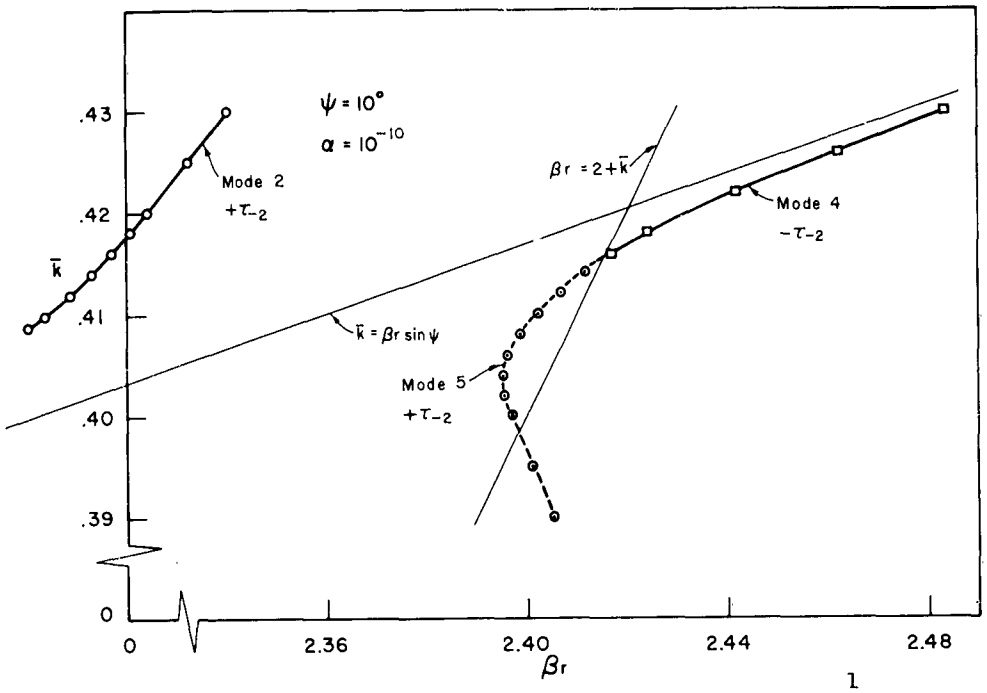

Figure 4.11a. The k - β_r diagram for the tape helix near $\bar{k}_{c4}^{-1}$: Mode 2, 4 and 5; $\psi = 10^{o}$, $\alpha = 10^{-10}$.

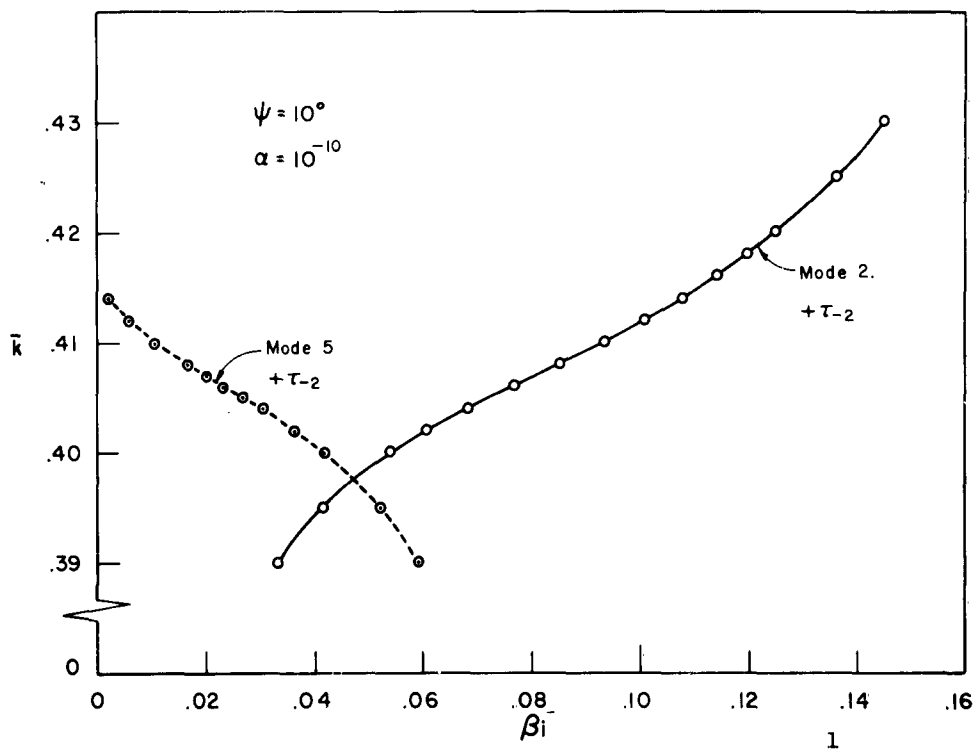

Figure 4.11b. The k - β_i diagram for the tape helix near $\bar{k}_{c4}^{-1}$: Modes 2, 4 and 5; $\psi = 10^{o}$, $\alpha = 10^{-10}$.

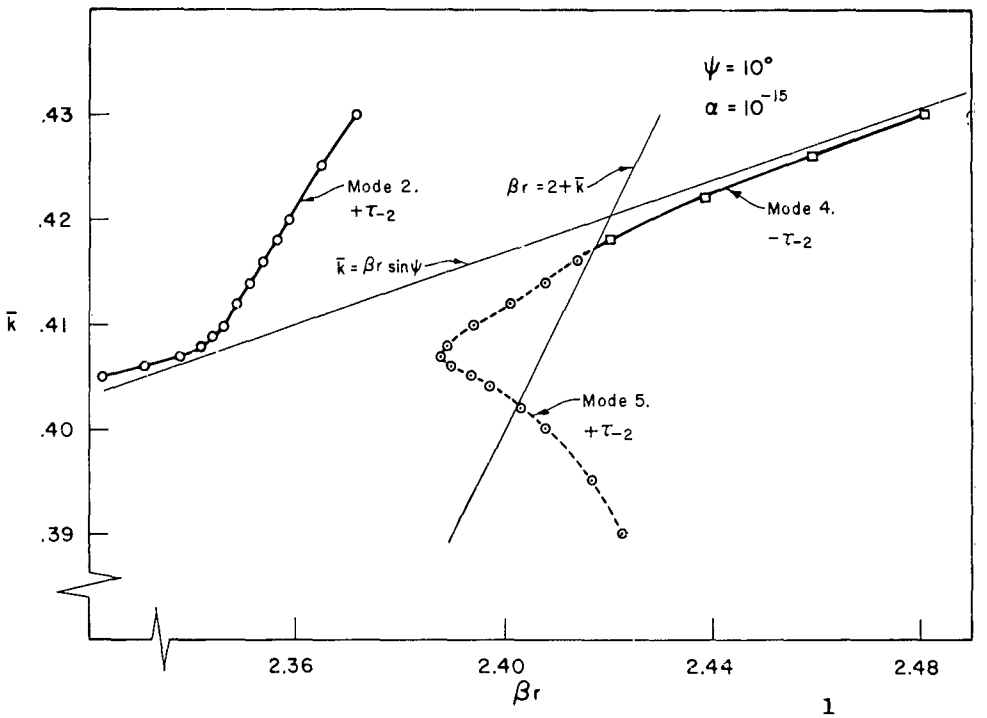

Figure 4.12a. The k - β_r diagram for the tape helix near $\bar{k}_{c4}^{-1}$: Modes 2, 4 and 5: $\psi = 10^{o}$, $\alpha = 10^{-15}$.

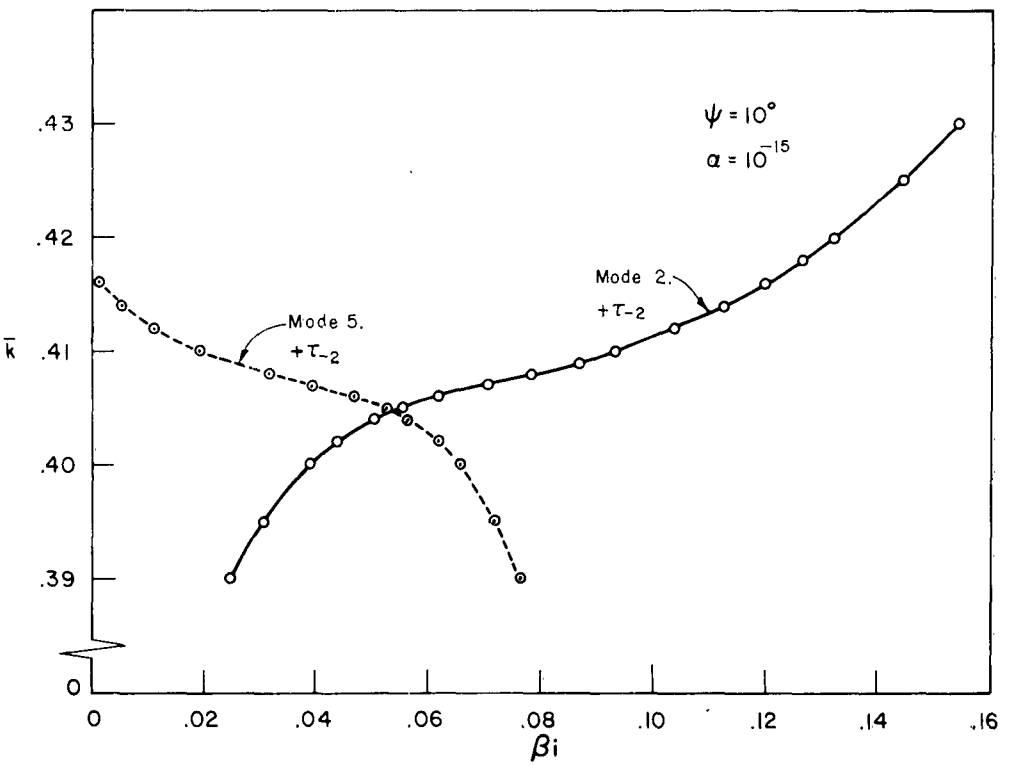

Figure 4.12b. The k - β_i diagram for the tape helix near $\bar{k}_{c4}^{-1}$: Modes 2, 4 and 5: $\psi = 10^{o}$, $\alpha = 10^{-15}$.

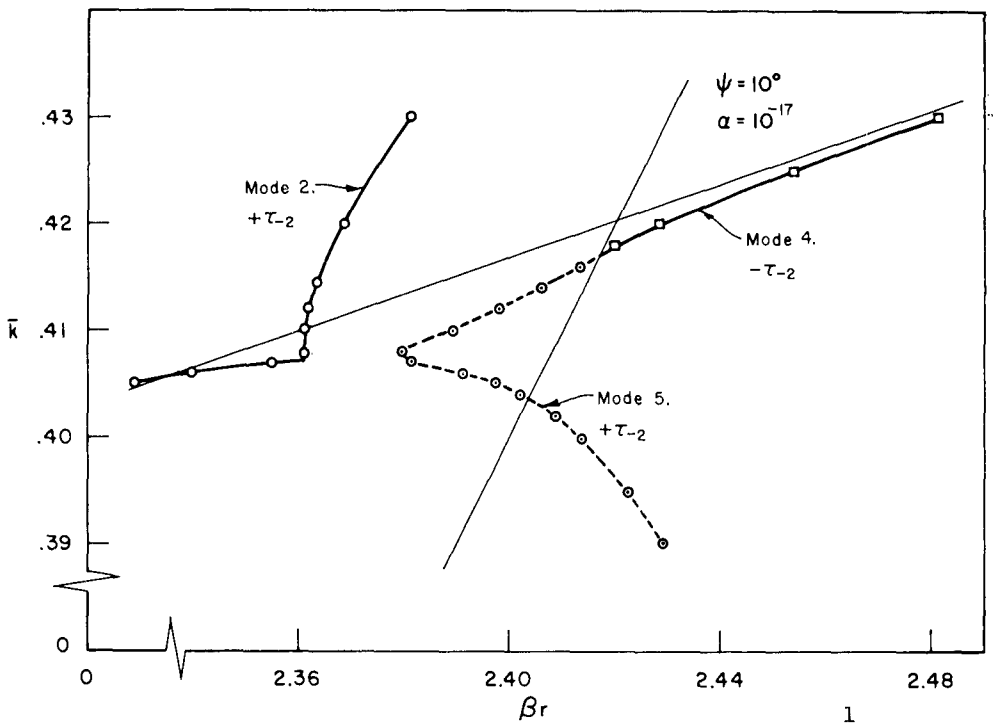

Figure 4.13a. The k - β_r diagram for the tape helix near $\bar{k}_{c4}^{1}$: Modes 2, 4, and 5; $\psi = 10^{o}$, $\alpha = 10^{-17}$.

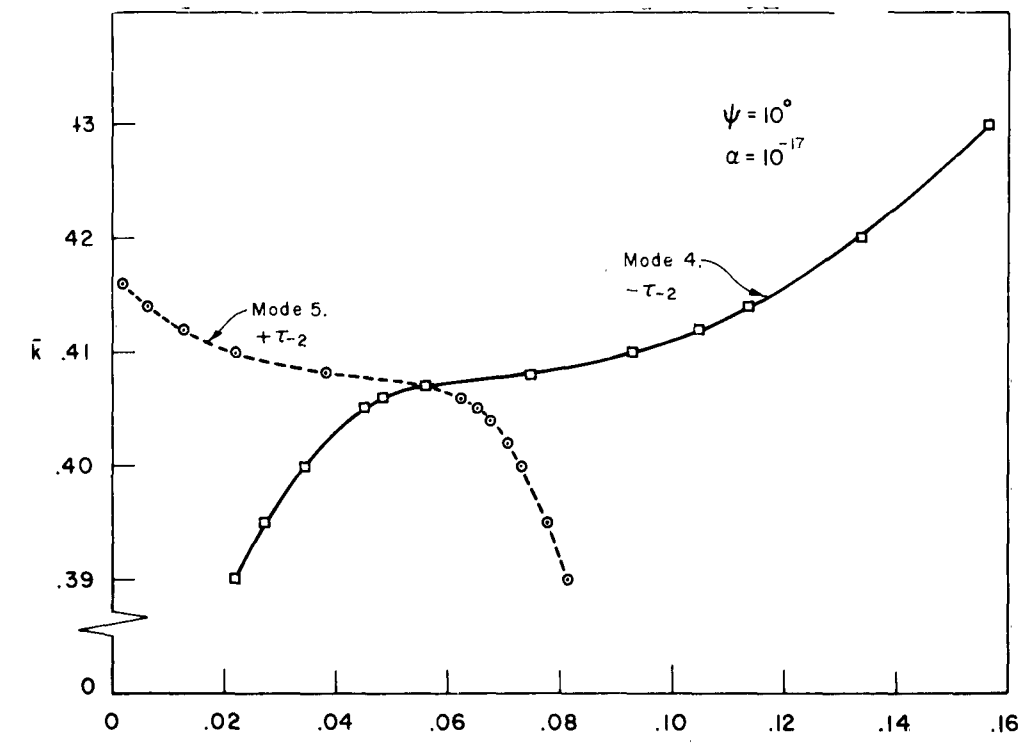

Figure 4.13b. The k - β_i diagram for the tape helix near $\bar{k}_{c4}^{1}$: Modes 2, 4, and 5; $\psi = 10^{o}$, $\alpha = 10^{-17}$.

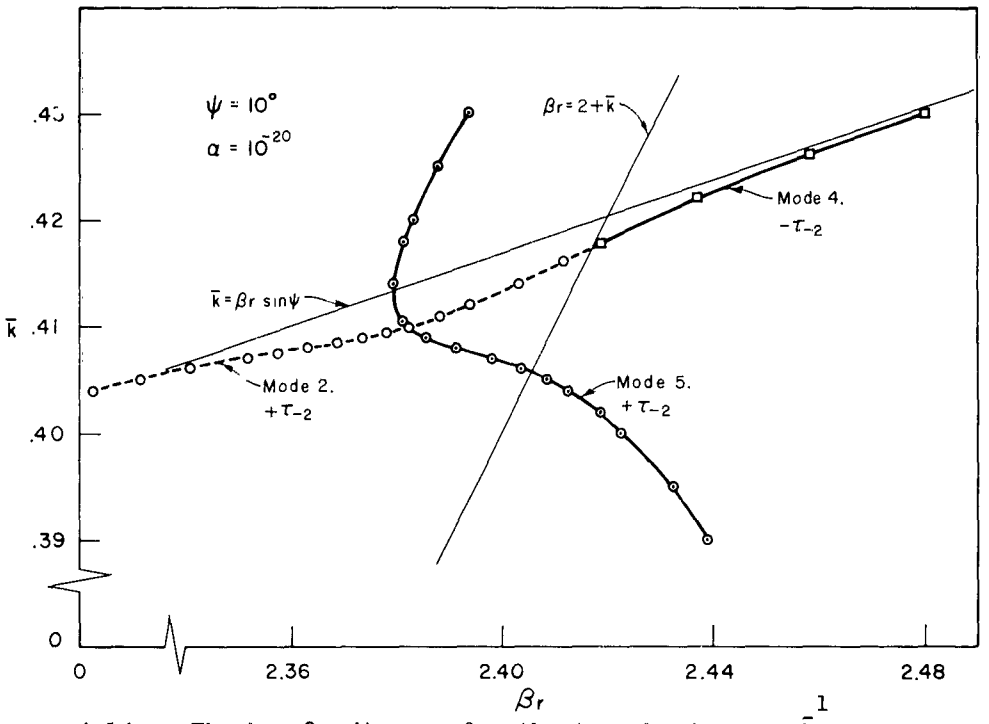

Figure 4.14a. The k - β_r diagram for the tape helix near $\bar{k}_{c4}^{1}$: Modes 2, 4, and 5; $\psi = 10^{o}$, $\alpha = 10^{-20}$.

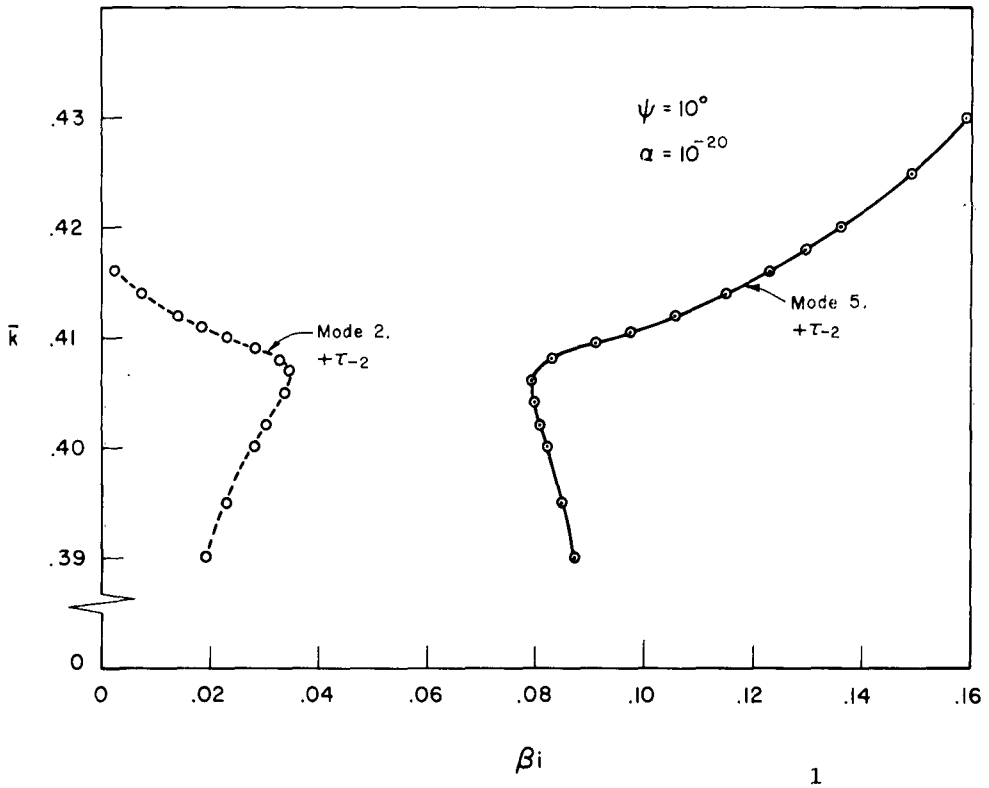

Figure 4.14b. The k - β_i diagram for the tape helix near $\bar{k}_{c4}^{1}$: Modes 2, 4, and 5; $\psi = 10^{o}$, $\alpha = 10^{-20}$.

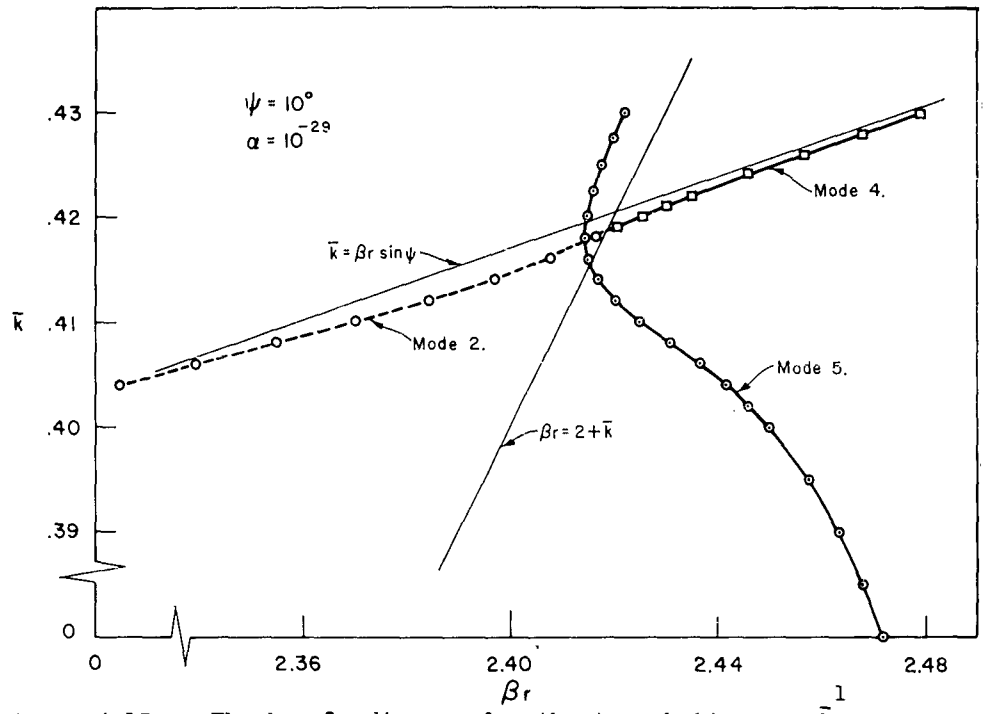

Figure 4.15a. The k - β_r diagram for the tape helix near $\bar{k}_{c4}^{1}$: Modes 2, 4 and 5; $\psi = 10^{o}$, $\alpha = 10^{-29}$.

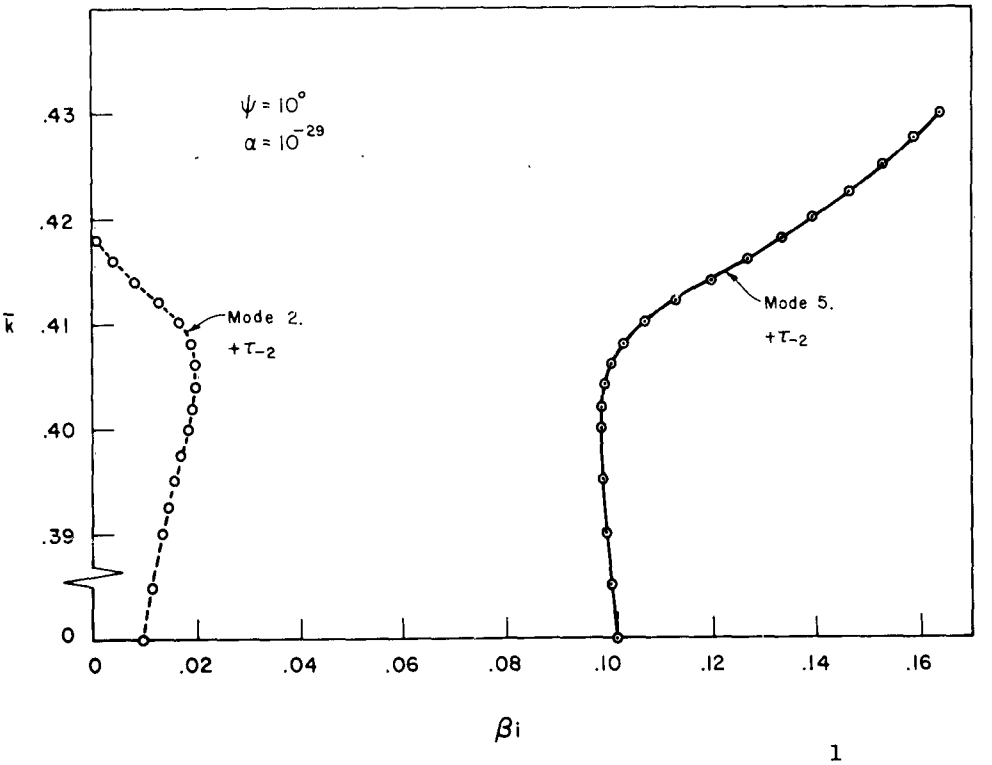

Figure 4.15b. The k - β_i diagram for the tape helix near $\bar{k}_{c4}^{1}$: Modes 2, 4 and 5; $\psi = 10^{o}$, $\alpha = 10^{-29}$.

4.2.8 Solution when the Tape Width is Infinitesimally Narrow.

Mittra[11] showed that as the tape width is made infinitesimally narrow the asymptotic solution for the determinantal equation, Equation (2.40) is given by

$$\beta = \frac{\bar{k}}{\sin \psi} \tag{4.3}$$

and

$$\beta = 1 \pm \bar{k}$$

A graph of the above solution is shown in Figure 4.16.

To show that the solution given in Equation (4.3) is the asymptotic solution consider the determinantal equation.

$$\beta^2 - \frac{\bar{k}^2}{\sin^2 \psi} = \frac{A_{+1} + A_{-1} - 2A_o}{2A_o} \tag{4.4}$$

Recall

$$A_j = \sum_{n=-\infty}^{\infty} I_{n+j} K_{n+j}(\tau_n) D_n$$

For an infinitesimally narrow tape $D_n = 1$. Now for $n \neq 0$

$$I_{n+j} K_{n+j}(\tau_n) \simeq \frac{1}{2} \frac{1}{[(n+j)^2 + \tau_n^2]^{1/2}}$$

as was shown by Sensiper[7]. If $\tau_{-1} \neq 0$, the numerator of the right hand

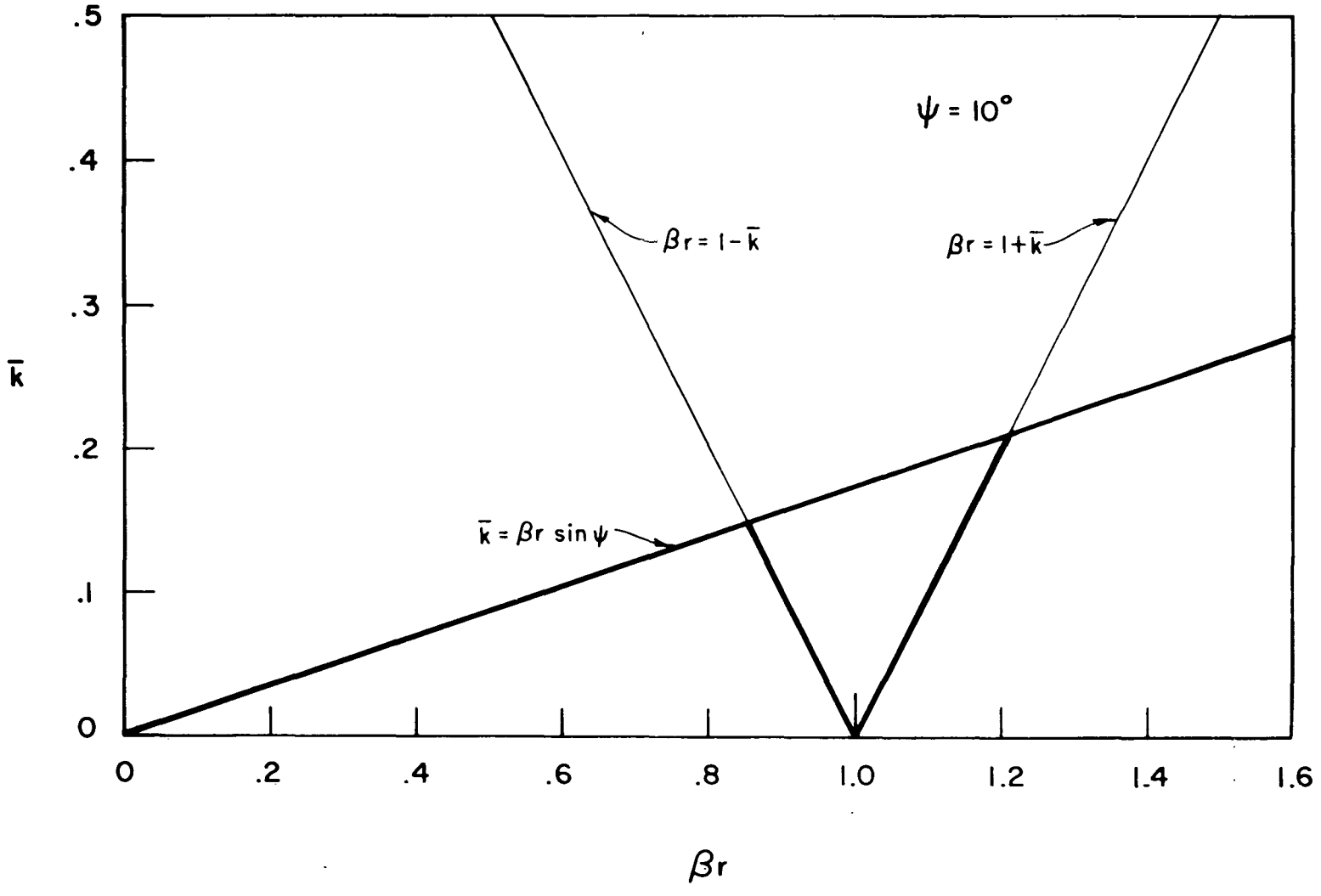

Figure 4.16. The k - β_r diagram for the tape helix: $\alpha = \bar{\delta} = 0$.

side of Equation (4.4) is finite. As τ_{-1} approaches zero the numerator of the right hand side becomes finite because the $I_o K_o(\tau_{-1})$ term has a logarithmic singularity (see Section 3.2). The denominator of the right hand side of Equation (4.4) for $|n| \gg 1$ behaves like the harmonic series and consequently the denominator of the right hand side is finite. The value of the right hand side of the determinantal equation, Equation (4.4), is zero if $\tau_{-1} \neq 0$ and indeterminant if $\tau_{-1} = 0$. The determinantal equation then has the asymptotic solution

$$\beta = \frac{\bar{k}}{\sin \Psi} \qquad \tau_{-1} \neq 0$$

and also has the solution

$$\tau_{-1} = 0, \text{ i.e. } \quad \beta = 1 \pm \bar{k}$$

The solution obtained when $\bar{\delta} = 10^{-308}$, a very narrow tape, agrees with the asymptotic solution. As the tape is made wider, but still very narrow e.g. corresponding to $\bar{\delta} = 10^{-30}$, the solution for the phase constant becomes complex for $\bar{k} > \bar{k}_{cl}$ and the real part of the phase constant deviates from the $\beta_r = \frac{\bar{k}}{\sin \Psi}$ line which is the asymptotic solution. For any tape corresponding to real dimensions, even very narrow tapes, the solution deviates from the asymptotic solution.

4.3 Choosing the Predominant Modes.

In this section it will be shown that modes 1, 2 and 4 are permitted by the interpretation of leaky mode theory, whereas modes 3, 5 and 6 are not physically admissable.

If only the r and z variation is considered, the fields outside the helix for r large may be written as

$$\psi(r,z) = e^{-i\frac{\beta}{p}z} \sum_{n=-\infty}^{\infty} a_n e^{-\tau_n \frac{r}{a}} \qquad (4.5)$$

because $I_m K_m(x)$ behaves like e^{-x} for large x. Now if $\beta = \beta_r - i\beta_i$, the z dependence is

$$e^{-i\frac{\beta_r}{p}z} \quad e^{-\frac{\beta_i}{p}z}$$

which corresponds to a wave traveling in the +z direction and decaying in the +z direction. For large r the fields are given by Equation (4.5). The only terms which could cause the fields to behave improperly are the terms corresponding to n = -1, -2 and -3. The argument τ_{-1}, τ_{-2} or τ_{-3}, which could cause the mode to behave improperly is shown for each mode in Figure 4.17 along with the r dependence for the field. In the r dependence shown in Figure 4.17 the real members a and b are positive. Consider the mode 1 solution. For $\beta_r < 1$ the r dependence is $e^{-ar}e^{-ibr}$ which corresponds to an outwardly traveling wave which is attenuated. Since $\beta_r < 1$ the radiation corresponding to the phase constant is in the backward direction, and decay in the transverse direction is proper for the leaky wave as was shown by Marcuvitz [18] and later discussed by Oliner [20]. For $\beta_r > 1$ the r dependence is $e^{ar}e^{-ibr}$ which corresponds to an outwardly traveling wave which is growing in amplitude. Since $\beta_r > 1$ the radiation corresponding to the phase constant is in the forward direction, and exponential growth in the transverse direction is

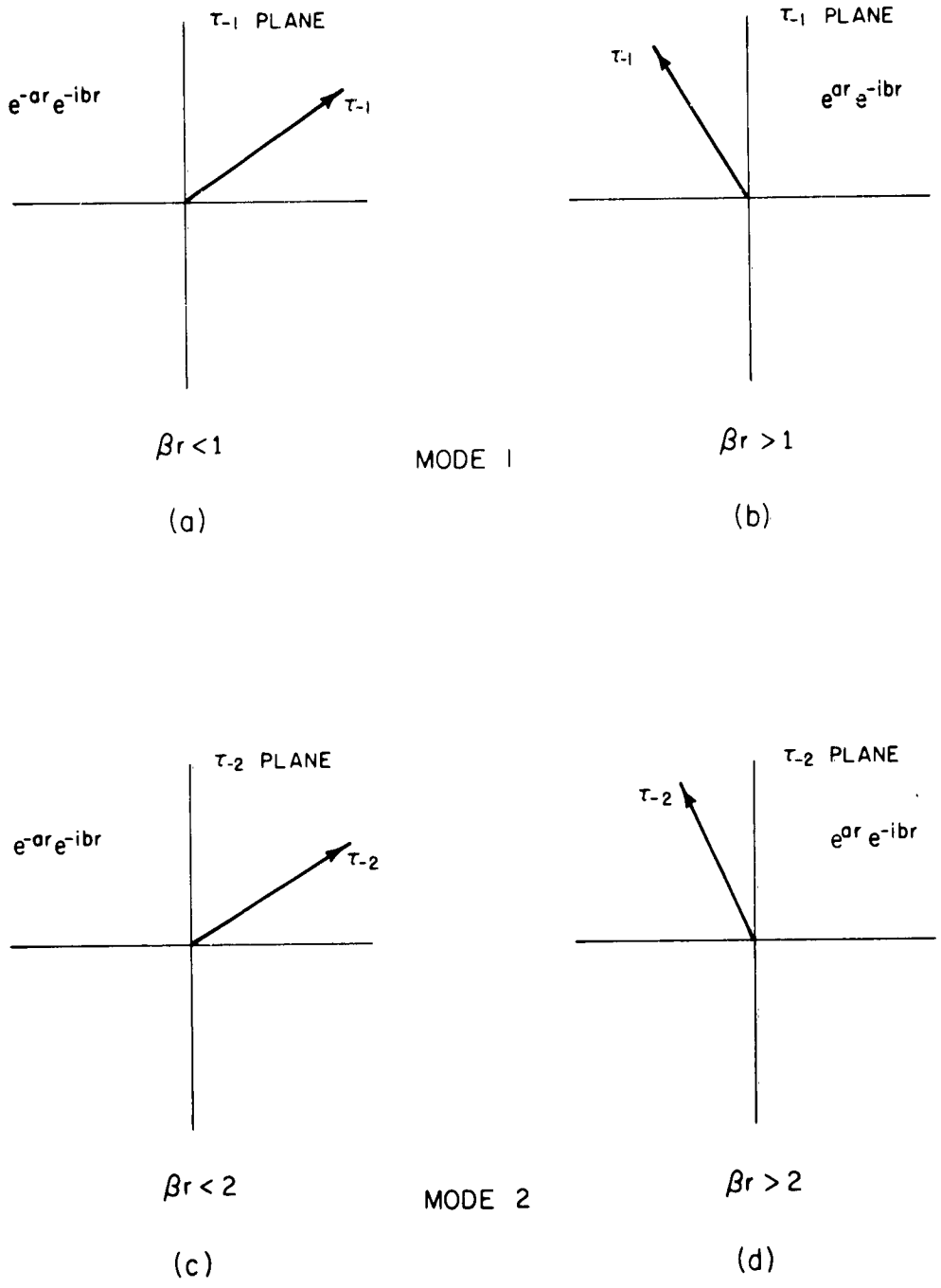

Figure 4.17a. Determination of τ_{-1} for Modes 1 and 2.

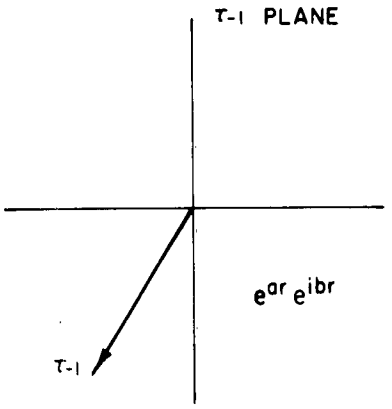

MODE 3

(e)

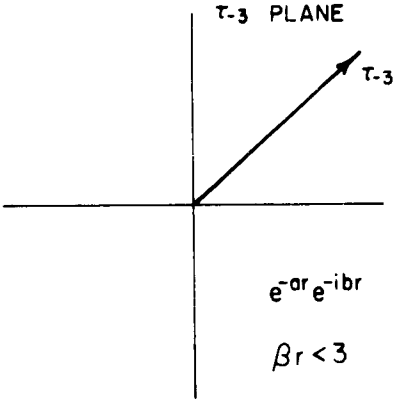

MODE 4

(f)

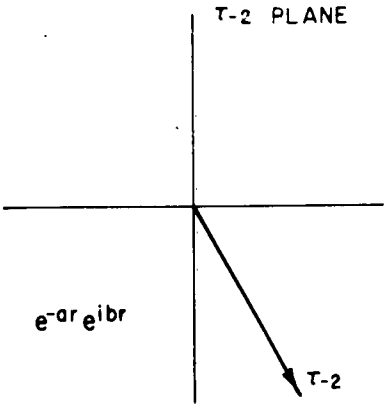

MODE 5

(g)

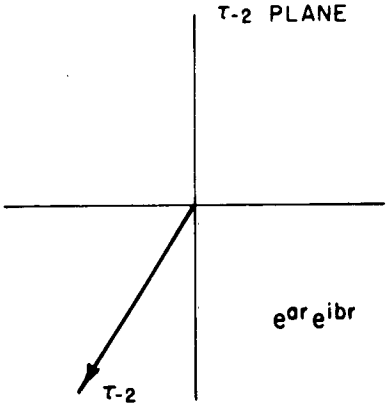

MODE 6

(h)

Figure 4.17b. Determination of τ_{-1} for Modes 3, 4, 5 and 6.

proper for the leaky wave as was shown by Marcuvitz. To understand the growth in the transverse direction consider a slotted waveguide shown schematically in Figure 4.18. The guide is fed at the origin, and radiation takes place in the forward direction. As z is increased less radiation occurs since the fields are decaying exponentially. The spacing of the lines in Figure 4.18 is inversely proportional to the power density. Note that at $z = z'$ the fields increase as x is increased from zero to a value of x related to the direction of radiation.

The mode 2 solution has exactly the same behavior for T_{-2} as the mode 1 solution has for T_{-1}, and consequently mode 2 has solutions which correspond to waves which are leaky waves. The mode 4 solution corresponds to waves which are leaky waves since the mode 4 solution behaves for T_{-3} the same as mode 1 and mode 2 solutions behave for T_{-1} and T_{-2} respectively.

However, this behavior of the fields is not the case for solutions corresponding to modes 3, 5, and 6. Each mode has a transverse behavior which is characterized by an inwardly traveling wave. If there is an inwardly traveling wave the field must increase in the z direction. The fields do not increase since the z dependence is

$$e^{-1\frac{\beta_r}{\bar{p}}z}\; e^{-1\frac{\beta_1}{\bar{p}}z} \qquad \beta_1 > 0$$

This contradiction between the wave traveling inwardly and the fields decaying in the $+z$ direction make the waves corresponding to the solutions of modes 3, 5, and 6 physically inadmissable for leaky waves.

If $\beta = \beta_r + i\beta_i$ is chosen as the solution to the determinantal equation, all of the arguments are the conjugates of the arguments when

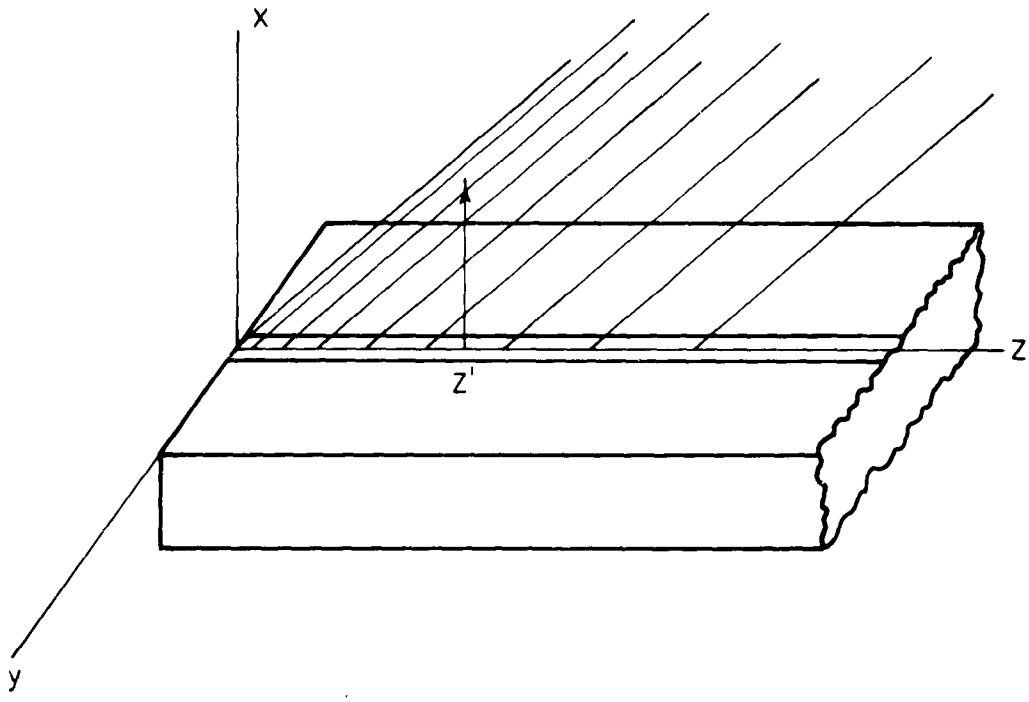

Figure 4.18. Leaky Waveguide

$\beta = \beta_r - i\beta_i$ is chosen as the solution to the determinantal equation. The property that T_n is its conjugate when β is its conjugate makes the discussion of admissable solutions when $\beta = \beta_r + i\beta_i$ similar to the above discussion when $\beta = \beta_r - i\beta_i$ and with the same results,

1) Modes 1, 2, and 4 are physically admissable for leaky modes and

2) Modes 2, 5 and 6 are not physically admissable for leaky modes.

If $-\beta$ is chosen as the solution to the determinantal equation, then attention must be focused on the terms containing T_{+1}, T_{+2} and T_{+3}. Here, as before, the discussion of the admissable solution is similar to that discussion above and with, or course, the identical results. The normalized frequency, $\bar{k}$, for which there is experimental data is less than $\bar{k}^1_{c4}$ where $\bar{k}^1_{c4}$ is the lowest value of $\bar{k}$ for which there exists a solution corresponding to mode 4. Therefore, only two modes will be of interest for $\bar{k} < \bar{k}^1_{c4}$. The modes of interest are modes 1 and 2 and will be called predominant modes.

4.4 Summary

The results of the solution of the determinantal equation have been presented in this chapter. It was seen that only modes 1, 2 and 4 are physically admissable. Mode 4 exists only for $\bar{k} > \bar{k}^1_{c4}$. Therefore, for $\bar{k} < \bar{k}^1_{c4}$ the current will be approximated by solutions from modes 1 and 2.

5. SOURCE PROBLEMS

5.1 Introduction

In contrast with the previous chapters that considered only an infinite tape helix without a source, this chapter is concerned with helices with a source. The source will be of small extent located at the origin. A description for the source is

$$E_{11} = \begin{cases} E_o & |\phi| \leq \phi_o \\ 0 & |\phi| \geq \phi_o \end{cases} \tag{5.1}$$

where ϕ_o is much less than one radian. In the limit E_{11} could be taken as

$$E_{11} = \delta(\phi) \tag{5.2}$$

Not only will the infinite helix be studied but also a finite helix symmetrical about the origin.

5.2 An Infinite Helix with a Source

In this section an infinite helix with a source as described in Equation (5.1) is considered. An equation for the amplitudes of the free modes is found following Sensiper[7]. In a range of frequencies of interest there are two modes. The solution for the relative amplitudes is shown graphically.

To derive the expression for the amplitudes one first writes the

assumed electric field Equation (5.1) as a Fourier integral viz.

$$E_{11} = \frac{E}{\pi} \int_{-\infty}^{\infty} \frac{\sin \frac{\beta\phi_o}{2}}{\beta} e^{-i\beta\phi} \, d\beta \tag{5.3}$$

since $\frac{E}{\pi\beta} \sin \frac{\beta \phi_o}{2}$ is the Fourier transform of the assumed electric field. The current on the tape is

$$I(\phi) = \int_{-\infty}^{\infty} I(\beta) \, e^{-i\beta\phi} \, d\beta \tag{5.4}$$

Now E_{11} may be calculated from the integral representation in Equation (2.32)

$$E_{11}(\phi,\zeta) = \frac{-i\omega\mu}{4\pi k^2 (a^2+\bar{p}^2)^{1/2}} \int_{-\infty}^{\infty} \left\{ \frac{\partial^2 I(\phi^1)}{\partial \phi^{12}} + k^2 I(\phi^1) \left[a^2 \cos(\phi-\phi^1) + \bar{p}^2 \right] \right\} \frac{e^{-ikR}}{R} d\phi^1$$

If the two equations for E_{11}, Equation (5.3) and Equation (2.32) are set equal to each other and the current and its derivative are replaced in Equation (2.32) by their Fourier integrals one obtains, after an interchange of order of integration, an expression containing $I(\beta)$ viz.

$$0 = \int_{-\infty}^{\infty} d\beta \left\{ \frac{E}{\pi} \frac{\sin \frac{\beta\phi_o}{2}}{\beta} e^{-i\beta\phi} + i \frac{I(\beta)}{4\pi\omega\epsilon (a^2+\bar{p}^2)^{1/2}} \int_{-\infty}^{\infty} \left[-\beta^2 + k^2 \left[a^2 \cos(\phi-\phi^1) + \bar{p}^2 \right] \right] e^{-i\beta\phi^1} \right.$$

$$\left. \frac{e^{-ikR}}{R} \, d\phi^1 \right. \tag{5.5}$$

If the integrand is set equal to zero an expression for I(β) is obtained. Now if the inverse transform of I(β) is taken the result is

$$I(\phi) = \int_{-\infty}^{\infty} e^{-i\beta\phi} \frac{\frac{-iE}{\pi} \frac{\sin\frac{\beta\phi_o}{2}}{\beta} e^{-i\beta\phi} 4\pi\omega\epsilon(a^2+\bar{p}^2)^{1/2}}{\int_{\infty}^{\infty} e^{-i\beta\phi^1}\left\{-\beta^2+k^2[a^2\cos(\phi-\phi^1)+\bar{p}^2]\right\}\frac{e^{-ikR}}{R}\, d\phi^1} d\beta \qquad (5.6)$$

The denominator of the integrand of Equation (5.6) is recognized as being proportional to E_{11} for a current $I = I_{oe}{}^{-i\beta\phi^1}$. The electric field E_{11} for the exponential current is given by substituting for I and $\frac{dI}{d\phi^1}$, in Equation (2.32) viz.

$$E_{11} = \frac{-i\omega\mu}{4\pi k^2(a^2+\bar{p}^2)^{1/2}} \int_{-\infty}^{\infty} \left\{-\beta^2+k^2[a^2\cos(\phi-\phi^1)+\bar{p}^2]\right\} e^{-i\beta\phi^1} \frac{e^{-ikR}}{R}\, d\phi^1 \qquad (5.7)$$

Now the electric field may also be found from Equation (2.23)

$$E_{11} = \frac{ie^{-i\beta\frac{\delta}{2\bar{p}}} I_o v_e e^{-i\beta\phi} \sin^2\psi}{4\pi k \epsilon \bar{p}} \left\{2A_o\left[\beta^2 - \frac{\bar{k}^2}{\sin^2\psi} - \bar{k}^2 \operatorname{ctn}^2\psi \frac{A_{-1}+A_{+1}-2A_o}{2A_o}\right]\right\} \qquad (5.8)$$

which was the electric field found in the derivation of the determinantal

equation by matching boundary conditions.

If Equations (5.7) and (5.8) are set equal to each other, one may substitute for the denominator of the integrand of Equation (5.6) the series expression, whose zeros have been found. The expression for $I(\phi)$ is

$$I(\phi) = \frac{\imath E\phi_o}{\pi} \frac{\bar{k} \epsilon \bar{p}}{\imath \sin^2\psi} \int_{-\infty}^{\infty} \frac{\sin \frac{\beta\phi_o}{2}}{\frac{\beta\phi_o}{2}} \epsilon^{\imath\beta \frac{\delta}{2\bar{p}}} \epsilon^{-\imath\beta\phi} \Big/ 2A_o \left[\beta^2 - \frac{\bar{k}^2}{\sin^2\psi} - \bar{k}^2 \operatorname{ctn}^2\psi \frac{A_{-1} + A_{+1} - 2A_o}{2A_o}\right] d\beta \tag{5.9}$$

Let

$$D(\beta) = 2A_o \left[\beta^2 - \frac{\bar{k}^2}{\sin^2\psi} - \bar{k}^2 \operatorname{ctn}^2\psi \frac{A_{-1} + A_{+1} - 2A_o}{2A_o}\right] \tag{5.10}$$

The expression $D(\beta)$ when set equal to zero is the determinantal equation. The roots of the determinantal equation are poles of the integrand in Equation (5.9). The integral in Equation (5.9) may be evaluated by using the residue theorem to find the current in terms of the free modes. The result is

$$I(\phi) = \frac{4\pi E\phi_o \bar{k} \epsilon \bar{p}}{v \sin^2\psi} \sum_{\imath=1,2} \frac{e^{-\imath\beta_\imath\phi}}{\frac{d}{d\beta} D(\beta)}\Big|_{\beta=\beta_\imath} \tag{5.11}$$

where use was made of the fact,

$$\frac{\sin \beta_i \frac{\phi_o}{2}}{\beta_i \frac{\phi_o}{2}} \; e^{i\beta_i \frac{\delta}{2p}} \simeq 1$$

for narrow tapes with a source of small extent. The summation in Equation (5.11) is taken over the two predominant modes.

Let the current on the tape be

$$I(\phi) = I_o[e^{-i\beta_1 \phi} + a\, e^{-i\beta_2 \phi}] \quad \phi > 0 \tag{5.12}$$

A calculation for the magnitude of a, $|a|$, was made for a helix with $\Psi = 12.6^{\circ}$ and $\delta = .15$. The results are shown in Figure 5.1. Note that as the frequency k is increased the relative amplitude of the second mode is increased.

The complex valued derivatives in Equation (5.11) were evaluated numerically by taking first an increment in the β_r direction and finding

$$\frac{\Delta D_r}{\Delta \beta_r} + i \frac{\Delta D_i}{\Delta \beta_r} \tag{5.13}$$

where $D = D_r + D_i$. Second an increment in the $i\beta_i$ direction was taken and the result

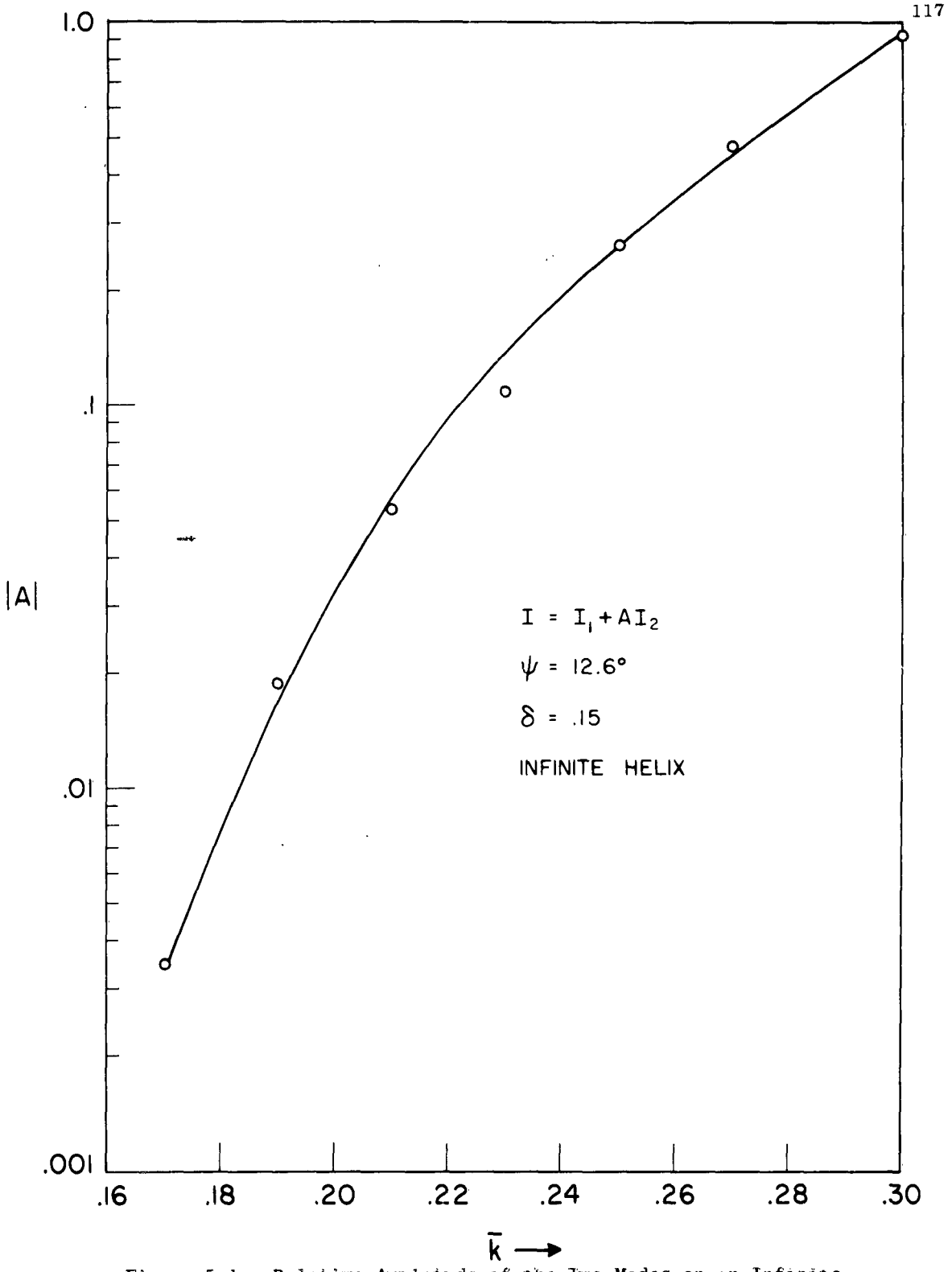

Figure 5.1. Relative Amplitude of the Two Modes on an Infinite Helix as a Function of Frequency.

$$\frac{\Delta D_i}{\Delta \beta_i} \quad -i \quad \frac{\Delta D_r}{\Delta \beta_i} \tag{5.14}$$

compared to Equation (5.14) to determine the derivative. This is, of course, doing nothing more than performing the difference quotient along two convenient rays. The function $D(\beta)$ is analytic in a region containing the zero under consideration, and the derivative is unique. The only reason that the difference quotient was evaluated along two different rays was to have a numerical check on the calculation.

5.3 A Finite Helix with Source

5.3.1 Introduction

This section will be concerned with relative amplitudes of the two predominant current modes that exist on a finite helix. The helix is symmetrical about the origin - $\phi_o \leq \phi \leq \phi_o$ and is fed at the origin. The two currents, $I_1(\beta_1)$ and $I_2(\beta_2)$, will be chosen such that each current will be zero at the ends of the helix, $\phi = \pm \phi_o$. This boundary condition excludes consideration of mode conversion at $\phi = \pm \phi_o$ i.e., no energy is taken from mode 1 and placed in mode 2 or conversely by the end discontinuity.

The currents that satisfy the boundary condition are

$$I_1 = \sinh \gamma_1 (\phi_o - |\phi|) \tag{5.15}$$

and

$$I_2 = \sin \beta_2 (\phi_o - |\phi|) \tag{5.16}$$

where γ_1 and β_2 are the propagation and phase constants for modes one and two respectively, which were found by solving the determinantal equation for an infinite helix with the same pitch angle, tape width and radius as the finite helix. The total current on the helix is

$$I = I_1 + AI_2 \tag{5.17}$$

where A is a complex constant which relates the relative amplitude of the two modes.

If one had a function of the total current which was stationary with respect to the current then it would be possible to find the complex constant A by a variational technique. This is how A is calculated. The relative amplitude of the two modes is then studied as a function of frequency for a finite helix of different lengths.

5.3.2 The Variational Expression

A variational expression that is stationary with respect to current for a symmetric helix was found by Tang [30]

The integral representation, Equation (2.31), for the electric field was found in Chapter 2. Equation (2.31) will be repeated here for convenience, viz.

$$E_{11} = \frac{-i\omega\mu}{4\pi k^2 (a^2+\bar{p}^2)^{1/2}} \int_{-\infty}^{\infty} I(\phi^1) \left\{ \frac{\partial^2}{\partial \phi^{12}} + k^2 [a^2 \cos(\phi-\phi^1) + \bar{p}^2] \right\} \frac{e^{-ikR}}{R} \, d\phi^1 \tag{5.18}$$

with

$$R^2 = [2a \sin \frac{\phi-\phi^1}{2}]^2 + [\bar{p}(\phi-\phi^1)]^2 + (\frac{\delta}{2})^2$$

The above R is linearized so that the kernel in Equation (5.18) is symmetric in $\phi - \phi^1$, i.e. $K(\phi - \phi^1) = K(\phi^1 - \phi)$, with

$$K(\phi-\phi^1) = \frac{-i\omega\mu}{4\pi k^2(a^2+\bar{p}^2)^{1/2}} \left\{\frac{\partial^2}{\partial\phi^2} + k^2[a^2\cos(\phi-\phi^1)+\bar{p}^2]\right\} \frac{e^{-ikR}}{R}$$

The approximation for the linearized R is good for large R since δ is compared to $\bar{p}(\phi-\phi^1)$ and is good for very small R since $4\ \bar{p}(\phi-\phi^1)$ is compared with δ.

If Equation (5.18) is written symbolically as $E = K\ I$

and if

$$\langle A,B\rangle = \int_{-\phi_o}^{\phi_o} AB d\phi$$

where the helix extends from $-\phi_o$ to ϕ_o, then the stationary function is the input impedance

$$Z_{in} = \frac{\langle I, KI\rangle}{I^2(0)} \qquad (5.19)$$

found by Tang[30].

The stationary function, Equation (5.19), is stationary with respect to current, i.e.,

$$\frac{\delta Z_{in}}{\delta I} = 0 \tag{5.20}$$

It follows from Equations (5.17) and (5.20) that

$$\frac{\delta Z_{in}}{\delta A} = 0 \tag{5.21}$$

If the indicated operation in Equation (5.21) is performed, the result for the complex constant A is

$$A = \frac{I_2(0)\mathcal{I}_{11} - I_1(0)\mathcal{I}_{12}}{I_1(0)\mathcal{I}_{22} - I_2(0)\mathcal{I}_{12}} \tag{5.22}$$

where

$$\mathcal{I}_{ij} = \int_{-\phi_o}^{\phi_o} \int_{-\phi_o}^{\phi_o} I_i(\phi)\, I_j(\phi^1)\, K(\phi-\phi^1)\, d\phi d\phi^1 \tag{5.23}$$

$$I_1(0) = \sinh \gamma_1 \phi_o$$

and

$$I_2(0) = \sin \beta_2 \phi_o$$

To evaluate the complex constant A it is necessary to evaluate the integrals in Equation (5.23).

5.3.3 Integration of $\mathcal{I}_{ij}$

The kernel in Equation (5.23) may be written as

$$K(\phi-\phi^1) = \frac{-i\omega\mu}{4\pi k^2(a^2+\bar{p}^2)^{1/2}} \left\{ -\frac{\partial}{\partial\phi^1} \frac{\partial}{\partial\phi} + k^2 f(\phi-\phi^1) \right\} G(\phi-\phi^1) \tag{5.24}$$

where

$$f(u) = a^2 \cos u + \bar{p}^2$$

$$G(u) = \frac{e^{-ikR}}{R}$$

with

$$R^2 = [2a \sin \frac{u}{2}]^2 + (\bar{p}u)^2 + (\frac{\delta}{2})^2$$

If

$$\mathcal{J}_{ij} = \frac{4\pi k^2(a^2+\bar{p}^2)^{1/2}}{-i\omega\mu} \mathcal{I}_{ij}$$

then

$$\mathcal{J}_{ij} = \int_{-\phi_o}^{\phi_o} d\phi I_i(\phi) \int_{-\phi_o}^{\phi_o} I_J(\phi) \left[-\frac{\partial}{\partial\phi^1} \frac{\partial}{\partial\phi} + k^2 f(\phi-\phi^1) \right] G(\phi-\phi^1) d\phi^1 \tag{5.25}$$

The inner integral is separated into two integrals, viz.

$$\int_{-\phi_o}^{0} I_j(\phi^1) \left[- \frac{\partial}{\partial \phi^1} \frac{\partial}{\partial \phi} + k^2 f(\phi-\phi^1) \right] G(\phi-\phi^1)\, d\phi^1$$

$$+ \int_{0}^{\phi_o} I_j(\phi^1) \left[- \frac{\partial}{\partial \phi^1} \frac{\partial}{\partial \phi} + k^2 (\phi-\phi^1) \right] G(\phi-\phi^1)\, d\phi^1$$

In the first integral above the change of variable $\phi^1 = -\phi^1$ is made and in addition use is made of $I_j(-\phi^1) = I_j(\phi^1)$ to yield

$$\mathcal{J}_{ij} = \int_{-\phi_o}^{\phi_o} d\phi I_i(\phi) \left\{ \int_{0}^{\phi_o} I_j(\phi^1) \frac{\partial}{\partial \phi^1} \frac{\partial}{\partial \phi} \left[G(\phi+\phi^1) - G(\phi-\phi^1) \right] d\phi^1 \right. \tag{5.26}$$

$$\left. + \int_{0}^{\phi_o} I_j(\phi^1)\, k^2 \left[f(\phi+\phi^1)\, G(\phi+\phi^1) + f(\phi-\phi^1)\, G(\phi-\phi^1) \right] d\phi^1 \right\}$$

The function of ϕ inside the braces, $\{\}$, is an even function as is the current $I_i(\phi)$. This simplifies Equation (5.26) to

$$\frac{1}{2} \mathcal{J}_{ij} = \int_{0}^{\phi_o} d\phi I_o(\phi) \left\{ \int_{0}^{\phi_o} I_j(\phi^1) \frac{\partial}{\partial \phi^1} \frac{\partial}{\partial \phi} \left[G(\phi+\phi^1) - G(\phi-\phi^1) \right] d\phi^1 \right.$$

$$\left. + \int_{0}^{\phi_o} I_j(\phi^1)\, k^2 \left[f(\phi+\phi^1)\, G(\phi+\phi^1) + f(\phi-\phi^1)\, G(\phi-\phi^1) \right] d\phi^1 \right\} \tag{5.27}$$

The first integral in Equation (5.27) may be integrated by parts twice, once with respect to ϕ and once with respect to ϕ^1 which gives

$$\int_0^{\phi_o}\int_0^{\phi_o} \frac{dI_i(\phi)}{d\phi}\ \frac{dI_j(\phi^1)}{d\phi^1}\ [G(\phi+\phi^1) - G(\phi-\phi^1)]\ d\phi d\phi^1 \qquad (5.28)$$

where use has been made of

$$I_i(\phi_o) = I_j(\phi_o) = 0 \text{ and}$$

$$G(\phi^1) - G(-\phi^1) = 0$$

If Equation (5.28) is substituted into Equation (5.27) the result is

$$\mathcal{J}_{ij} = \int_0^{\phi_o}\int_0^{\phi_o} \frac{dI_i(\phi)}{d\phi}\ \frac{dI_j(\phi^1)}{d\phi^1}\ [G(\phi+\phi^1) - G(\phi-\phi^1)]\ d\phi d\phi^1$$

$$+ \int_0^{\phi_o}\int_0^{\phi_o} I_j(\phi^1)\ I_i(\phi)\ k^2[f(\phi+\phi^1)\ G(\phi+\phi^1) + f(\phi-\phi^1)\ G(\phi-\phi^1)]d\phi d\phi^1 \qquad (5.29)$$

It will be reiterated that Equation (5.29) holds only when the following are true:

1) $I_{ij}I_j$ are even functions and vanish at ϕ_o

2) R is linearized, i.e., $R(\phi-\phi^1) = R(\phi^1-\phi)$.

The integrals in Equation (5.29) are two dimensional integrals and need to be integrated once analytically to be suitable for numerical computation. The reason for this is that the integrands are rapidly varying functions of the variable of integration and numerical integration requires either a very small step size or a variable step size technique. Either of the two techniques is prohibitive in the amount of machine time required for two dimensional integrals.

However, one is indeed fortunate that after a change of variable the integrals may be integrated analytically once. The resulting one dimensional integrals are then numerically integrated by a variable step size technique.

Let

$$\begin{aligned} u &= \phi+\phi^1 \\ v &= \phi-\phi^1 \end{aligned} \tag{5.30}$$

Recall that

$$I_1(\phi) = \sinh \gamma_1(\phi_o-\phi) \qquad \frac{dI_1(\phi)}{d\phi} = -\gamma_1 \cosh \gamma_1(\phi_o-\phi)$$

$$I_2(\phi^1) = \sin \beta_2(\phi_o-\phi^1) \qquad \frac{dI_2(\phi^1)}{d\phi^1} = -\beta \cos \beta_2(\phi_o-\phi^1)$$

If the change of variable in Equation (5.30) is made then

$$I_1(\phi)\ I_1(\phi^1) = \frac{1}{2}\left[\cosh \gamma_1(2\phi_o-u) - \cosh \gamma_1 v\right] \tag{5.31}$$

$$\frac{dI_1(\phi)}{d\phi}\ \frac{dI_1(\phi^1)}{d\phi^1} = \frac{\gamma_1^2}{2}\ [\cosh\ \gamma_1(2\phi_o-u) + \cosh\ \gamma_1 v] \qquad (5.32)$$

$$I_1(\phi)\ I_2(\phi^1) = \frac{i}{2}\ [\cosh\ \gamma_3(2\phi_o-u)\ \cosh\ \gamma_2 v - \sinh\ \gamma_3\ (2\phi_o-u)\ \sinh\ \gamma_2 v$$

$$- \cosh\ \gamma_2(2\phi_o-u)\ \cosh\ \gamma_3 v + \sinh\ \gamma_2(2\phi_o-u)\ \sinh\ \gamma_3 v] \qquad (5.33)$$

$$\frac{dI_1(\phi)}{d\phi}\ \frac{dI_2(\phi^1)}{d\phi^1} = \frac{\gamma_1\beta}{2}\ [\cosh\ \gamma_3(2\phi_o-u)\ \cosh\ \gamma_2 v - \sinh\ \gamma_3(2\phi_o-u)\ \sinh\ \gamma_2 v$$

$$+ \cosh\ \gamma_2(2\phi_o-u)\ \cosh\ \gamma_3 v - \sinh\ \gamma_2(2\phi_o-u)\ \sinh\ \gamma_3 v] \qquad (5.34)$$

$$I_2(\phi)\ I_2(\phi^1) = \frac{1}{2}\left\{\cos\ \beta_2 v - \cos\ \beta_2(2\phi_o-u)\right\} \qquad (5.35)$$

$$\frac{dI_2(\phi)}{d\phi}\ \frac{dI_2(\phi^1)}{d\phi^1} = \frac{\beta_2^2}{2}\ [\cos\ \beta_2\ (2\phi_o-u) + \cos\ \beta_2 v] \qquad (5.36)$$

where

$$\gamma_2 = \frac{\gamma_{1+i}\beta_2}{2}$$

and

$$\gamma_3 = \frac{\gamma_1 - i\beta_2}{2}$$

Since the assumed currents are exponential in form and, of course, have the property $e^{(x+y)}=e^x e^y$, the products of the currents and their derivatives separate into products of functions of the form U(u) V(v), where U is a function of u alone and V is a function of v alone. This particular property of the currents permits the two dimensional integrals, Equation (5.29) to be integrated once analytically.

The integrals, Equation (5.29), are now of the form

$$\frac{1}{2}\mathcal{J}_{ij} = \int_0^{\phi_o}\int_0^{\phi_o} F_1(\phi+\phi^1)\ F_2(\phi-\phi^1)\ d\phi d\phi^1 \qquad (5.37)$$

The Jacobian of the transformation given in Equation (5.30) is $\frac{1}{2}$. The integral in Equation (5.37) may then be written as

$$\frac{1}{2}\mathcal{J}_{ij} = \iint_{R_{uv}} F_1(u)\ F_2(v)\ dudv \qquad (5.38)$$

where R_{uv} is shown in Figure 5.2.

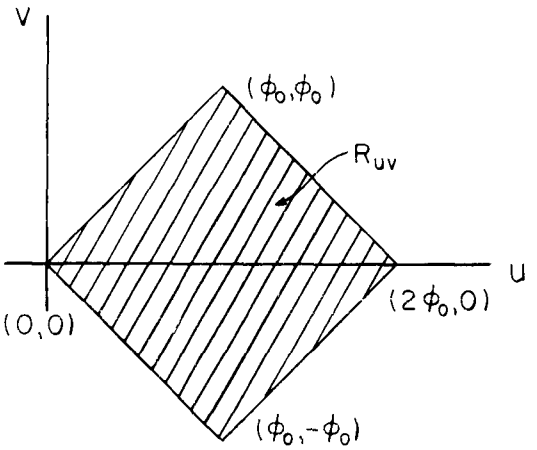

Figure 5.2

If the integration with respect to u is to be integrated first, i.e., able to be integrated analytically, Equation (5 38) is written as

$$\frac{1}{2}\mathcal{J}_{ij} = \int_0^{\phi_o} \frac{F_2(v) + F_2(-v)}{2}\, dv \int_v^{2\phi_o - v} F_1(u)\, du \tag{5.39}$$

On the other hand if the integration with respect to v is to be performed first, Equation (5.38) is written

$$\frac{1}{2}\mathcal{J}_{ij} = \frac{1}{2}\int_0^{\phi_o} F_1(u)\ du \int_{-u}^{u} F_2(v)\ dv + \frac{1}{2}\int_{\phi_o}^{2\phi_o} F_1(u)\, du \int_{-2\phi_o+u}^{2\phi_o-u} F_2(v)\, dv \tag{5.40}$$

If the currents and their derivatives, Equations (5.31) through (5.36), are substituted into Equations (2.39) and (3.40), and the integrations first are performed, the results for the integrals, Equation (5.29), are obtained after considerable analytical integration. The results are

$$\mathcal{J}_{11} = \int_0^{\phi_o} \left\{ [\gamma_1^2 + k^2 f(u)] \, [u \cosh \gamma_1 (2\phi_o - u) - 2 (\phi_o - u) \cosh \gamma_1 u] \right.$$

$$\left. + [\gamma_1^2 - k^2 f(u)] \left[\frac{2 \sinh \gamma_1 u - \sinh \gamma_1 (2\phi_o - u)}{\gamma_1} \right] \right\} G(u) \, du$$

$$+ \int_{\phi_o}^{2\phi_o} \left\{ [\gamma_1^2 + k^2 f(u)] (2\phi_o - u) \cosh \gamma_1 (2\phi_o - u) \right.$$

$$\left. + [\gamma_1^2 - k^2 f(u)] \, \frac{\sinh \gamma_1 (2\phi_o - u)}{\gamma_1} \right\} G(u) \, du \qquad (5.41)$$

$$\mathcal{J}_{12} = \int_0^{\phi_o} G(u) \left[[\gamma_1 \beta_2 - i \, k^2 f(u)] \left\{ \frac{\sinh \gamma_3 u}{\gamma_3} \cosh [\gamma_2 (2\phi_o - u)] \right. \right.$$

$$\left. \left. - \cosh \gamma_2 u \, \frac{\sinh [\gamma_3 (2\phi_o - u)] - \sinh \gamma_3 u}{\gamma_3} \right\} \right.$$

$$+ [\gamma_1 \beta_2 + i \, k^2 f(u)] \left\{ \frac{\sinh \gamma_2 u}{\gamma_2} \cosh [\gamma_3 (2\phi_o - u)] \right.$$

$$- \cosh \gamma_3 u \quad \frac{\sinh [\gamma_2(2\phi_o - u)] - \sinh \gamma_2 u}{\gamma_2} \Bigg\} \Bigg] \, du$$

$$+ \int_{\phi_o}^{2\phi_o} G(u) \left\{ [\gamma_1 \beta_2 - ik^2 f(u)] \frac{\sinh \gamma_3(2\phi_o - u)}{\gamma_3} \cosh [\gamma_2(2\phi_o - u)] \right. \tag{5.42}$$

$$\left. + [\gamma_1 \beta_2 + i k^2 f(u)] \frac{\sinh \gamma_2(2\phi_o - u)}{\gamma_2} \cosh [\gamma_3(2\phi_o - u)] \right\} du$$

$$\mathcal{J}_{22} = \int_0^{\phi_o} [\beta_2^2 + k^2 f(u)] \left[\frac{2 \sin \beta_2 u - \sin \beta_2(2\phi_o - u)}{\beta_2} \right]$$

$$\left. + [\beta_2^2 - k^2 f(u)] [u \cos \beta_2(2\phi_o - u) - 2 (\phi_o - u) \cos \beta_2 u] \right\} G(u) \, du$$

$$+ \int_{\phi_o}^{2\phi_o} \left\{ [\beta_2^2 + k^2 f(u)] \frac{\sin \beta_2(2\phi_o - u)}{\beta_2} + [\beta_2^2 - k^2 f(u)] (2\phi_o - u) \cos \beta_2(2\phi_o - u) \right\} G(u) du \tag{5.43}$$

where

$$f(u) = a^2 \cos u + \bar{p}^2$$

$$G(u) = \frac{e^{-ikR}}{R}, \qquad R^2 = [2a \sin \frac{u}{2}]^2 + (\bar{p}u)^2 + (\frac{\delta}{2})^2$$

$$\gamma_2 = \frac{\gamma_{1+i} \beta_2}{2}, \qquad \gamma_3 = \frac{\gamma_{1-i} \beta_2}{2}$$

The integrals are now in a form suitable for numerical evaluation and hence the complex constant A may be found from Equation (5.22) which is repeated here for convenience after the numerator and denominator on the right hand side are multiplied by a constant.

$$A = \frac{I_2(0)\mathcal{I}_{11} - I_1(0)\mathcal{I}_{12}}{I_1(0)\mathcal{I}_{22} - I_2(0)\mathcal{I}_{12}} \tag{5.44}$$

with

$$I_1(0) = \sinh \gamma_1 \phi_o$$

and

$$I_2(0) = \sin \beta_2 \phi_o$$

5.3.4 Results of the Numerical Integration

The integrals in Equation (5.44) were evaluated using a variable step size technique and the value of A was determined for helices with a total of 8, 12, and 16 turns. All helices have a pitch angle Ψ = 12 6 and a tape width δ = .15.

One is interested in how much of the second mode is launched as compared to the first mode. For this reason the results for A are not given, but the values for $|a| = \frac{A}{\sinh \gamma_1 \phi_o}$ are given. The magnitude of a, $|a|$, approximately equals the ratio of the amplitude of the first mode. The approximation arises from ignoring the term $e^{-2\gamma_1 \phi_o}$ as compared to unity. The approximation is better than 2% on the worst case and often better than .05%.

In Figure 5.3 |a| is plotted as a function of frequency for the three different length helices. It is to be noted as frequency is increased the general trend is for an increase in second mode. This functional variation is identical to what was found for the infinite helix as shown in Figure 2.1.

The oscillations in the amplitude of a may be caused by the variation of input impedance of the helix. The minimums of |a| occur near values of $\bar{k}$ which correspond to values of β_{r2} that make the helix resonant.

The magnitude of the total current on a helix of 12 turns for two different frequencies is shown in Figures 5.4 and 5.5. At the lower frequency, k = .17, the attenuation for the first mode was smaller than at the higher frequency, k = .29. Consequently, the total current does not decay as fast at the lower frequency. In addition, the amplitude of the second mode is less at the lower frequency. Therefore, the second mode does not give the pronounced standing wave as at the higher frequency. Figures 5.6a, 6b, and 6c show that $\bar{k} - \beta$ diagram in the region of interest in this chapter.

5.4 Summary

Two source problems were investigated in this chapter, one an infinite helix and the other a finite helix. Both problems were similar in that the helices were fed at the origin with sources of small extent, essentially δ - sources. In both problems the object was to find the relationship between the amplitudes of the two predominant modes constituting the current on the helix. The phase constants determined by solving the determinantal equation in previous chapters were used in finding the relative amplitudes of the two modes.

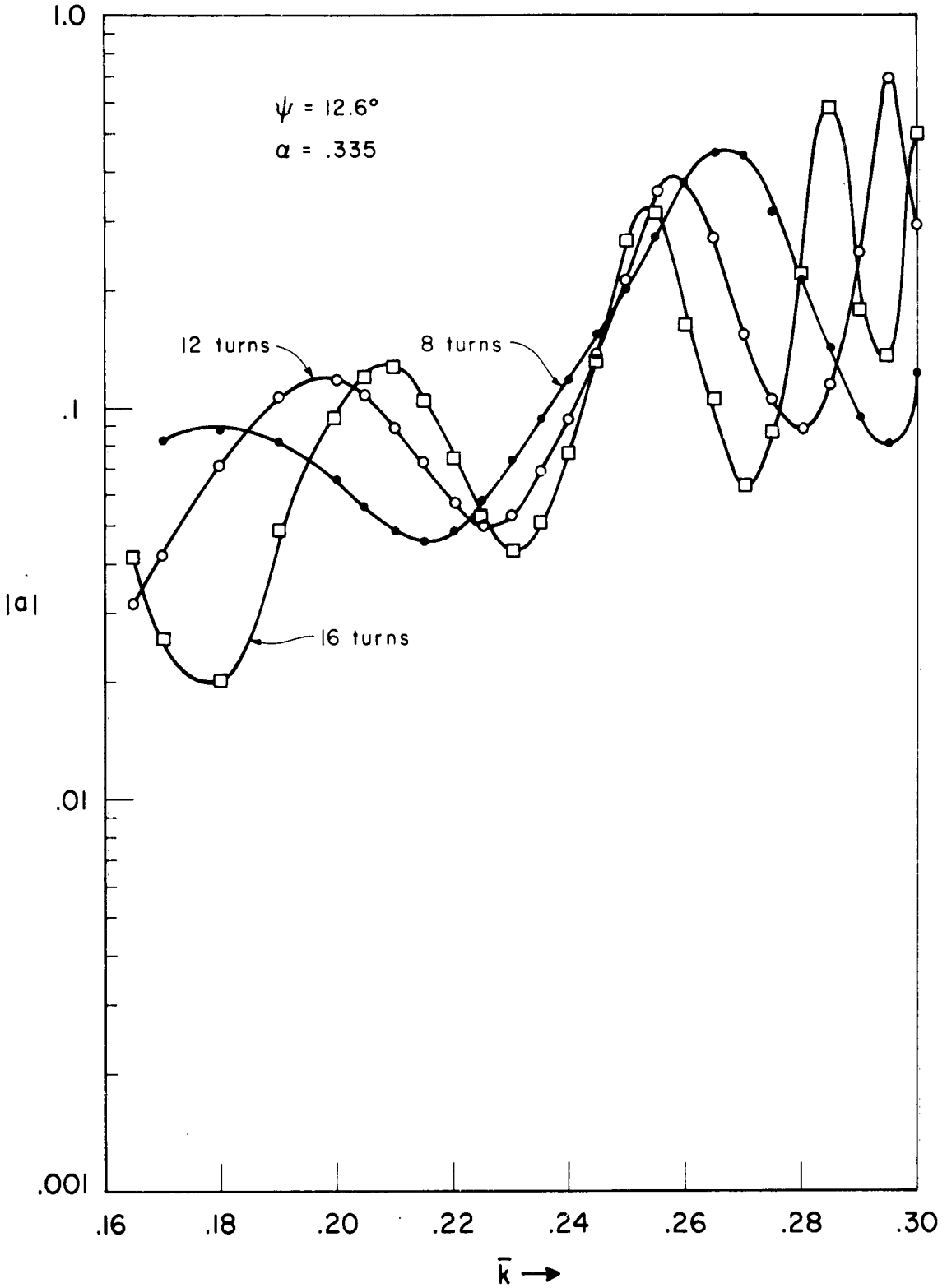

Figure 5.3. Relative Amplitude of the Two Modes on a Finite Helix as a Function of Frequency.

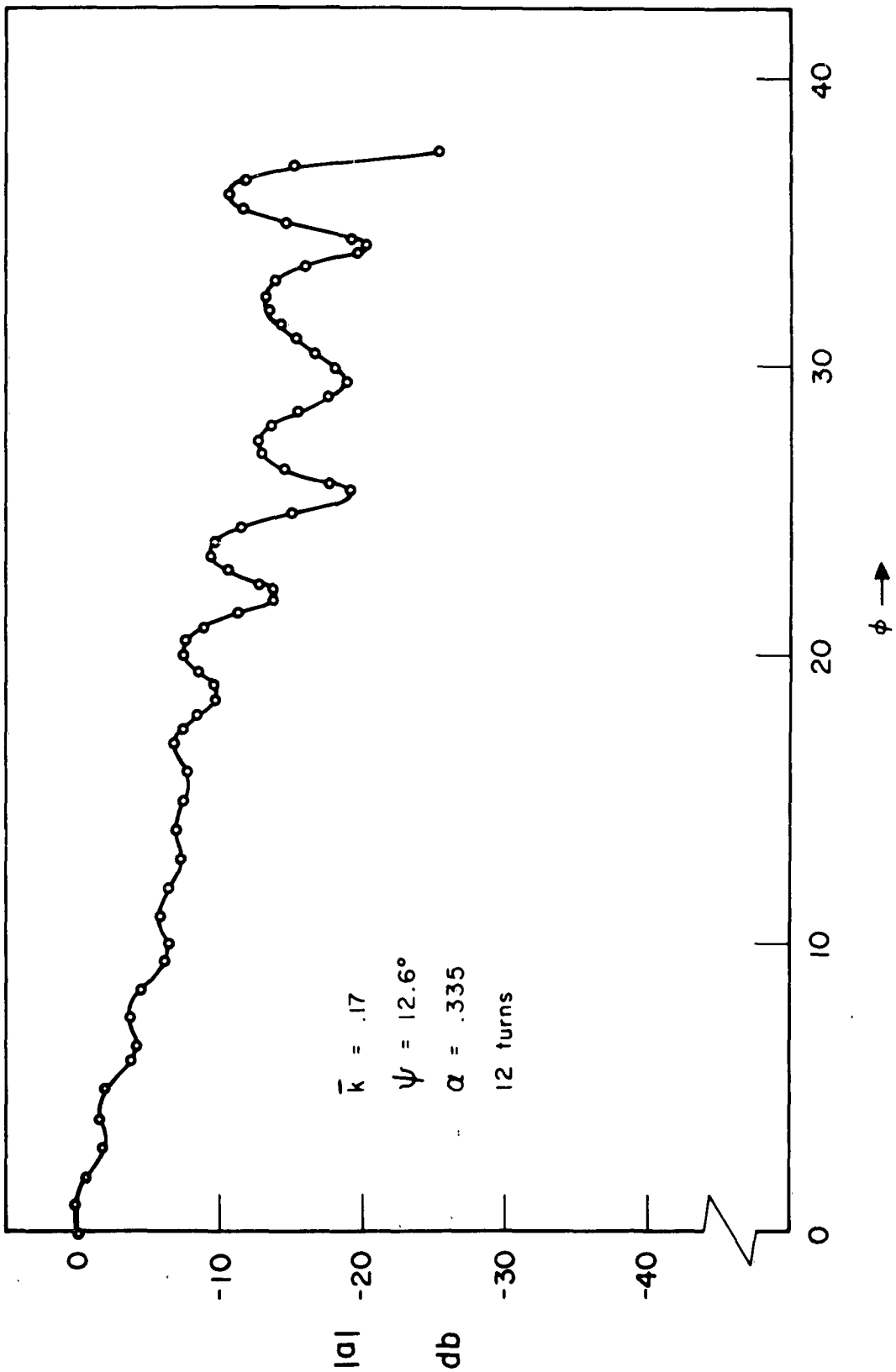

Figure 5.4. Magnitude of the Current on a Finite Helix: $\bar{k} = .17$.

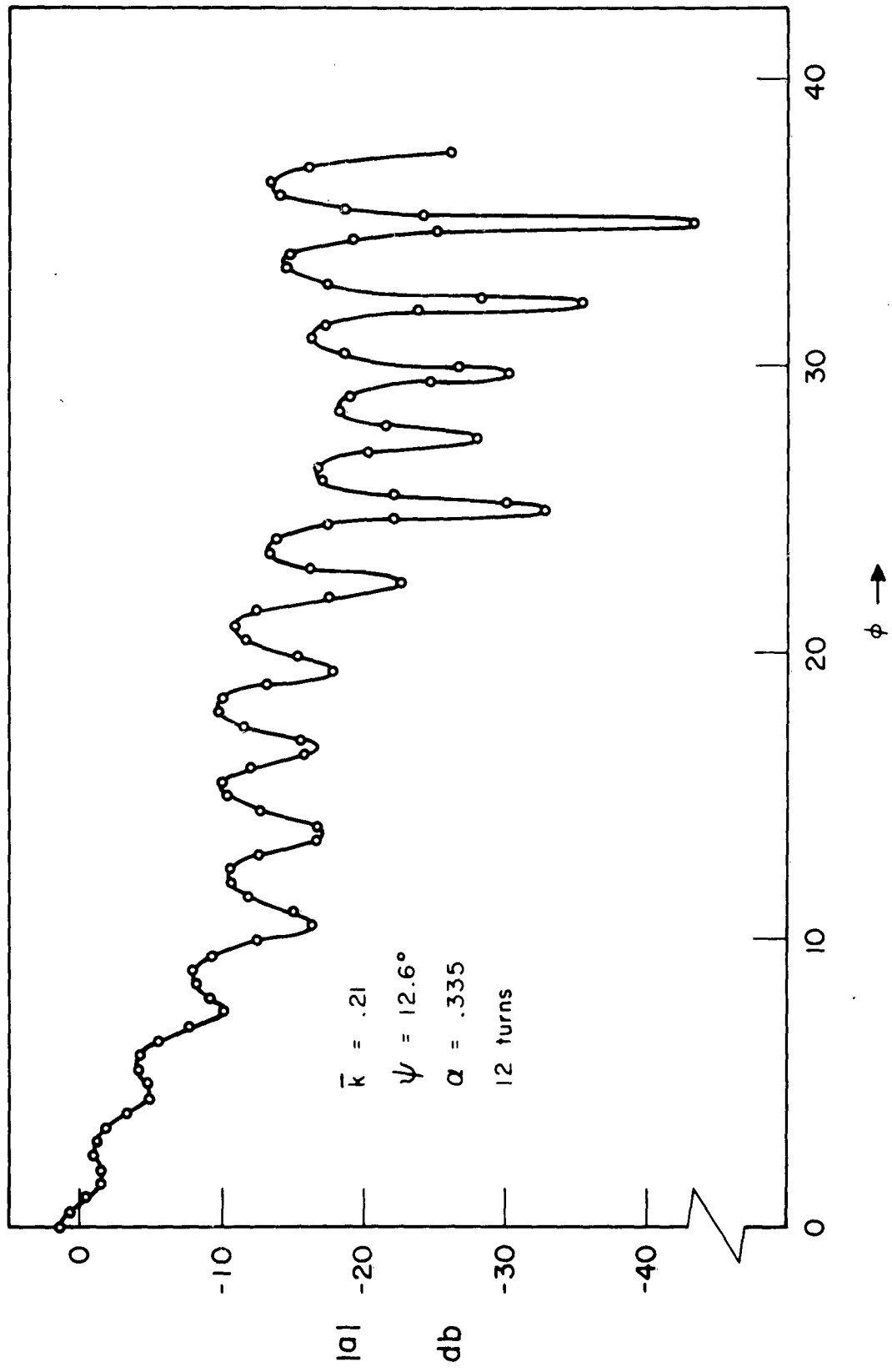

Figure 5.5. Magnitude of the Current on a Finite Helix: $\bar{k} = .21$.

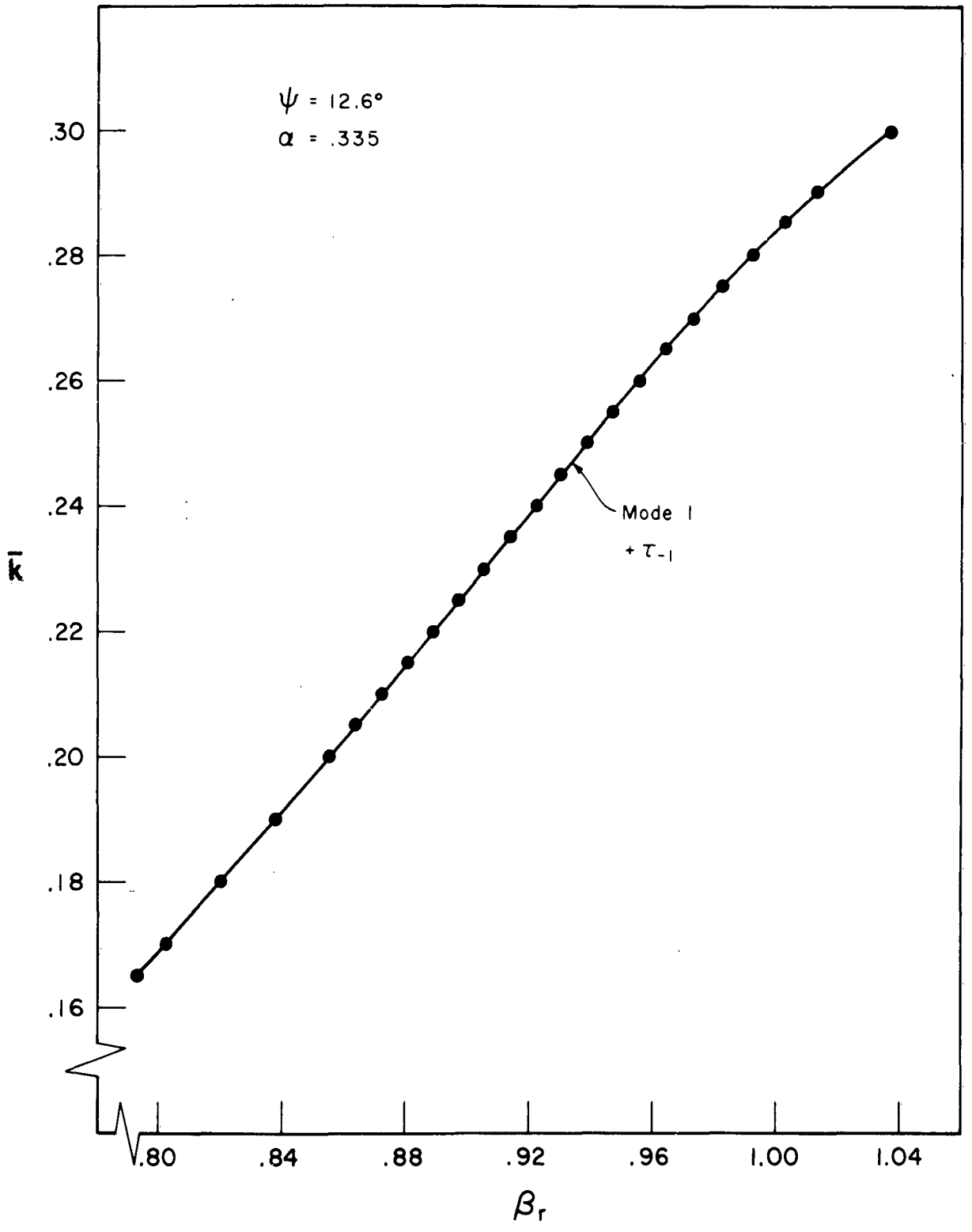

Figure 5.6a. The k - β_r diagram for the tape helix near $\bar{k}_{c1}$; Mode 1; $\psi = 12.6^{\circ}$, $\alpha = .335$.

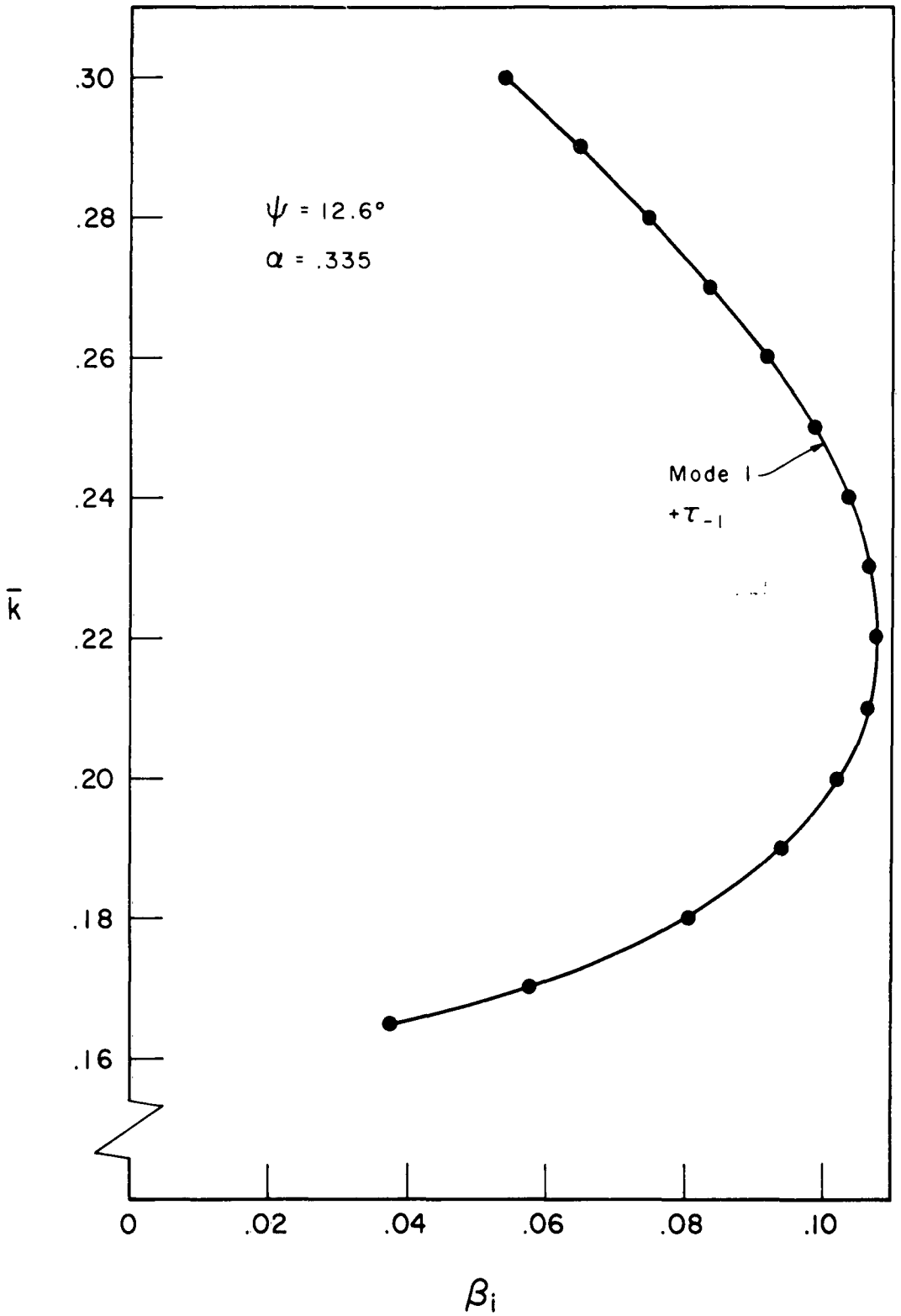

Figure 5.6b. The $k - \beta_i$ diagram for the tape helix near $\bar{k}_{c1}$; Mode 1; $\psi = 12.6^{\circ}$, $\alpha = .335$.

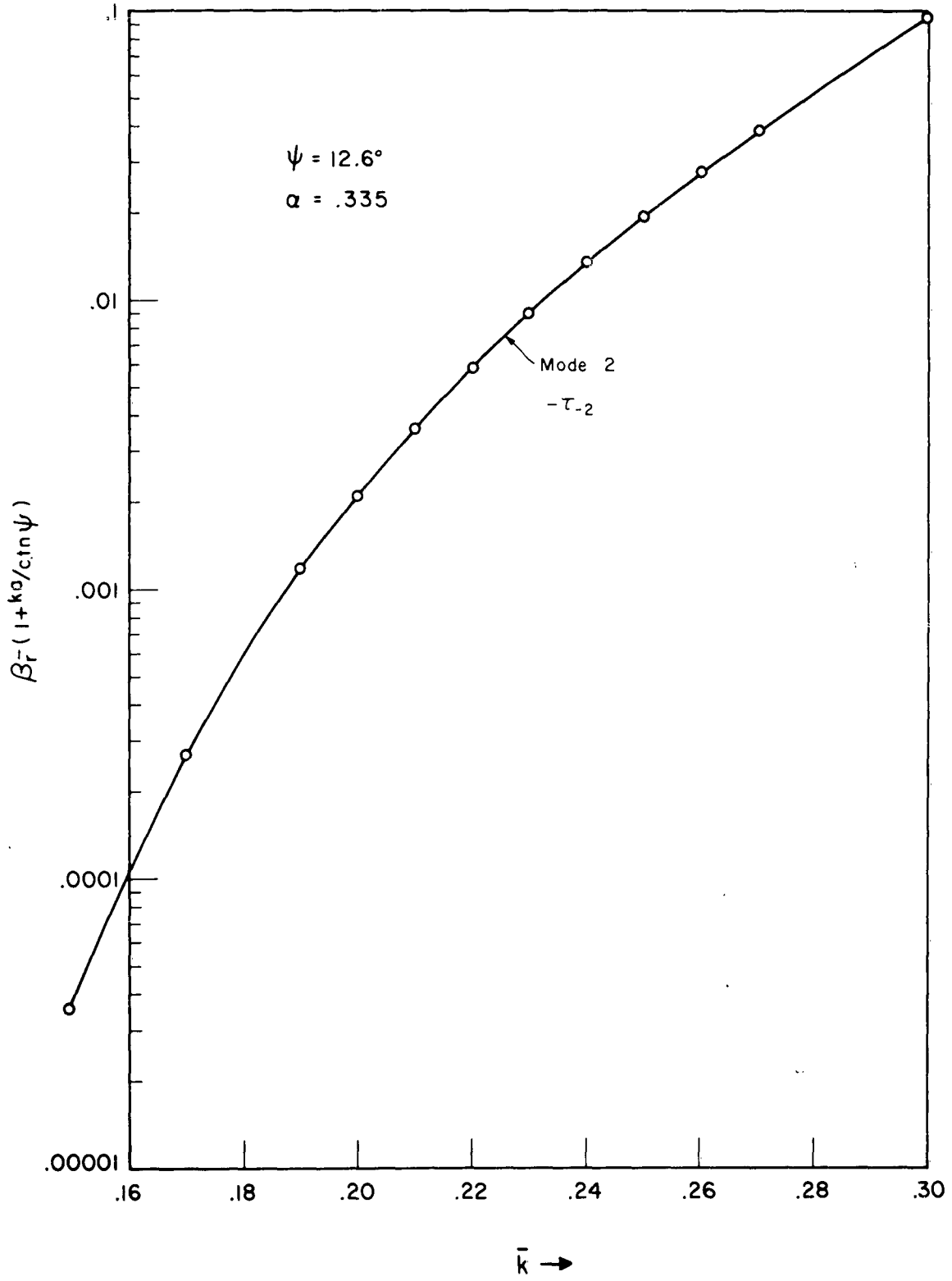

Figure 5.6c. The k - β_r diagram for the tape helix near $\bar{k}_{c1}$; Mode 2; $\psi = 12.6^{\circ}$, $\alpha = .335$.

The relative amplitude of the two modes in the case of the infinite helix was found by evaluating the contribution made by the leaky wave poles to the inverse Fourier transform of the source problem. The leaky wave poles are the solutions to the determinantal equation.

The relative amplitude of the two modes in the case of the finite helix was found by using a variational formulation to find the relative amplitude to give the best input impedance in terms of the two current waves which correspond to solutions of the determinantal equation.

It was found that the second mode increased in amplitude as the frequency was increased for both problems. In addition, when the helix was truncated, there was an end effect and the oscillations of the relative amplitude agree well with the expected variations of the input impedance for the second mode.

6. COMPARISON WITH EXPERIMENTS

6.1 Marsh's Experiment

6.1.1 Introduction

In 1950 Marsh[18] reported that he had measured the current distribution of a six turn helix fed against a ground plane. In addition to measuring the current he was able to empirically fit the results by assuming two current modes each of which was reflected from the end. For the empirical results he chose the current as

$$I = e^{-(\alpha_1+i\beta_1)z} + ae^{-i\beta_2 z} + be^{(\alpha_1+i\beta_1)z} + ce^{i\beta_2 z}$$

The real constants α_1, β_1, and β_2 and the complex constants a, b, and c were chosen by Marsh to fit his measured data. He obtained excellent agreement.

6.1.2 Phase Constants

The phase constants calculated by solving the determinantal equation agree well with Marsh's empirically determined phase constants as shown in TABLE I.

TABLE I

	α_1		β_1		β_2	
$\bar{k}$	Marsh	Calculated	Marsh	Calculated	Marsh	Calculated
.1488	.0078	0	.681	.69	1.193	1.15
.1734	.0636	.069	.795	.808	1.173	1.175
.2115	.1548	.1065	.969	.875	1.356	1.212

The calculated phase constants in TABLE I correspond to tape helix parameters, $\psi = 12.6^{o}$, a = 4.305 cm and $\delta = .15a$. The empirically determined phase constants by Marsh correspond to parameters $\psi = 12.6^{o}$ and a = 4.305 cm. The wire diameter is not reported by Marsh and a tape width was chosen to be approximately equal to the wire diameter inferred from a photograph in Marsh's report. For β_1 Marsh used β_o corresponding to a wave traveling down the wire with the velocity of light.

6.1.3 Amplitude Constants

The solution for the helix fed against the ground plane was not attempted. However, it is interesting to compare the magnitude of the amplitude coefficients obtained for: 1) The infinite helix fed at origin; 2) the finite helix fed at the origin, and 3) Marsh's empirical results for the helix fed against a ground plane. The comparison is shown in Figure 6.1. Note that, as k is increased, one in general expects the second mode amplitude to increase relative to the first mode amplitude. Marsh, in empirically determining the amplitude coefficients, did not insist on zero current for each mode or total at the end of the helix. He permitted energy propagation down the helix in mode 2 to be converted into mode 1 to be reflected. This is reasonable since at the discontinuity the waves are "relaunched" and mode 1 is easier to excite than mode 2 as shown by the calculations of Chapter 5. Since only a portion of the mode 2 current returns this may permit a larger mode 2 current to be launched and hence a larger relative amplitude, a. In Chapter 5, where source problems were investigated, each mode current was forced to be zero at the end of the helix.

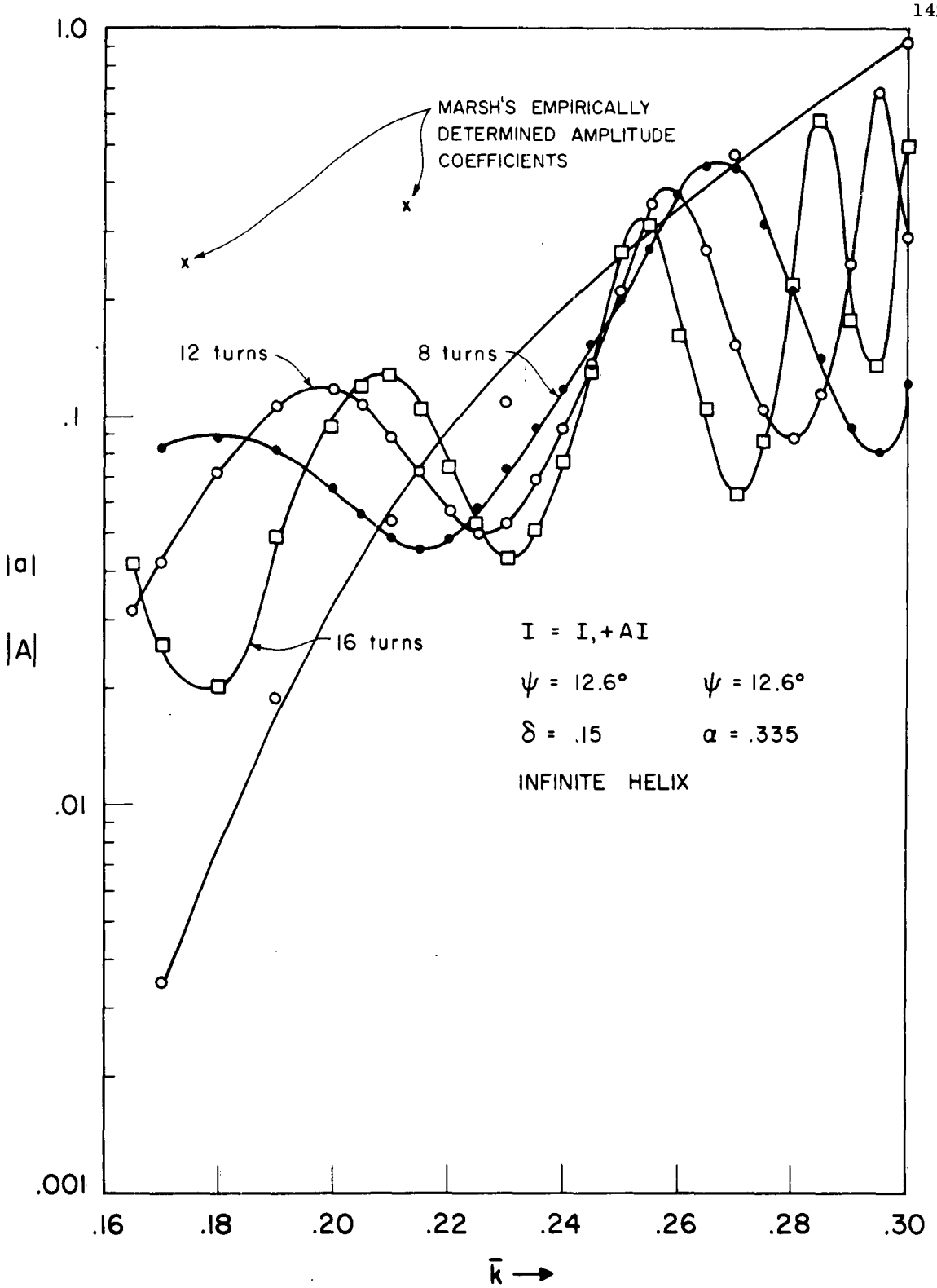

Figure 6.1. Relative amplitude of the two modes compared for a) infinite helix, b) finite helix and c) Marsh's empirical work.

6.1.4 Summary

Marsh was able to empirically fit the measured current distribution on a six turn helix fed against a ground plane by assuming two current waves each reflected at the end. The phase constants calculated in this report agree well with Marsh's empirically determined phase constants. In addition the amplitude coefficients calculated in Chapter 5 behave similarly to Marsh's coefficients.

6.2 Other Experiments

Both McClelland,[31] on the conical equiangular spiral, and Patton,[12] on the bifilar helix fed out of phase, have performed experiments which support the use of the approximation for the current by only the two modes. The bifilar helix fed out of phase has a determinantal equation which is related to the determinantal equation for the monofilar helix studied in this report. The determinantal equation for the bifilar helix has only the terms corresponding to n odd as coefficients to D_n as compared to the determinantal equation for the monofilar helix. One expects similar behavior of the solution near $\beta_r = 2$ but certainly different solutions near $\beta_r = 2$ since the terms containing T_{-2} are missing. The conical equiangular spiral is the log-periodic version of the bifilar helix. Both works, McClelland's and Patton's, support the calculations reported here in the following manner:

1) As the frequency is increased above a value corresponding to $\bar{k}_{c1}$, the current decays, indicating radiation. The higher $\bar{k}$ the more attenuation, indicating β_i increasing as $\bar{k}$ is increased.

2) As $\bar{k}$ is increased still further the current has a small standing wave component occurring indicating that mode 2 is present.

The foregoing experimental results are exactly what would be predicted from the solution of the determinantal equation and the corresponding study of the source problem.

7. SUMMARY

7.1 Original Work Done

Sensiper formulated and solved the determinantal equation for the tape helix treating the phase constant, β, as a real variable but Sensiper and Pierce doubted the existence of complex-valued solutions for the determinantal equation. This present work reports the solution of the determinantal equation for various values of the parameters of the tape helix, where the phase constant is complex-valued. The determinantal equation was interpreted as a complex-valued equation where the arguments of the IK products are shown to be continuous functions of k and β. In determining how the various arguments of the IK products should be interpreted it was found useful to study two simplified equations which exhibited solutions, in certain regions of β_r, similar in character to the solutions for the determinantal equation.

Two source problems were investigated, the first an infinite helix, the second a finite helix, both fed at the origin. The amplitudes of the free modes representing the current on the infinite helix were found following Sensiper[7] but with the phase constant, β, as a complex variable. On the problem of a finite helix a variational technique was used to find the relative amplitude of the two modes representing the current which yields the best input impedance for a current approximated by two modes which correspond to solutions of the determinantal equation. Tang[30] used the variational technique to find the input impedance of the helical antenna (finite helix) assuming the current to be the sum of two components, the first was sinusoidal and corresponded to waves

traveling at the velocity of light; the second was also sinusoidal but with the phase constant twice the value corresponding to phase constant for a wave traveling at the velocity of light.

The variational technique was used in the present report to find the relative amplitude of the two assumed modes which were used to represent the current on the finite helix. The phase constants corresponding to the assumed modes are the complex-valued solutions to the determinantal equation.

7.2 Conclusions

This report indicates that it is possible to approximate the current on a helix with current waves whose complex-valued phase constants are found solving the determinantal equation. The value and the behavior of the roots as a function of the helix parameters of the determinantal equation is just that behavior which causes the corresponding current to agree with experimental results.

The solution of the determinantal equation for $\alpha = 10^{-308}$, an extremely narrow tape, corresponds to the asymptotic solution obtained by Mittra[11] for the limiting case where the tape width tends to zero. As the tape is made wider but still very narrow, e.g., corresponding to $\alpha = 10^{-30}$, the phase constant becomes complex valued and in addition the real part of the phase constant deviates from the line $\bar{k} = \beta_r \sin \psi$, representing a wave traveling down the tape with the velocity of light. The wider the tape the greater is the value of β_i, the imaginary part of the phase constant. Also the wider the tape the greater is the deviation of the real part of the phase constant from the line corresponding to the velocity of light.

For the mode 1 solution the imaginary part of the phase constant increases rapidly as the frequency is increased above $\bar{k} = \bar{k}_{c1}$.

As the pitch angle, ψ, is increased the real part of the phase constant tends toward the line corresponding to the velocity of light. Also as the pitch angle is increased the maximum value of the imaginary part of the phase constant decreases.

The amplitude coefficients calculated in connection with the source problems permit the calculation of the total current on the helix. Corresponding to a frequency just above $\bar{k} = \bar{k}_{c1}$ the current is predominantly mode 1 type current and shows exponential decay away from the source. For a higher value of $\bar{k}$ the current shows the relative increase of mode 2 type which is typified by a definite standing wave of current near the reflected end for the finite helix.

7.3 Further work

7.3.1 The Bifilar Helix

The determinantal equation has been derived for the bifilar helix when the currents are assumed balanced. This determinantal equation has only the terms on the right hand side which have form factors, i.e., the even terms are zero. Although simplified Equation (1), Section 3.2, gives an insight into the behavior of the solution, a more exact solution might be found. After one obtains the roots for the infinite bifilar helix, the source problem could be investigated with the end results the calculation of patterns. These could be checked against Patton's[12] calculated and measured results.

7.3.2 A Conducting Cylinder Inside the Helix

Following the method similar to that used in this report, the

determinantal equation for a concentric conducting cylinder inside the helix may be obtained. The behavior of the solutions could then be used to verify the preliminary measurements [12] indicating that the radius of cylinder has small effect on the fields outside the helix.

BIBLIOGRAPHY

1. H.C. Pocklington, "Electrical Oscillations in Wires", Proc. Camb. Phil. Soc., Vol. 9, p. 324; 1897.

2. J.W. Nicholson, "Resistance and Inductance of a Helical Conductor", Phil. Mag., Vol. 19, p. 77, 1910.

3. F. Ollendorf, Die Grundlagen der Hochfrequenztechnik J. Springer, Berlin, Ger., p. 79, 1926.

4. R.S. Phillips and H. Malin, "A Helical Wave Guide II", Res. Rep. 170-3, New York Univ. Math. Res. Group; August, 1947 - June 1948.

5. E.T. Kornhauser, "Electromagnetic Wave Propagation on Helical Structures", Cruft Lab. Tech. Report No. 88, Aug. 1949.

6. S. Sensiper, "Electromagnetic Wave Propagation on Helical Structures", Proceedings of the IRE, Vol. 43, No. 2, February, 1955, pp. 149-161.

7. S. Sensiper "Electromagnetic Wave Propagation on Helical Conductors," Thesis, M.I.T., 1951.

8. J.R. Pierce and P.K. Tien, "Coupling of Modes in Helices", Proceedings of I.R.E., 42 pp. 1389-1396, September 1954.

9. J.R. Pierce, "Coupling of Modes of Propagation", J. Appl. Phy., 25, pp. 179-183, February 1954.

10. J.Y. Wong and R.S. Thomas, "Bibliography on the Helical Beam Antenna", N.R.C. No. 5264, National Research Council of Canada, Radio and Elec. Eng. Division, Ottawa, May 1959.

11. R. Mittra, "Wave Propagation in Helices" Abstract of Paper from the URSI-IRE Joint Spring Meeting Held April 30 - May 3, 1962 Washington, D.C., IRE Trans. PTGAP, AP-10, No. 4, July 1962, Accepted for pub. as corres. in IRE Trans PTGAP.

12. Patton, W.T., "The Backfire Bifilar Helical Antenna", Antenna Laboratory Tech. Report No. 61, U. of I., AF33(657)-8460, September 1962.

13. T.S.M. Maclean, "The Helical Aerial: A Comparative Study of the Tape Helix Approach", Memo 108, E.E. Dept. University of Birmingham, 1962.

14. T.S.M. Maclean, "An Engineering Study of the Helical Aerial", Memo 97, E.E. Dept. Univ. of Birmingham, Accepted for Publication, I.E.E. pt.b., 1962.

15. T.S.M. Maclean, "The Sheath-Helix Approach to the Helical Aerial", The Institution of Electrical Engineers, London, Monograph No. 519E, May 1962. To be republished in part C of the Proceedings of the Institution.

16. J.D. Kraus and Williamson "Characteristics of the Helical Antennas Radiating in the Axial Mode", J. Appl. Phys. 19, 87(1948).

17. E.T. Kornhauser, "Radiation Field of Helical Antennas with Sinusoidal Current" J. Appl. Phys., 22: 887-91, July 1951. Also Cruft Lab., Tech. Report No. 115 Sept., 1950.

18. James Marsh "Current Distributions on Helical Antennas" Project Report No. 339-10, The Ohio State University Research Foundation, February 28, 1950.

19. N. Marcuvitz, "On Field Representations in Terms of Leaky Modes or Eigenmodes" Trans. IRE, Vol. AP-4, pp. 192-4, July 1956.

20. Arthur A. Oliner, "Leaky Waves in Electromagnetic Phenomena" Report PIBMRI-1064-62, Polytechnical Institute of Brooklyn, Contract No. AF-19(604)-7499, 2 August 1962.

21. L.O. Goldstone and A.A. Oliner "Leaky Wave Antennas I: Rectangular Waveguides" PIB-534, Research Report R-606-57, AF Cambridge Research Center Contract No. AF-19(604)-2031, August 11, 1957. IRE Trans. PTGAP Vol. AP-7 No. 4 October, 1959.

22. L.O. Goldstone and A.A. Oliner "Leaky Wave Antennas II: IRE Trans. PTGAP Vol. AP-9, May 1961, No. 3 p. 280.

23. A. Hessel, "On the Influence of Complex Poles on the Radiation Pattern of Leaky-Wave Antennas", Trans IRE PTGAP, Vol. AP-10, 5, p. 646.

24. S.K. Kogan, "The Propagation of Waves Along on Endless Helix", Compt. Rend. Acad. Sci. (USSR), Vol. 66, June 1949; p. 867.

25. D.A. Watkins, Topics of Electromagnetic Theory, John Wiley and Sons, Inc. New York, 1958.

26. G.A. Deschamps, "Generalized Floquet Theorem", (Unpublished) Univ. of Illinois Ant. Lab., 1963.

27. G.A. Campbell and R.M. Foster "Fourier Integrals for Practical Application", Bell Telephone System Monograph B-584 Sept. 1931.

28. Higher Transcendental Functions, Vol II, A. Erdelyi, Editor, Calif. Inst. of Tech. Bateman Manuscript Project, McGraw-Hill Book Company, Inc., 1953.

29. Klock, P. and R. Mittra. "Complex-Valued Phase Constants for the Sheath Helix and Their Realtion to the Solutions for the Tape Helix", Quarterly Report 2, March 1963, AF33(657)-10474.

30. C.H. Tang, "Input Impedances of Some Curved Wire Antennas", Ant. Lab. Tech. Report No. 56, Univ. of Illinois, June 1962, Contract AF33(657)-8460.

31. O.L. McClelland, "An Investigation of the Near Fields of the Conical Equiangular Spiral Antenna", Univ. of Illinois Ant. Lab. Tech., Report No. 55, May 1962, Contract AF33(657)-8460.

AF 33(657)-10474

DISTRIBUTION LIST

One copy each unless otherwise indicated

Armed Services Technical Information Agency
Attn: TIP-DR
Arlington Hall Station
Arlington 12, Virginia (20 copies)

Air Force Systems Command (SCSE)
Andrews Air Force Base
Washington 25, D. C.

Aeronautical Systems Divsion
Attn: ASRNCF-3
Wright-Patterson Air Force Base
Ohio (5 copies)

Aeronautical Systems Division
Attn: ASNSED, Mr. Mulligan
Wright-Patterson Air Force Base
Ohio

Aeronautical Systems Division
Attn: ASAPRL
Wright-Patterson Air Force Base
Ohio

Aeronautical Systems Division
Attn: ASRSA - Library
Wright-Patterson Air Force Base
Ohio

Aeronautical Systems Division
Attn: ASNPRS
Wright-Patterson Air Force Base
Ohio

Commander
Air Force Systems Command
Aeronautical Systems Division
Wright-Patterson Air Force Base
Ohio
Attn: ASNCSO

Commander
Air Force Systems Command
Attn: ASNPOT, Mr. Finocharo
Aeronautical Systems Division
Wright-Patterson Air Force Base
Ohio

Commander
Foreign Technology Division
Attn: TD-El
Wright-Patterson Air Force Base
Ohio

Air Force Cambridge Research Laboratory
Attn: CRRD
Laurence G. Hanscom Field
Bedford, Massachusetts

Commander
Air Force Missile Test Center
Technical Library
Patrick Air Force Base
Florida

Commander
Air Force Missile Development Center
Attn: Technical Library
Holloman Air Force Base
New Mexico

Air Force Ballistic Missile Division
Attn: Technical Library, Air Force Unite Post Office
Los Angeles, California

Commanding Officer
USARDVL
Attn: SIGRA/SL-NAI
Ft. Monmouth, New Jersey

Chief, Bureau of Ships
Attn: Code 312
Main Navy Building
Washington 25, D. C.

Commander
Air Proving Ground Center (AFSC)
Headquarters 3208th Test Group
Eglin Air Force Base, Florida

Director
Ballistics Research Laboratory
Attn: Ballistics Measurement Lab.
Aberdeen Proving Ground, Maryland

National Aeronautics & Space Adm.
Attn: Librarian
Langley Field, Virginia

Rome Air Development Center
Attn: RALTM
Griffiss Air Force Base
New York

Rome Air Development Center
Attn: RAWED, Mr. R. F. Davis
Griffiss Air Force Base
New York

Commander
Research & Technology Division
Attn: RTHR, Maj. J. Gregory
Bolling Air Force Base
Washington 25, D. C.

Office of Chief Signal Officer
Engineering & Technical Division
Attn: SIGNET-5
Washington 25, D. C.

Commanding Officer
U. S. Army Electronics R&D Activity
Attn: SELWS-ED
White Sands, Missile Range, New Mexico

Director
Surveillance Department
Evans Area
Attn: Technical Document Center
Belman, New Jersey

Commander
U. S. Naval Air Test Center
Attn: WST-54, Antenna Section
Patuxent River, Maryland

Material Laboratory, Code 932
New York Naval Shipyard
Brooklyn 1, New York

Director
Naval Research Laboratory
Attn: Code 5200
Washington 25, D. C.

Director
Air University Library
Attn: 3T-AUL-59-30
Maxwell Air Force Base
Alabama

Commanding General
White Sands Missile Range
Attn: ORDBS-OM-Tech Library RR-312
New Mexico.

Commanding Officer
Diamond Ordnance Fuse Laboratories
Attn: 240
Washington 25, D. C.

Director
U. S. Navy Electronics Laboratory
Attn: Library
San Diego 52, California

Adams-Russell Company
200 Sixth Street
Attn: Library (Antenna Section)
Cambridge, Massachusetts

Aero Geo Astro
Attn: Security Officer
1200 Duke Street
Alexandria, Virginia

NASA Goddard Space Flight Center
Attn: Antenna Section, Code 523
Greenbelt, Maryland

Airborne Instruments Labs., Inc.
Attn: Librarian (Antenna Section)
Walt Whitman Road
Melville, L.I., New York

American Electronic Labs
Box 552 (Antenna Section)
Lansdale, Pennsylvania

Andrew Alfred Consulting Engineers
Attn: Librarian (Antenna Section)
299 Atlantic Avenue
Boston 10, Massachusetts

Amphenol-Borg Electronic Corporation
Attn: Librarian (Antenna Section)
2801 S. 25th Avenue
Broadview, Illinois

Bell Aircraft Corporation
Attn: Technical Library
(Antenna Section)
Buffalo 5, New York

Bendix Radio Division of
Bendix Aviation Corporation
Attn: Technical Library
(For Dept. 462-4)
Baltimore 4, Maryland

Antenna Systems, Inc.
Manager Documentation
Grenier Field
Manchester, New Hampshire

Boeing Airplane Company
Aero Space Division
Attn: Technical Library
M/F Antenna & Radomes Unit
Seattle, Washington

Boeing Airplane Company
Attn: Technical Library
M/F Antenna Systems Staff Unit
Wichita, Kansas

Chance Vought Aircraft, Inc.
THRU: Bu AER Representative
Attn. Technical Library
M/F Antenna Section
P. O. Box 5907
Dallas 22, Texas

Collins Radio Company
Research Division
Attn: Technical Library
Cedar Rapids, Iowa

Convair
Ft. Worth Division
Attn: Technical Library (Antenna
Section)
Grants Lane
Fort Worth, Texas

Convair
Attn. Technical Library
(Antenna Section)
P. O. Box 1050
San Diego 12, California

Dalmo Victor Company
Attn: Technical Library
(Antenna Section)
1515 Industrial Way
Belmont, California

Dorne & Margolin, Inc.
Attn: Technical Library
(Antenna Section)
30 Sylvester Street
Westbury, L. I., New York

Dynatronics, Inc.
Attn: Technical Library
(Antenna Section)
Orlando, Florida

Electronic Communications, Inc.
Research Division
Attn: Technical Library
1830 York Road
Timonium, Maryland

Fairchild Engine & Airplane Corporation
Fairchild Aircraft & Missiles Division
Attn Technical Library
(Antenna Section)
Hagerstown 10, Maryland

Georgia Institute of Technology
Engineering Experiment Station
Attn· Technical Library
M/F Electronics Division
Atlanta 13, Georgia

General Electric Company
Electronics Laboratory
Attn: Technical Library
Electronics Park
Syracuse, New York

General Electronic Labs., Inc.
Attn: Technical Library
(Antenna Section)
18 Ames Street
Cambridge 42, Massachusetts

General Precision Lab., Division of
General Precision, Inc.
Attn: Technical Library
(Antenna Section)
63 Bedford Road
Pleasantville, New York

Goodyear Aircraft Corporation
Attn: Technical Library
M/F Dept. 474
1210 Massilon Road
Akron 15, Ohio

Granger Associates
Attn: Technical Library
(Antenna Section)
974 Commercial Street
Palo Alto, California

I-T-E Circuit Breaker Company
Special Products Division
Attn: Research Library
601 E. Erie Avenue
Philadelphia 34, Pennsylvania

General Mills Electronics Division
Attn: Dr. H. P. Raabe
2003 East Hennepin Avenue
Minneapolis 13, Minnesota

Grumman Aircraft Engineering Corporation
Attn: Technical Library
M/F Avionics Engineering
Bethpage, New York

The Hallicrafters Company
Attn: Technical Library
(Antenna Section)
4401 W. Fifth Avenue
Chicago 24, Illinois

Hoffman Laboratories, Inc.
Attn: Technical Library
(Antenna Section)
Los Angeles 7, California

John Hopkins University
Applied Physics Laboratory
8621 Georgia Avenue
Silver Springs, Maryland

Hughes Aircraft Corporation
Attn: Technical Library
(Antenna Section)
Florence & Teal Street
Culver City, California

ITT Laboratories
Attn: Technical Library
(Antenna Section)
500 Washington Avenue
Nutley 10, New Jersey

U. S. Naval Ordnance Laboratory
Attn: Technical Library
Corona, California

Lincoln Laboratories
Massachusetts Institute of Technology
Attn: Document Room
P. O. Box 73
Lexington 73, Massachusetts

Litton Industries
Attn: Technical Library
(Antenna Section)
4900 Calvert Road
College Park, Maryland

John Hopkins University
Radiation Laboratory
Attn: Library
1315 St. Paul Street
Baltimore 2, Maryland

Lockheed Missile & Space Division
Attn: Technical Library (M/F Dept-
58-40, Plant 1, Bldg. 130)
Sunnyvale, California

The Martin Company
Attn: Technical Library
(Antenna Section) Mail No. T-38
P. O. Box 179
Denver 1, Colorado

The Martin Company
Attn: Technical Library (Antenna
Section)
Baltimore 3, Maryland

The Martin Company
Attn: Technical Library (M/F
Microwave Laboratory)
Box 5837
Orlando, Florida

W. L. Maxson Corporation
Attn: Technical Library
(Antenna Section)
460 West 34th Street
New York 1, New York

McDonnell Aircraft Corporation
Attn: Technical Library
(Antenna Section)
Box 516
St. Louis 66, Missouri

Melpar, Inc.
Attn: Technical Library
(Antenna Section)
3000 Arlington Blvd.
Falls Church, Virginia

University of Michigan
Radiation Laboratory
Willow Run
201 Catherine Street
Ann Arbor, Michigan

Mitre Corporation
Attn: Technical Library (M/F Electronic
Warefare Dept. D-21)
Middlesex Turnpike
Bedford, Massachusetts

Northeastern University
Attn: Dodge Library
Boston 15, Massachusetts

North American Aviation, Inc.
Attn: Technical Library (M/F
Engineering Dept.)
4300 E. Fifth Avenue
Columbus 16, Ohio

North American Aviation, Inc.
Attn: Technical Library
(M/F Dept. 56)
International Airport
Los Angeles, California

Northrop Corporation
NORAIR Division
1001 East Broadway
Attn: Technical Information (3924-3)
Hawthorne, California

Ohio State University Research
Foundation
Attn: Technical Library
(M/F Antenna Laboratory)
1314 Kinnear Road
Columbus 12, Ohio

Ohio State University Research
Foundation
Attn: Dr. C. H. Walter
1314 Kinnear Road
Columbus 12, Ohio

Philco Corporation
Government & Industrial Division
Attn: Technical Library
(M/F Antenna Section)
4700 Wissachickon Avenue
Philadelphia 44, Pennsylvania

Westinghouse Electric Corporation
Air Arms Division
Attn: Librarian (Antenna Lab)
P. O. Box 746
Baltimore 3, Maryland

Wheeler Laboratories
Attn: Librarian (Antenna Lab)
Box 561
Smithtown, New York

Electrical Engineering Research
Laboratory
University of Texas
Box 8026, University Station
Austin, Texas

University of Michigan Research
Institute
Electronic Defense Group
Attn: Dr. J. A. M. Lyons
Ann Arbor, Michigan

Radio Corporation of America
RCA Laboratories Division
Attn: Technical Library
(M/F Antenna Section)
Princeton, New Jersey

Radiation, Inc.
Attn: Technical Library (M/F)
Antenna Section
Drawer 37
Melbourne, Florida

Ramo-Wooldridge Corporation
Attn: Librarian (Antenna Lab)
Canoga Park, California

Rand Corporation
Attn: Librarian (Antenna Lab)
1700 Main Street
Santa Monica, California

Rantec Corporation
Attn: Librarian (Antenna Lab)
23999 Ventura Blvd.
Calabasas, California

Raytheon Corporation
Equipment Division
Library - J. Portsch
P. O. Box 520
Waltham 54, Massachusetts

Republic Aviation Corporation
Applied Research & Development
Division
Attn: Librarian (Antenna Lab)
Farmingdale, New York

Sanders Associates
Attn: Librarian (Antenna Lab)
95 Canal Street
Nashua, New Hampshire

Southwest Research Institute
Attn: Librarian (Antenna Lab)
8500 Culebra Road
San Antonio, Texas

H. R. B. Singer Corporation
Attn: Librarian (Antenna Lab)
State College, Pennsylvania

Sperry Microwave Electronics Company
Attn: Librarian (Antenna Lab)
P. O. Box 1828
Clearwater, Florida

Sperry Gyroscope Company
Attn: Librarian (Antenna Lab)
Great Neck, L. I., New York

Stanford Electronic Laboratory
Attn: Librarian (Antenna Lab)
Stanford, California

Stanford Research Institute
Attn: Librarian (Antenna Lab)
Menlo Park, California

Sylvania Electronic System
Attn: Librarian (M/F Antenna &
Microwave Lab)
100 First Street
Waltham 54, Massachusetts

Sylvania Electronic System
Attn: Librarian (Antenna Lab)
P. O. Box 188
Mountain View, California

Technical Research Group
Attn: Librarian (Antenna Section)
2 Aerial Way
Syosset, New York

Ling Temco Aircraft Corporation
Temco Aircraft Division
Attn: Librarian (Antenna Lab)
Garland, Texas

Texas Instruments, Inc.
Attn: Librarian (Antenna Lab)
6000 Lemmon Avenue
Dallas 9, Texas

A. S. Thomas, Inc.
Attn: Librarian (Antenna Lab)
355 Providence Highway
Westwood, Massachusetts

New Mexico State University
Head Antenna Department
Physical Science Laboratory
University Park, New Mexico

Bell Telephone Laboratories, Inc.
Whippany, New Jersey
Attn: Technical Reports Librarian
Room 2A-165

Robert G. Hansen
Aerospace Corporation
Box 95085
Los Angeles 45, California

Dr. Richard C. Becker
10829 Berkshire
Westchester, Illinois

Dr. W. M. Hall
Raytheon Company
Surface Radar and Navigation
Operations
Boston Post Road
Wayland, Massachusetts

Dr. Robert L. Carrel
Collins Radio Corporation
Antenna Section
Dallas, Texas

Dr. A. K. Chatterjee
Vice Principal and Head of the De-
partment of Research
Birla Institute of Technology
P. O. Mesra
District-Ranchi (Bihar) India

University of Dayton
Research Institute
Attn: Professor Douglas Hanneman
300 College Park
Dayton, Ohio

Technische Hochschule
Attn: H. H. Meinke
Munich, Germany

NASA Goddard Space Flight Center
Attn: Antenna Branch
Mr. Lantz
Greenbelt, Maryland

Aeronautic Division
Ford Motor Company
Ford Road - Attn: Mr. J. M. Black
Newport Beach, California

Professor A. A. Oliver
Polytechnic Institute of Brooklyn
Microwave Research Institute
55 Johnson Street
Brooklyn 1, New York

U. S. Naval Ordnance Laboratory
Attn: Technical Library
Corona, California

Avco Corporation
Research and Advanced Development
Division
Attn Research Library, T.A. Rupprecht
201 Lowell Street
Wilmington, Massachusetts

Raytheon Company
Missile and Space Division
Attn: Research Library
Bedford, Massachusetts

Teledyne Systems, Incorporated
Attn: Technical Library, Antenna Section
1625 E. 126th Street
Hawthorne, California

National Research Council
Attn. Microwave Section
Ottawa 2, Canada

Sichak Associates
Attn: W. Sichak
518 Franklin Avenue
Nutley, New Jersey

W. T. Patton
2208 New Albany Road
Cinn. Township
Riverton Post Office
New Jersey

Radio Corporation of America
Missile and Service Radar Division
Attn Manager, Antenna Engineering
Skill Center
Moorestown, New Jersey

Advanced Development Laboratories, Inc.
Haines Street
Nashua, New Hampshire

Cornell Aeronautical Lab.
Attn: Research Library
Buffalo, New York

Fairchild Stratos Corporation
Aircraft-Missiles Division
Attn: Technical Library (Antenna Section)
Hagerstown 10, Maryland

General Electric Company
Light Military Electronics Department
French Road
Utica, New York

General Electric Company
General Engineering Laboratory
Bldg 371, Room 478
Schenectady, New York

Goodyear Aircraft Corporation
Antenna Department
Litchfield Park
Phoenix, Arizona

Laboratory for Electronics, Inc.
Antenna Department
1079 Commonwealth Avenue
Boston 15, Massachusetts

Lockheed Aircraft
Electronic and Armaments System Office
Burbank, California

Motorola, Inc.
Western Military Electronics Division
P. O. Box 1417
Scottsdale, Arizona

Philco Corporation
Antenna Section
3875 Fabian Way
Palo Alto, California

Space Technology Laboratory
Attn: Research Library
P. O. Box 95100
Los Angeles 45, California

Avco Corporation
Electronic and Ordnance Division
Attn: Technical Library
Cincinnati 41, Ohio

Bendix Corporation
Research Labs Division
Attn: G. M. Peace
Southfield (Detroit), Michigan

Douglas Aircraft Co., Inc.
Attn: MSSD Technical Library
(Antenna Section)
3000 Ocean Park Blvd.
Santa Monica, California

Emerson and Cuming, Inc.
Attn: E. J. Luoma
869 Washington Street
Canton, Massachusetts

ANTENNA LABORATORY

TECHNICAL REPORTS AND MEMORANDA ISSUED

Contract AF33(616)-310

"Synthesis of Aperture Antennas," Technical Report No. 1, C. T. A. Johnk, October, 1954.*

"A Synthesis Method for Broadband Antenna Impedance Matching Networks," Technical Report No. 2, Nicholas Yaru, 1 February 1955. * AD 61049.

"The Assymmetrically Excited Spherical Antenna," Technical Report No. 3, Robert C. Hansen, 30 April 1955.*

"Analysis of an Airborne Homing System," Technical Report No. 4, Paul E. Mayes, 1 June 1955 (CONFIDENTIAL).

"Coupling of Antenna Elements to a Circular Surface Waveguide," Technical Report No. 5, H. E. King and R. H. DuHamel, 30 June 1955.*

"Input Impedance of A Spherical Ferrite Antenna with A Latitudinal Current," Technical Report No. 6, W. L. Weeks, 20 August 1955.

"Axially Excited Surface Wave Antennas," Technical Report No. 7, D. E. Royal, 10 October 1955.*

"Homing Antennas for the F-86F Aircraft (450-2500 mc), Technical Report No. 8, P. E. Mayes, R. F. Hyneman, and R. C. Becker, 20 February 1957, (CONFIDENTIAL).

"Ground Screen Pattern Range," Technical Memorandum No. 1, Roger R. Trapp, 10 July 1955.*

Contract AF33(616)-3220

"Effective Permeability of Spheriodal Shells," Technical Report No. 9, E. J. Scott and R. H. DuHamel, 16 April 1956.

"An Analytical Study of Spaced Loop ADF Antenna Systems," Technical Report No. 10, D. G. Berry and J. B. Kreer, 10 May 1956. AD 98615.

"A Technique for Controlling the Radiation from Dielectric Rod Waveguides," Technical Report No. 11, J. W. Duncan and R. H. DuHamel, 15 July 1956.*

"Direction Characteristics of a U-Shaped Slot Antenna," Technical Report No. 12, Richard C. Becker, 30 September 1956.**

"Impedance of Ferrite Loop Antennas," Technical Report No. 13, V. H. Rumsey and W. L. Weeks, 15 October 1956. AD 119780.

"Closely Spaced Transverse Slots in Rectangular Waveguide," Technical Report No. 14, Richard F. Hyneman, 20 December 1956.

"Distributed Coupling to Surface Wave Antennas," Technical Report No. 15, R. R. Hodges, Jr., 5 January 1957.

"The Characteristic Impedance of the Fin Antenna of Infinite Length," Technical Report No. 16, Robert L. Carrel, 15 January 1957.*

"On the Estimation of Ferrite Loop Antenna Impedance," Technical Report No. 17, Walter L. Weeks, 10 April 1957.* AD 143989.

"A Note Concerning a Mechanical Scanning System for a Flush Mounted Line Source Antenna," Technical Report No. 18, Walter L. Weeks, 20 April 1957.

"Broadband Logarithmically Periodic Antenna Structures," Technical Report No. 19, R. H. DuHamel and D. E. Isbell, 1 May 1957. AD 140734.

"Frequency Independent Antennas," Technical Report No. 20, V. H. Rumsey, 25 October 1957.

"The Equiangular Spiral Antenna," Technical Report No. 21, J. D. Dyson, 15 September 1957. AD 145019.

"Experimental Investigation of the Conical Spiral Antenna," Technical Report No. 22, R. L. Carrel, 25 May 1957.** AD 144021.

"Coupling between a Parallel Plate Waveguide and a Surface Waveguide," Technical Report No. 23, E. J. Scott, 10 August 1957.

"Launching Efficiency of Wires and Slots for a Dielectric Rod Waveguide," Technical Report No. 24, J. W. Duncan and R. H. DuHamel, August 1957.

"The Characteristic Impedance of an Infinite Biconical Antenna of Arbitrary Cross Section," Technical Report No. 25, Robert L. Carrel, August 1957.

"Cavity-Backed Slot Antennas," Technical Report No. 26, R. J. Tector, 30 October 1957.

"Coupled Waveguide Excitation of Traveling Wave Slot Antennas," Technical Report No. 27, W. L. Weeks, 1 December 1957.

"Phase Velocities in Rectangular Waveguide Partially Filled with Dielectric," Technical Report No. 28, W. L. Weeks, 20 December 1957.

"Measuring the Capacitance per Unit Length of Biconical Structures of Arbitrary Cross Section," Technical Report No. 29, J. D. Dyson, 10 January 1958.

"Non-Planar Logarithmically Periodic Antenna Structure", Technical Report No. 30, D. E. Isbell, 20 February 1958. AD 156203.

"Electromagnetic Fields in Rectangular Slots," Technical Report No. 31, N. J. Kuhn and P. E. Mast, 10 March 1958.

"The Efficiency of Excitation of a Surface Wave on a Dielectric Cylinder," Technical Report No. 32, J. W. Duncan, 25 May 1958.

"A Unidirectional Equiangular Spiral Antenna," Technical Report No. 33, J. D. Dyson, 10 July 1958. AD 201138.

"Dielectric Coated Spheroidal Radiators," Technical Report No. 34, W. L. Weeks, 12 September 1958. AD 204547.

"A Theoretical Study of the Equiangular Spiral Antenna," Technical Report No. 35, P. E. Mast, 12 September 1958. AD 204548.

Contract AF33(616)-6079

"Use of Coupled Waveguides in a Traveling Wave Scanning Antenna," Technical Report No. 36, R. H. MacPhie, 30 April 1959. AD 215558.

"On the Solution of a Class of Wiener-Hopf Integral Equations in Finite and Infinite Ranges," Technical Report No. 37, R. Mittra, 15 May 1959.

"Prolate Spheriodal Wave Functions for Electromagnetic Theory," Technical Report No. 38, W. L. Weeks, 5 June 1959.

"Log Periodic Dipole Arrays," Technical Report No. 39, D. E. Isbell, 1 June 1959. AD 220651.

"A Study of the Coma-Corrected Zoned Mirror by Diffraction Theory," Technical Report No. 40, S. Dasgupta and Y. T. Lo, 17 July 1959.

"The Radiation Pattern of a Dipole on a Finite Dielectric Sheet," Technical Report No. 41, K. G. Balmain, 1 August 1959.

"The Finite Range Wiener-Hopf Integral Equation and a Boundary Value Problem in a Waveguide," Technical Report No. 42, R. Mittra, 1 October 1959.

"Impedance Properties of Complementary Multiterminal Planar Structures," Technical Report No. 43, G. A. Deschamps, 11 November 1959.

"On the Synthesis of Strip Sources," Technical Report No. 44, R. Mittra, 4 December 1959.

"Numerical Analysis of the Eigenvalue Problem of Waves in Cylindrical Waveguides, Technical Report No. 45, C. H. Tang and Y. T. Lo, 11 March 1960.

"New Circularly Polarized Frequency Independent Antennas with Conical Beam or Omnidirectional Patterns," Technical Report No. 46, J. D. Dyson and P. E. Mayes, 20 June 1960. AD 241321.

"Logarithmically Periodic Resonant-V Arrays," Technical Report No. 47, P. E. Mayes and R. L. Carrel, 15 July 1960. AD 246302.

"A Study of Chromatic Aberration of a Coma-Corrected Zoned Mirror," Technical Report No. 48, Y. T. Lo, June 1960.

"Evaluation of Cross-Correlation Methods in the Utilization of Antenna Systems," Technical Report No. 49, R. H. MacPhie, 25 January 1961

"Synthesis of Antenna Products Patterns Obtained from a Single Array," Technical Report No. 50, R. H. MacPhie, 25 January 1961.

"On the Solution of a Class of Dual Integral Equations," Technical Report No. 51, R. Mittra, 1 October 1961. AD 264557.

"Analysis and Design of the Log-Periodic Dipole Antenna," Technical Report No. 52, Robert L. Carrel, 1 October 1961. AD 264558.

"A Study of the Non-Uniform Convergence of the Inverse of a Doubly-Infinite Matrix Associated with a Boundary Value Problem in a Waveguide," Technical Report No. 53, R. Mittra, 1 October 1961. AD 264556.

Contract AF33(616)-8460

"The Coupling and Mutual Impedance Between Balanced Wire-Arm Conical Log-Spiral Antennas," Technical Report No. 54, J. D. Dyson, June 1962.

"An Investigation of the Near Fields on the Conical Equiangular Spiral Antenna," Technical Report No. 55, O. L. McClelland, May 1962.

"Input Impedance of Some Curved Wire Antennas," Technical Report No. 56, C. H. Tang, June 1962.

"Polygonal Spiral Antennas," Technical Report No. 57, C. H. Tang. O. L. McClelland, June 1962.

"On Increasing the Effective Aperture of Antennas by Data Processing," Technical Report No. 58, R. H. MacPhie, July 1962.

"Theoretical Study of a Class of Logarithmically Periodic Circuits," Technical Report No. 59, R. Mittra, July 1962.

"Backward Wave Radiation from Periodic Structures and Application to the Design of Frequency-Independent Antennas," Technical Report No. 60, P. E. Mayes, G. A. Deschamps, and W. T. Patton, December 1962.

"The Backfire Bifilar Helical Antenna," Technical Report No. 61, W. T. Patton, September 1962.

"On the Mapping by a Cross-Correlation Antenna System of Partially Coherent Radio Sources," Technical Report No. 62, R. H. MacPhie, October 1962.

"On a Conical Quad-Spiral Array," Technical Report No. 63, J. D. Dyson, September 1962.

"Antenna Impedance Matching by Means of Active Networks," Technical Report No. 64, S. Laxpati, R. Mittra, November 1962.

---

*Copies available for a three-week loan period.

** Copies no longer available